High fat diet induces metabolic disorder in the fruit fly *Drosophila melanogaster*

Dissertation

zur Erlangung des Doktorgrades

der Mathematisch-Naturwissenschaftlichen Fakultät

der Christian-Albrechts-Universität zu Kiel

Vorgelegt von

Muhammad Naeem Faisal

aus Pakistan.

Kiel, 2014

Referent:	**Prof Dr Thomas Roeder**
Koreferent:	**Prof. Dr Holger Heine**
Tag der Möndlichen Prüfung	**25/02/2015**
Zum Druck genehmigt:	_____
Gez. Dekan:	_____

With the name of *almighty* ALLAH, the most merciful and beneficent, his holy prophet Hazrat Muhammad peace be upon him.

and

With the prayers of my parents, my beloved wife maliha, my son Humayal and my daughter Hoor.

TABLE OF CONTENTS

SUMMARY

Different diets have a great impact on our health. HFD (High fat diet) have been linked to epidemic development of various metabolic disorders. Manifestation of metabolic disorders in the gut may be causally associated with several chronic diseases such as IBD, IBS, insulin resistance and ultimately with cancer. Thus, the effects of HFD on various aspects of the gut structure and physiology were studied using the fruit fly *Drosophila melanogaster* as a mod**e**l.

HFD induces substantial changes in the gut. Most importantly, it activates regeneration of the intestinal epithelium. This nutritional intervention induced stem cells to divide and produce enteroblasts with a small time delay. These enteroblasts develop into enterocytes and enteroendorine cells. The structure of the intestine is different following HFD, as the number of enteroendocrine cells was increased for longer periods indicating modified hormonal system in response to this intervention. Structural changes in the intestine were seen even after a short period of HFD. Apparently, the induction is triggered by HFD mediated expressioj of the cytokine upd3. This induction appears to be meditaed via the JNK-pathway. This induction is independent on the microbiota, as gnotobiotic animals show the same effect. Nevertheless, HFD has a strong impact on the structure of the microbiota, meaning that the number of bacteria is much higher following HFD.

In addition to the JNK-Upd3 axis, other signaling pathways are also activated in response to HFD. Ca^{2+}-signaling, indicated by the CaLexA system was chronically increased. Moreover, the stress sensing pathway Nrf2 as well as the Notch-pathway were activated in enterocytes in response to HFD. An activation of the intestinal innate immune response could not be observed.

Physiologically, the consistency and structure of defecation products was changed in response to HFD. The pH range was shifted towards more neutral values. Moreover, the defecation rate was reduced, indicative for constipation and a reduced intestinal transit process.

Taken together, HFD has a major impact on various aspects of the intestinal physiology, including a long lasting modification of the intestinal hormonal system.

Zusammenfassung

Unterschiedliche Nahrungsbestandteile haben starke Einflüsse auf unsere Gesundheit. Hochfett Diäten (HFD) konnten mit der als epidemisch zu bezeichnenden Zunahme metabolischer Erkrankungen verknüpft werden. Das Entstehen unterschiedlicher sich primär im Darm manifestierender Erkrankungen kann ebenfalls in mit HFD assoziiert werden. Zu diesen Erkrankungen gehören entzündliche Erkrankungen des Darm, Krebs und Typ2 Diabetes. Um ein besseres Verständnis dieser Vorgänge zu ermöglichen wurden Untersuchungen an einem einfachen Modell, der Taufliege *Drosophila melanogaster* durchgeführt.

HFD induziert starke Änderungen in der Struktur des Darms der Taufliege. Diese Intervention induziert die regenerative Kapazität des Darmepithels. Die Stammzellen des Darms teilen sich vermehrt als Antwort auf eine HFD und produzieren vermehrt Enteroblasten. Aus den Enteroblasten entwickeln sich Enterocyten und Enteroendokrine Zellen. Die Struktur des Darms ändert sich, da die Anzahl der Enteroendokrinen Zellen langfristig erhöht bleibt. Das lässt vermuten, dass die Hormonfunktion des Darms eine chronische Änderung erfährt, ein Befund, der auch nach sehr kurzer HFD zu beobachten ist. Verantwortlich für diese Induktion ist eine Steigerung der Upd3 Expression, die wiederum direkt von einer Aktivierung des JNK-Signalwegs abhängt. Diese Induktion ist nicht abhängig von der endogenen Microbiota, da keimfreie Tiere eine sehr vergleichbare Induktion zeigen. Nichtsdestotrotz hat eine HFD einen Effekt auf die Microbiota, sie führt zu einer Vermehrung der Anzahl dieser Bakterien.

Zusätzlich zu der Aktivierung der JNK-Upd3-Achse werden weitere Signalwege aktiviert. Dazu gehört der Ca^{2+}-Signalweg, was mit Hilfe des CaLexA-Systems gezeigt wurde. Außerdem werden der Nrf2- sowie der Notch-Signalweg in den Enterozyten aktiviert. Eine Aktivierung des intestinalen Immunsystems konnte nicht beobachtet werden.

HFD führte auch zu wesentlichen Änderungen des physiologischen Zustands des Darms. Der pH-Wert der Defäkationsprodukte änderte sich hin zu einem eher neutralen Wert. Außerdem wurde die Defäkationsrate reduziert, was auf Verstopfungen hinweist. Das lässt auf einer Verzögerung der Darmmotilität schließen.

Zusammengefasst kann gesagt werden, dass HFD zu wesentlichen Änderungen der Darmphysiologie und Darmstruktur führt, wobei die langfristige Änderung des Hormonsystems herauszuheben ist.

List of Abbreviation

ATP	**Adenoaintriphosphat**
CaCl2x2H2O	**calcium chloride dihydrate**
cDNA	**complementary deoxyribonucleic acid**
CF	**CapFinder**
CTP	**cytidine triphosphate**
ddH2O	**double-distilled water**
DEPC	**diethylene pyrocarbonate**
DNA	**deoxyribonucleic acid**
dNTPs	**deoxyribonucleoside**
DTT	**dithiothreitol**
EDTA	**ethylenediaminetetraacetic acid**
EGFP	**Epithelial green fluorescent protein**
EtOH	**ethanol**
EYFP	**Epithelial yellow fluorescent protein**
g	**acceleration of gravity**
GFP	**green fluorescent protein**
GNBP	**Gram-negative binding protein**
GTP	**guanosine triphosphate**
H2O	**water**
HCl	**hydrochloric acid**
KCl,	**potassium chloride**
KH2PO4	**potassium dihydrogen phosphate**
MgCl2	**magnesium chloride**
MgSO4x7H2O	**magnesium sulphate heptahydrate**

MnCl2	**manganese chloride**
NaHCO3	**sodium bicarbonate**
Na2HPO4-7H2O	**disodium hydrogen phosphate heptahydrate**
NaCl	**sodium chloride**
PBS	**phosphate-buffered saline**
PAMP	**pathogen Associated Molecule Pattern**
PCR	**polymerase chain reaction**
PGRP	**Peptidoglycan recognition protein**
PRR	**Pattern Recognition Receptor**
RNA	**ribonucleic acid**
rpm	**revolutions per minute**
RT	**reverse transcriptase**
SSC	**solution Salznatriumcitrat**
T7	**T7 RNA polymerase**
LaTaq	**LaTaq polymerase**
TBE	**Tris-borate-EDTA buffer**
Tris	**Tris (hydroxymethyl) aminomethane**
Bp	**bas pair**
Min	**minute**
PBS	**phosphate bufferend saline**
Ng	**nanogram**
Rpm	**rounds per minute**
Sec	**second**
Taq	**thermos aquaticus**
Ml	**millilitre**
uM	**micro molor**
KB	**kilo base**

UPD3	**unpaired-3**
ISCs	**Intestinal stem cell**
EBs	**Enteroblast**
ECs	**Enterocytes**
EEs	**Enteroendocrine**

LIST OF TABLES

LIST OF FIGURES

INTRODUCTION

A special type of immune response against various forms of injury, infection that involves the recruitment of professional immune cells to the site of injury/infection is known as inflammation. Although inflammatory responses are very important to fight infections, their deregulation may lead to multiple complex diseases and disorders such as cardiovascular diseases, cancer, neurodegenerative and metabolic disorders as well as autoimmune diseases. Inflammation can occur as an acute and chronic form. Acute inflammation has a very quick onset and is fast, while chronic inflammation is the continuation of the acute inflammation and may last for very long periods, even if the primary reason for launching an inflammation is resolved (Toshio H and Masaaki M in 2012; Ferrero ML et al., 2007). Chronic inflammation of the intestine for example underlies various forms of disorders and composite diseases, like Crohn's disease and ulcerative colitis. Crohn's disease and ulcerative colitis are the two major forms of chronic inflammatory diseases of the gut, which are known as inflammatory bowel disease (Hugot JP., et al 2001; Masaaki M and Toshio H., 2012).

1.1 Intestinal epithelium

The intestinal epithelium makes the barrier between the lymphoid tissues associated with the gut and the outside world, most importantly, with the endogenous microbiota resident in the gut lumen of vertebrates and invertebrates. It is not only a physical but also a chemical barrier that has to block entry of e.g. microbes, antigens and toxins. IECs (Intestinal epithelial cells) are the most important cell population as they make the majority of cells within the epithelium (David A and Lance WP in 2014).

Homeostasis of the intestinal epithelium depends upon the equilibrium between self proliferation and differentiation of epithelial cells during the entire lifetime. The intestinal epithelium niche is made by the closely association cellular part with the sheath of intestinal pericryptal fibroblasts, which are also known as sub epithelial myofibroblasts (Mills JC and Gordon JI in 2001; Schofield R in 1978). It is established that these cells releases various types of important growth factors, hormones and cytokines that are essential for the induction of epithelial proliferation (Powell DW et al., 1999; Bjerknes M and Cheng H in 2006, Marshman E et al., 2002). In mammals it is believed that six stem cells are in each

crypt. Stem cell resides from position +4 from the crypt bottom, while the Paneth cells contain the first 3 positions (Potten CS et al., 1974).

Paneth cells are important epithelial cells and play pivotal roles in the innate immunity of the small intestine. Paneth cells release proteins and peptides with antimicrobial activities such as, defensins and lysozymes. Releasing of this specific antimicrobial peptides and lysozymes into the gastrointestinal flora is required to shape the microbial community while fighting against potential invaders. The life span of a Paneth cell is approximately three weeks (Van Es JH et al 2005). In addition to their location at the position 1-3, the positions 5-7 relative to the crypt base can be taken. Paneth cells are the only differentiating cells that can change in direction to the crypt's bottom (Bastide P et al., 2007).

Goblet cells are secretory cells of the gut epithelium. Mucin and trefoil proteins are secreted by them. Both products play pivotal roles in gut movement and ejection of the gut contents into the intestine towards lower parts of the gut. It also provides protection against chemical and physical damage of the epithelium. The division and distribution of the Goblet cells throughout the intestine is variable. It is approximately 4 % in duodenum and approximately 16% in the descending colon relative to all epithelial cells (Karam SM 1999).

Notch signalling plays a vital role in differentiation of goblet cells. Huge numbers of epithelial cells differentiate into goblet cells after the loss of Notch function in the epithelium (Katz JP et al., 2002; Van Es JH et al., 2005 and Crosnier C et al., 2005).

Enterocytes (ECs) are also knows as columnar cells and are extremely polarized. Enterocytes (ECs) contains brush border on the apical surface through which absorption takes place and are also responsible for nutrient movement in the entire epithelium. About 80% of the whole intestinal epithelium consists of enterocytes (ECs) (Jensen J et al., 2000).

Enteroendocrine cells (EEs) are also secretory cells that release different hormones and also Known as neuroendocrine cells. They contribute to gut functioning through the release of various peptide hormones. On the basis of marker gene expression, morphology and release of various specific hormones they can be differentiating into 15 various subtypes. Enteroendocrine (EEs) responsible for approximately 1% of the total epithelial cell lining and they are distributed through the whole intestinal epithelium organized as single cells. (Schonohoff SE et al., 2004).

The notch signalling pathway plays a pivotal role in differentiation of various epithelial cells as well as the development of enteroendocrine cells (EEs) or other secretory epithelial cells such as goblet cells. The bHLH transcription factor Beta 2, which is also known as NeuroD is very important for secretin and cholecystokinin producing enteroendocrine cells. Different types of other genes such as, homeodomain transcription factors Pdx-1, Nkx2.2, Pax4, and Pax6 are also relevant for the fate of specification of enteroendorine cells (EEs) (Naya FJ et al., 1997; Desai S et al., 2008; Larsson LI et al., 1998).

1.2 Intestinal immune system

The immune system protects multicellular organisms against various types of pathogenic bacteria, viruses, fungi, protozoan and parasites. Most animals depend on their innate immune system including engulfment of invaders through the process of phagocytosis or encapsulation of larger invaders (Lemaitre et al., 1996; Silverman et al., 2008; Leclerc et al., 2004). The innate immune system is the most ancient, fast and active type of immune defence system, which protects the intestinal epithelium and the whole individual from pathogens trying to invade the body. In all epithelia throughout the animal kingdom the major characteristics appear to be similar. Even humans depend on this ancient and very active immune system against infection caused by pathogens (Miller et al., 2007; Glaser et al., 2005; Lemaitre et al., 2007). The intestinal epithelium also provides the physical barrier against every pathogen. Epithelial cells are tightly bound to each other and leave no space for the entry of pathogens. This physical barrier function is impaired in inflammatory responses, where the tight junction between epithelial cell are damaged, making a pathogen entry through this path possible (Turner JR in 2006). Moreover, some pathogens have the ability to utilizing different enzymes such as proteases to disturb the tight junctions of the epithelium. This route allows the penetrators and other types of compounds to penetrate this barrier (Hackett et al., 2011; Sajjan et al., 2008; Jacquet A et al., 2011; Xiao et al., 2011).

PAMPs (pathogen associated molecular patterns) are invariable products of microorganisms. They are being recognized by various receptors of the innate immune system located on epithelial cells. These PRRs (Pathogen recognition receptors) comprise TLRs (Toll-like receptors), NLRs (Nucleotide-binding domain and leucine-rich repeats), C-type lectins, peptidoglycan recognition proteins (PGRPs) and also the retinoic acid-inducible gene I-like receptors (Rakoff N S et al., 2008). The response of the epithelium to confrontation with pathogen is the production and release of antimicrobial compounds such as AMPs

(antimicrobial peptides) or the production and release of cytokines to alert other parts of the immune system. Usually, any type of alteration or deregulation of the homeostasis may follow activation of immune responses and the onset of inflammation. As pointed out above, inflammation may lead to recovery or it persists towards a chronic inflammation of the epithelium (Weber B et al., 2009; Rakoff NS et al., 2008). The intestinal immune system is unable to differentiate between pathogens and beneficial microbes regarding their PAMPs. Other products also have the ability to activate intestinal responses comprise uric acid, nucleic acid, mitochondrial and ribosomal components released after tissue necrosis or damage (Cavassani KA et al., 2008; Shi Y et al 2003) thus acting as danger signals. Various mechanisms aim to reduce immune and inflammatory responses in the gut. Alkaline phosphatase and acyloxyacyl hydrolase are released by the enterocytes. These enzymes can diminish the inflammation through degradation of LPS, which is the most relevant PAMP (Van SM et al., 2006; McVay et al., 2006). Moreover, enterocytes maintain homeostasis through the production of various cytokines to activate different mobile cells of the immune system (Zaph C et al., 2007; Nenci A et al., 2007). Macrophages are among these mobile cells that have the potential to phagocytose invaded pathogens taking place in the intestinal lamina propria (Smythies LE et al., 2005; Weber B et al., 2009).

In mammals adaptive immune responses play a highly important role for fighting intestinal infections. B cell-mediated release of various types of different antibodies against pathogens plays a central role in this context (Mac pherson AJ et al., 2008). T helper cell and the cytokine IL-23 contribute to cause inflammation at the site of infection especially during chronic inflammatory diseases, although they hold the ability to protect the intestinal epithelium against bacteria and other types of harmful pathogens (Abraham C and Cho J., 2009; Hue S et al., 2006). IL23, IL17 and other cytokines likewise are required to maintain homeostasis in the gut and to regulate the immune system (Deretic V and Levine B in 2009).

1.3 Metabolic disorder caused by imbalances in metabolic profiles and the microbiota

The gastrointestinal tract (GIT) is the only single passage for food, water and drug administration. GIT is generally the first organ to be exposed directly to foreign particles, microbes, pathogen and other kinds of compounds through the diet (Srigiridhar K et al., 200; Brown ED et al., 1995; Aw TY in 1998; Gopaul NK et al., 2000; Kanner J and Lapidot T in 2001; Halliwell B et al., 2000; Zhao K et al 2001; Long LH et al., 1999; Long LH et al., 2000; Hiramoto K et al., 2001). High fat diet specially has been reported to activate mast cells and Toll-like receptors (TLRs) (Chamulitrat W in 1999).

Various types of metabolites are in a diet and particularly high fat diets appear to have a massive impact on the commensal microbiota and on the epithelial layer of gut. High fat diet changes the motility of the small intestine but also plays an important role to deposit fat droplets in epithelial cells with yet almost unknown consequences (Qin et al., 2010; Tasnya JT et al., 2007). Maintaining the homeostasis in the intestine is very important to keep the balance in the commensal microbiota. Imbalanced microbiota can cause several diseases, including gastrointestinal infections, metabolic imbalances, inflammatory bowel diseases (IBDs), colorectal cancer (Garrett et al., 2010; Ryu et al., 2008). Microbiota hold the potential to alter gut morphology and function (Nichole A et al., 2014).

1.3.1 Inflammatory bowel disease

IBD (Inflammatory bowel disease) collectively describes two clinical forms, Crohn's disease (CD) and Ulcerative colitis (UC). IBDs are complex and composite disorders showing high prevalence's. Individuals are on high risk to develop colorectal cancer (CRC) if they are suffering with inflammatory bowel disease (IBD) (Ekbom A et al., 1990; Langholz E et al., 1992; Choi PM et al., 1994; Gyde S et al., 1982; Carter MJ et al., 2004). Generally 1-2 % of the total cases of ulcerative colitis and Crohn's disease converts into colorectal cancer (CRC). The rate of death is one in six of all death in IBD individuals. Patients with the disease located to the rectum only are at low risk to develop CRC, while those patients where the whole colon (Pancolitis) is involved are more prone to develop CRC (Satsangi J et al., 2006; Choi PM et al., 1994; Gyde SN et al., 1982; Gyde SN et al., 1988; Eaden JA et al., 2001).

Colorectal cancer is the second leading cause of deaths among all cancers in the United States according to the American Cancer Society.

1.3.2 Obesity

High fat diet is not only characterised by the high calorie intake, but if taken permanently, it promotes to consume higher intake volumes. Thus, hyperphagia is one of the side-effects of high-fat dieting. It has been discussed that the increased availability of nutritionally unbalanced diets favours an increase in especially high-caloric nutrients. This hypothesis is called "protein leverage hypothesis" and means that protein consumption is directly regulated by the consumption of carbohydrates and fat. Lowering the consumption of protein in a diet will provoke higher levels of consumption of carbohydrates and fat. Increasing the level of protein consumption will lower the consumption of fat and carbohydrates. Studies have revealed that ad libitum feeding for animals on high fat diet progress to hyperphagia and consequently cause obesity. This is associated with leptin and insulin resistance (Wood SC et al., 2003; Simpson SJ and Rauben H D in 2005; Lissner L et al., 1987; Tremblay A et al., 1989).

Obese patients are more susceptible to a great variety of different disorders including those of the oesophageal motility, such as GERD (Gastroesophageal reflux disease) or diffuse oesophageal spasm (less spasm) and nutcracker oesophagus. Similar results are seen in the group of the morbidly obese patients. Obese patients have higher prevalence's of malfunctioning in magnitude of contraction in the middle oesophagus (Schneider JM et al 2009; Fornari F et al 2011; Biccas BN et al., 2009; Hong D et al., 2004; Jaffin BW et al., 1999). Patients with GERD that lose weight show a generally beneficial development (Djarv T et al., 2012; Friedenberg FK et al., 2008).

A great number of hormones play pivotal roles for the body's response to high fat diet consumption. Faster gastric emptying is mediated by ghrelin. A delay in gastric emptying and appetite inhibition is induced by CCK, Peptide YY (PYY), leptin and glucagon like peptide (GLP-1). Fat in the diet stimulates production e.g. CCK, PYY and GLP-1 (Stewart JE et al., 2011; Hellstrom PM et al 2006; Camilleri M et al., 2009; Delgado AS et al., 2002; Schirra J et al., 2002). Basal pyloric pressure is increased due to the infiltration of fatty acids in the intraduodenal tract. More important are the CCK and PYY levels in the blood stream. Free fatty acids can provoke appetite, as well as release and inhibition of various gastrointestinal hormones (Little TJ et al., 2007).

1.4 Model organisms

The use of model organisms to explore and understand human diseases has been out forward for a long period (Hergovich et al., 2006; Rogina and Helfand in 2003). Suited models should be easy to handle and amenable to genetic manipulation. Moreover, they should have a short life cycle and they should be cost effective. In addition to murine models there are different other model organisms used frequently, such as *yeast*, *Caenorhabditis elegans*, and *Drosophila melanogaster*. *Drosophila melanogaster*, commonly referred to as the fruit fly, was first used for genetic experiments more than a century ago by William Earnest Castle and his colleagues, who studied breeding and selection, which was published in 1906. It was through Castle's influence that *Drosophila melanogaster* became known to the geneticists T.H. Morgan culminating in the 1933 Nobel Prize in Medicine for identifying chromosomes as the vector of inheritance for genes (Snell and Reed in 1993). The major advantage of the fly compared to other invertebrate model organisms in the organ composition that is similar to vertebrates. *Drosophila melanogaster* has been used extensively for investigating fundamental biological processes such as cell proliferation, growth, cell death and cell migration. In addition, behavioural studies have shown that *Drosophila* can perform complex behaviour such as learning and memory, circadian rhythms, sleep and aggression (Bellen et al., 2010). Some of which were previously assumed to be exclusively performed by mammals (Adams and Sekelsky, 2002; Venken and Bellen, 2005; Venken and Bellen, 2007).

Drosophila melanogaster has a short generation time of approximately 10-12 days at 25 ºC and an average life span of 50-60 days. The fly genome has been completely sequenced and annotated (Adam et al., 2000). It requires only little labour and is cost effective to maintain fly stock. Mutant flies and transgenic flies are available from public stock centres at low cost and only small space is required for their maintenance. Importantly, it has been estimated that nearly 75% of all human disease associated genes are conserved in *Drosophila melanogaster* (Bier in 2005). The fruit fly has evolved an intricate defence system against various microbes. Fruit fly and other insects have strong innate immune responses to fight invading pathogens. The primary defence is located at various barriers including the peritrophic membrane the cuticle and the airway epithelium utilizing either the physical barriers (Dessens et al., 2001; Gooday and Sampson in 1998; Granados and Wang in 1997) or chemical barriers based on the production of antimicrobial peptides (AMPs), lysozymes, dual oxidases and other antimicrobial compounds (Apidianakis et al., 2005; De G et al., 2001; Ha et al., 2005). The response of the fruit fly to any kind of wound is very sophisticated and quick. This response

to wound is not only at locally but also raises a systemic response as well (Buchon et al 2009b; Hoffmann and Lemaitre in 2007; Apidianakis et al., 2007).

There are several tools and techniques available in *Drosophila,* but I will only mention those that are relevant for disease models particularly for those of metabolic disorders. One very important tool is the transposon-mediated transgenesis. The fly community has generated a number of transposon insertion lines that can be used for insertional mutagenesis. Another powerful and versatile approach in *Drosophila* is the GAL4/UAS system. It is a bipartite transcription activation system (Perrimon and Brand in 1993; Rubin and Spradling, 1982), which allows a gene of choice to be expressed in a defined set of cells or tissue of interest. In this system one transgene consists of a yeast transcriptional factor (GAL4), driven by a tissue specific promoter such as specific driver for Intestinal cell's Dl (ISC), Notch (EB), Amon (EE) and NP1 (EC). The second transgene consists of a gene of interest that is under the control of the UAS (upstream activation sequence), which drives transcription in response to GAL4 binding. This could be for example a reporter gene such as green fluorescent protein (GFP), or an RNAi construct. RNAi stands for RNA interference, which is very attractive and useful method that enables to knock down the gene of interest. This approach capitalizes on the finding that double stranded RNA (ds-RNA) molecules corresponding in sequence to endogenous transcripts can trigger the degradation of the endogenous transcripts. It requires the construction of a transgenic construct bearing an inverted repeat sequence corresponding to the target transcript (Kalidas and smith, 2002; Whitworth, 2011; Guo, 2012). This, in combination with the GAL4/UAS system to target expression of the dsRNA to the desired tissue, can simply be achieved by performing the appropriate cross diagram below,

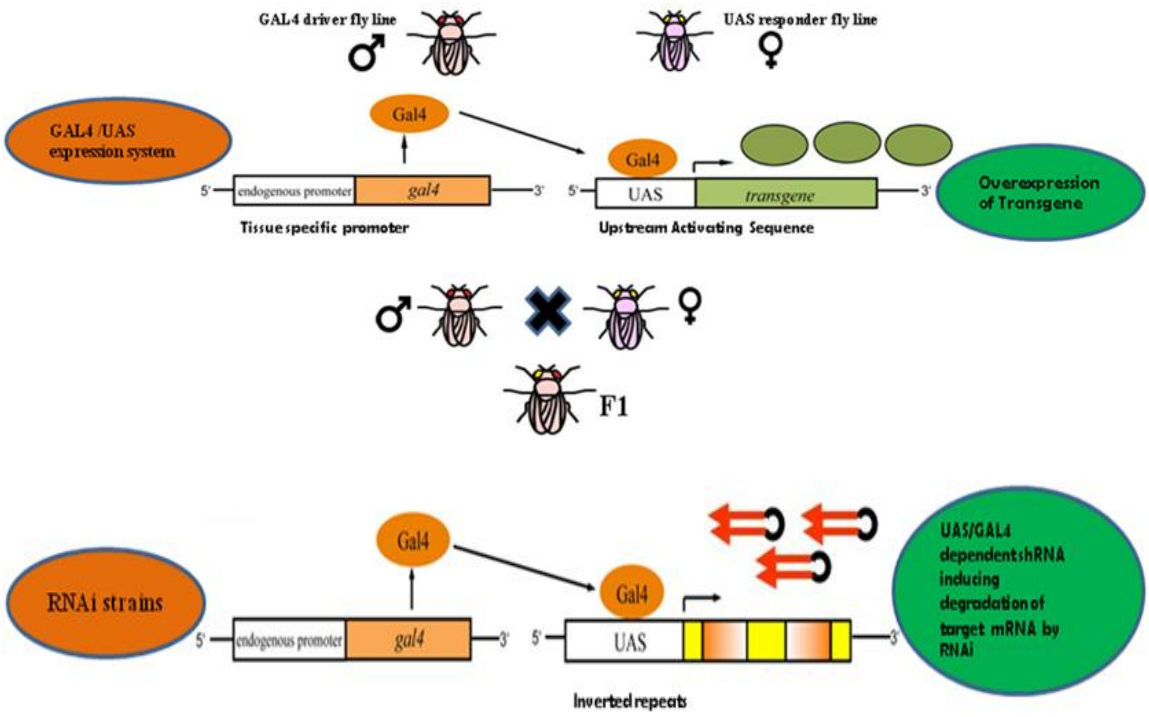

Figure1. In *Drosophila* the **UAS/Gal4 expression system** has been used to over express genes of interest in the tissue of interest. The transcript of the targeted gene will be expressed in the F1 generation in the cells of interest. **RNAi lines** have been used in *Drosophila* to silence genes of interest. The transcript of the targeted gene will be in the silenced in F1 generation after crossing of GAL4/UAS.

Different specific GAL4 cell markers are convenient because they collectively mark all midgut cells, without detectable overlap between them. An accurate percentage of each cell type can thus be calculated (by obtaining the ratio, multiplied by 100, of cells stained positively for a given cell type over the total number of stained cells) as a function of a particular experimental condition.

It has been suggested that *Drosophila melanogaster* is an ideal to monitor for the biology of stem cells. The gut of adult flies contains different types of cell population. The mother cell is called ISC (Intestinal stem cell), which is scattered through the entire gut on the basal membrane (Perrimon and Micchelli in 2006; Spradling and Ohlstein in 2006; Batlle and Casali in 2009). Under normal condition the ISC divides and give rise to another daughter ISC cell and an enteroblast (EB). EBs further differentiates into ECs (Enterocyte) or EEs

(Enteroendocrine). ECs are bigger in size and occupy the entire gut, while EEs are smaller in size (Perrimon and Micchelli in 2006; Spradling and Ohlstein in 2006).

1.5 Intestinal epithelium of *Drosophila melanogaster*

Gastrointestinal tissues in human and fruit fly share various anatomical and physiological similarities (Pitsouli et al., 2009; Hertenstein and Tepass in 1994; Kedinger et al., 1987; Rubin in 2007; Amcheslavsky A et al., 2014). The intestinal epithelium consists of a monolayer of cuboidal or columnar cells known as ECs (Enterocyte). In the midgut of *Drosophila* there are no crypts or villi, as they are present like in the mammalian systems, but cytoplasmic villi-like structures on the apical surface of the ECs have the same functional role (Tripathi and Shanbhag in 2009; Crosnier et al., 2006; Amcheslavsky A et al., 2014).

To protect the mid- and hindgut of insects from direct contact with the gut contact, including microbes, a chitinous layer known as pritrophic membrane is produced by the proventriculus (Vodovar et al., 2005; Gooday in 1999; Baumann in 2001; Garner in 1970; Tripathi and Shanbhag in 2009, Hegedus et al., 2009).

A network of circular and longitudinal muscles are present directly adjacent to the basal membrane. These longitudinal and circular muscles are responsible for the peristaltic movements in the gastrointestinal tract and both types of muscles are innervated and oxygenated (Jiang and Edgar in 2009; MacDonald and Sengupta in 2007; Kvietys and Granger in 1986; Rhee et al., 2009). In addition, to the immune competence of epithelial cells, hemocytes, macrophage-like cells in *Drosophila* play a vital part in the intestinal immunity (Komuro and Hashimoto in 1990; Hoffmann and Lemaitre in 2007).

Intestinal stem cells are located at the basal membrane. ISCs proliferate and give rise to another daughter ISCs and one EB. ISCs can be identified by their smaller nuclear size and their expression of the Notch ligand Delta (Dl) (Spradling and Ohlstein in 2006; Perrimon and Micchelli in 2006). EBs is smaller in size than ECs but bigger in size then ISCs and EEs. EBs and ISCs are also known as midgut precursor cells and both express the transcription factor escargot (esg), which is a member of the snail/ slug family of transcription factors (Perrimon and Micchelli in 2006).

EBs (Enteroblast) undergoes further differentiation into ECs. ECs can be differentiated by their larger size. ECs express Pdm1 and have large endoreplicating nuclei. EBs differentiates approximately at a rate of 90% into ECs (Perrimon and Micchelli in 2006; Singh et al., 2012).

EBs differentiates also into smaller cells known as EEs. They are small and have secretory function. EEs can be identified on the basis of Prospero (Pros) expression and their smaller size. EEs release different hormones (Spradling and Ohlstein in 2006; Perrimon and Micchelli in 2006; Singh et al., 2012; Scopelliti A et al., 2014).

It is been established that the Hippo signalling pathway has a vital role for ISC proliferation under normal and stress conditions (Herranz et al., 2012a and Herranz et al., 2012b; Poernbacher et al., 2012; Ren et al., 2010; Shaw et al., 2010; Staley and Irvine in 2010). ISC proliferation is under the inhibitory control of the Hippo pathway (Huang et al., 2005). The exact role of microRNAs for ISC renewal and differentiation is still not known, but it plays a role for proliferation and differentiation within the intestinal epithelium. *Bantam* microRNA is one of these microRNAs and regulation of ISC proliferation is directly related to the activity of bantam in the gut epithelium. Injury induces *Bantam* microRNA over expression. EGFR and Notch signaling pathways influence the activity of *Bantam* microRNA (Herranz et al., 2010a; Cohen and Thompson in 2006; Becam et al., 2011; Herranz et al., 2012b). Increased proliferation of the ISCs can also be seen following over expression of the Wnt signaling pathway in the intestinal epithelium. Hyper proliferation and hyperplasia of ISCs may result in multilayering of the intestinal epithelium. This reaction may be the first in a series leading to cancer in the gut epithelium (Lee et al., 2009; Cordero et al., 2009). Signaling systems such as the JNK, INSR (insulin receptor pathways) and Wnt signaling pathway collaborate to control proliferation of ISCs in the gut. JNK activates the Wnt signaling pathways, while as INSR activates Wnt signaling for ISCs proliferation (Scoville et al., 2008; Nateri et al., 2005). Moreover, mutations or deregulation in *K-Ras/Ras1* gene outcome can result in the formation of intestinal cancer (Pagliarini and Xu in 2003; Uhlirova et al., 2005). It has been noted that mutation in the *Ras1* gene cause abnormal growth of the epithelium, oncogenesis, multilayering, impaired differentiation as well as change in apical and basal polarity (Apidianakis et al., 2009; Jiang and Edgar in 2009).

1.6 Intestinal immune system of *Drosophila melanogaster*

The intestinal immune system of *Drosophila* precludes the entry and infection from various microbes through physical and chemical barriers (Ferrandon 2013). The first protection to block the microbial entry is made by the peritrophic membrane or peritrophic matrix.

Damaged peritrophic membrane increase the frequency of successful infections via the oral route (Kuraishi et al., 2011; Hegedus et al., 2009).

The host microbe interaction in the fly gut depends on various signaling pathways such as, Wingless, JAK/ STAT, JNK and Notch (Liu et al., 2010; Jiang et al., 2009; Lin et al., 2008; Ohlstein and Spradling in 2007). Principally, the primary immune response to any type of infection and injury of the epithelium is local, but may develop into a systemic response (Girardin and Philpott in 2004; Lemaitre and Hoffmann in 2007; Lemaitre et al., 1996; Nehme et al., 2007; Rosetto et al., 1995). After infection, various signaling pathways including those acting on NF-κB (nuclear factor kappa B) will be activated) (Buchon et al., 2009b). In response to infection in the gut epithelium production of AMPs (Antimicrobial peptides) could be observed. AMPs are most important for the gut immunity to fight back various harmful pathogens. It is established that Imd pathways has role in maintaining homeostasis by controlling long term activation of various immune responses. PGRP-LB is released in gut lumen to control the response to an infection by inhibiting the activation of the Imd pathway. Permanent activation of the NF-κB pathways would have catastrophic effects for the gut homeostasis (Zaidman R et al., 2006; Berkey et al., 2009).

The most important part of the intestinal immune system is the local production of Reactive Oxygen Species (ROS) by the enzyme dual oxidase (Duox). To activate the membrane bound Duox, cytosolic Ca^{2+} is necessary. Calcium levels are increased through activation of G-protein coupled receptors that recognise bacterial uracil. This reaction activates the PLC-ß that in turn activate the production of IP3 and there with the release of Ca2+ from intracellular stores (Razzell W et al., 2013; Sung HK and Won JL in 2014, Ha et al., 2009b).

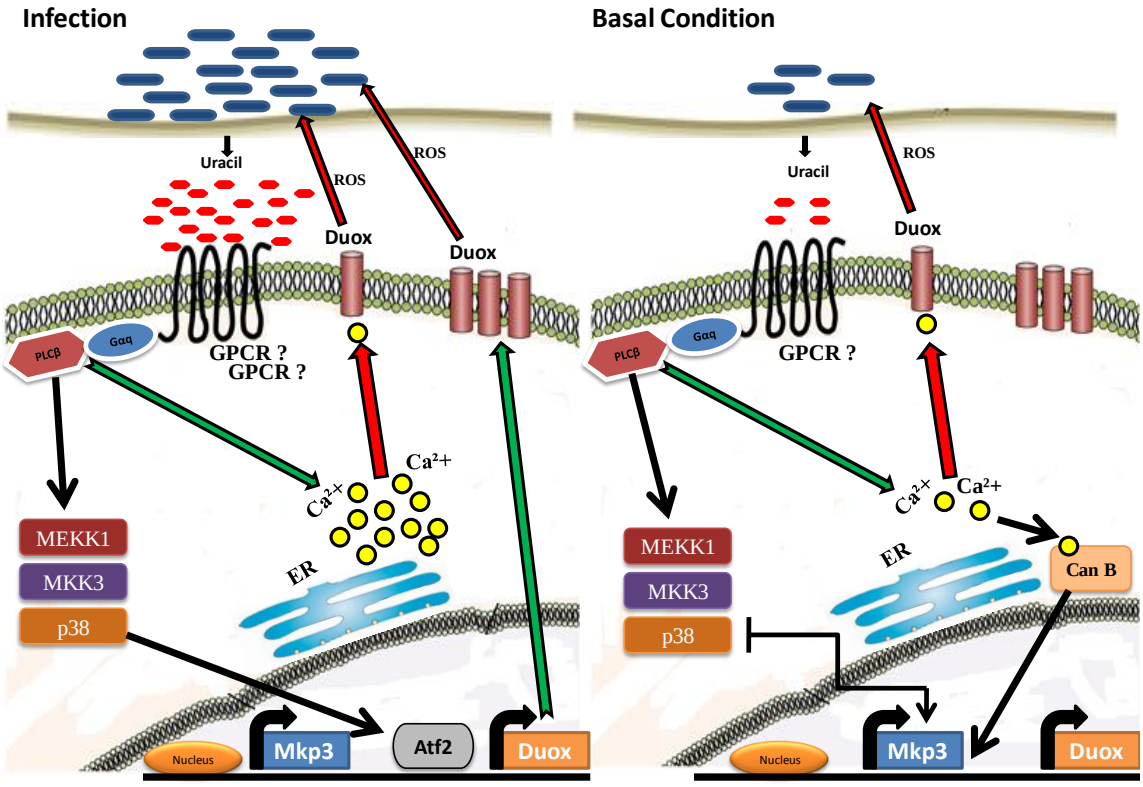

Figure2. Calcium signaling pathways play a role in the local release of ROS. Uracil activates a GPCR that leads in turn to activation of the PLCß and there with to Ca^{2+} release, which activates Duox. This figure is modified after (Sung HK and Won JL2014).

Stress mediated signals in the intestinal epithelium

Various compounds have been shown to be able to induce ISC proliferation (Biteau et al., 2008; Choi et al., 2008a; Choi et al 2008b). *Drosophila* feeding of dextrin sodium sulphate, bleomycin and hydrogen peroxide induce strong cell damages leading to proliferation and differentiation of cell progenitors in the gut epithelium (Biteau et al., 2008; Chatterjee and Ip in 2009; Choi et al., 2008b; Amcheslavky et al., 2009). The effect on the gut epithelium is different according to severity and damage to the epithelium. Some agents are cytotoxic and damage the cell so the response of the epithelium in regeneration through activation of ISCs (Biteau et al., 2008). INSR plays a role in regeneration of the intestinal epithelium after injury or cytotoxic effect caused by dextrin sodium sulphate or bleomycin (Amcheslavsky et al., 2009).

The above mentioned stressors will activate the JAK/ STAT pathway, induced by the secretion of different cytokines (Upd, Upd2, Upd3) from the damaged epithelial cells (Buchon et al., 2009b; Cronin et al., 2009; Jiang et al., 2009). In response to these cytokines from the injured or damaged ECs a higher rate of proliferation and differentiation of ISCs is induced. Huge activities ISCs cause multilayering in the gut epithelium. The homolog in mammals of these cytokines is IL-6 (Buchon et al., 2009b; Ha et al., 2009b; Ha et al., 2009a).

Nrf2 is a family of CnC (cap and collar) transcription factors (Lee et al., 2005; Maher and Yamamoto in 2010; Hayes and McMahon in 2009). The role of Nrf2 is vital under stress conditions (Inoue et al., 2005; Sykiotis and Bohmann in 2008). SKN1 is involved in life span extension and maintenance of tissue homeostasis (Curran et al., 2009). Keap 1 (Kelch-like ECH-associated protein 1) is a cytoplasmic repressor and that negatively regulates Nrf2 in *Drosophila* as well as in vertebrates (Hayes and MaMahon in 2009; Nguyen et al., 2009; Sykiotis and Bohmann in 2008; Toledano in 2009). Nrf2 degradation occurs through the Cul3-uniquitin ligase and its adapter Keap1. Life span is increased if Keap1 is inhibited. It has a direct role in activating of tolerance towards stress factors (Sykiotis and Bohmann in 2008).

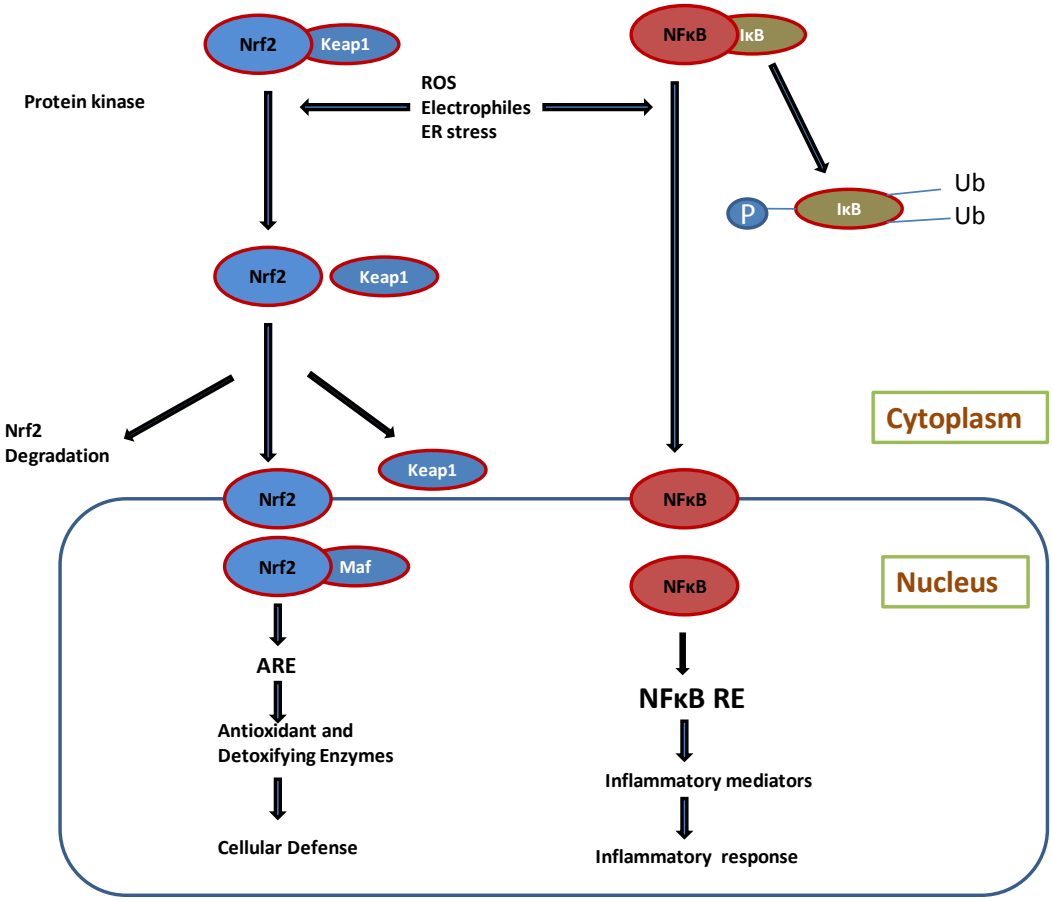

Figure3. Nrf2 pathway plays an important role under stress conditions. Antioxidant agents and detoxifying enzymes are activated following Nrf2 signaling. This figure is modified after (Hyun J K and Nosratola DV, 2010).

Keeping the homeostasis in the gut epithelium of *Drosophila* is one of the tasks of Notch signaling. ISC proliferation and differentiation is important to maintain homeostasis after activation of Notch signaling (Perrimon and Micchelli in 2006; Spradling and Ohlstein in 2006; Spradling and Ohlstein in 2007). Notch signaling is especially important for differentiation of ISCs (Crosnier et al., 2006; Ligoxygakis et al., 1999; Perrimon and Micchelli in 2006; Spradling and Ohlstein in 2006). Over expression or inactivation of Notch signaling results in critical changes of the gut epithelium. Inactivation of Notch signaling will result in the multilayering of the epithelium (Ren et al., 2010; Poernbacher et al., 2012; Staley and Irvine in 2010; Shaw et al., 2010).

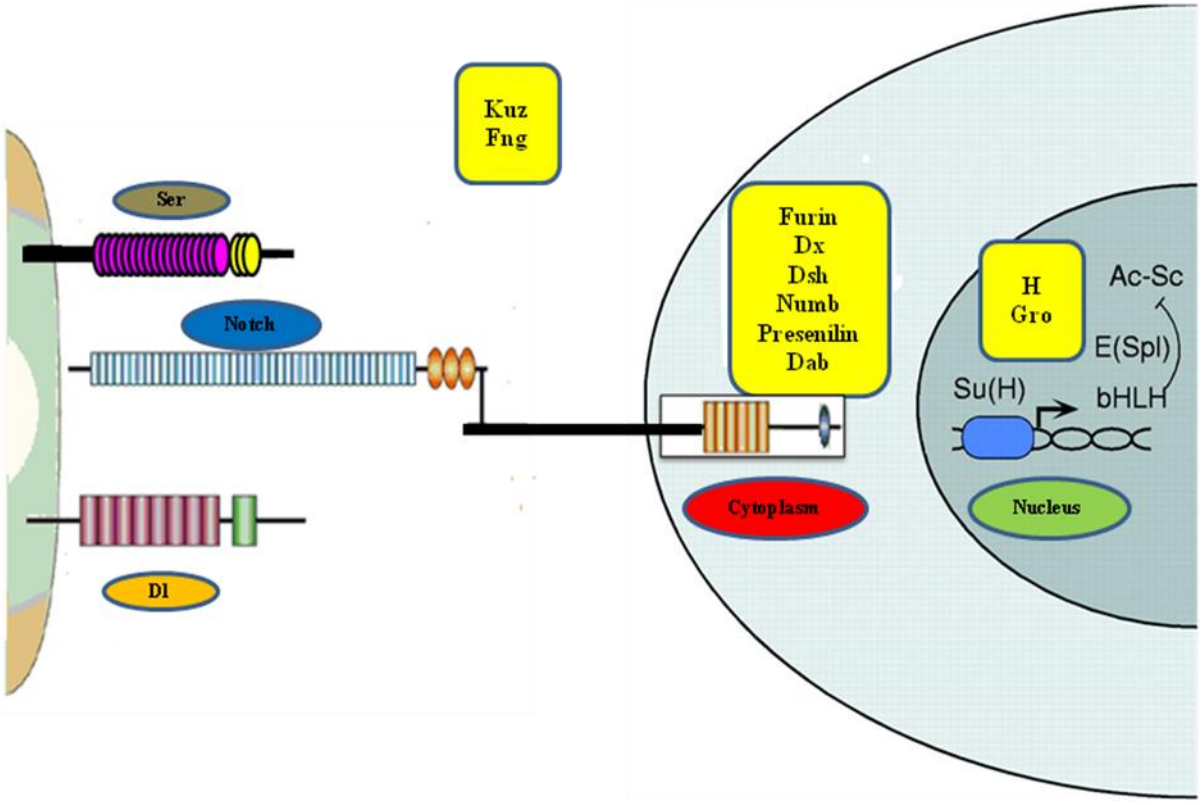

Figure 4, Both Notch and Delta are single-pass transmembrane proteins. Both play their role for controlling proliferation by the interaction between Delta and Notch. Notch and Delta require proteolysis process to function. This figure is modified after Amsen D et al 2009.

JNK (c-Jun N-terminal kinase) signaling pathways are important in response to stress or apoptotic signals. JNK pathways are also activated in response to various cytokines such as TNF (Tumor necrosis factor), which is one of the proinflammatory cytokines after stress situations (Liu et al., 1996; Moreno et al., 2002; Ryoo et al., 2004; Xia et al., 1995). JNK signaling requires different kinases cascades to form a signaling pathway (Neisch et al., 2010). Activation of JNK depends on one important factor, named Hipks (homeodomain-interacting protein kinase), which belongs to the family serine/threonine kinases (Hoffmann et al., 2003; Lan et al., 2007; Li et al., 2005; Choi et al., 2005; Kim et al., 1998; Sung et al., 2005; Zhang et al., 2003). Although Hipk factors play important roles in morphogenesis and apoptosis, the link in between JNK and Hipk is not yet understood (Inoue et al., 2010; Isono et al., 2006; Link et al., 2007; McEwen et al 2000; Zhang et al., 2003). JNK signaling has a vital role in ISCs activation and proliferation especially under oxidative stress conditions and during aging (Biteau et al., 2008; Choi et al., 2008b).

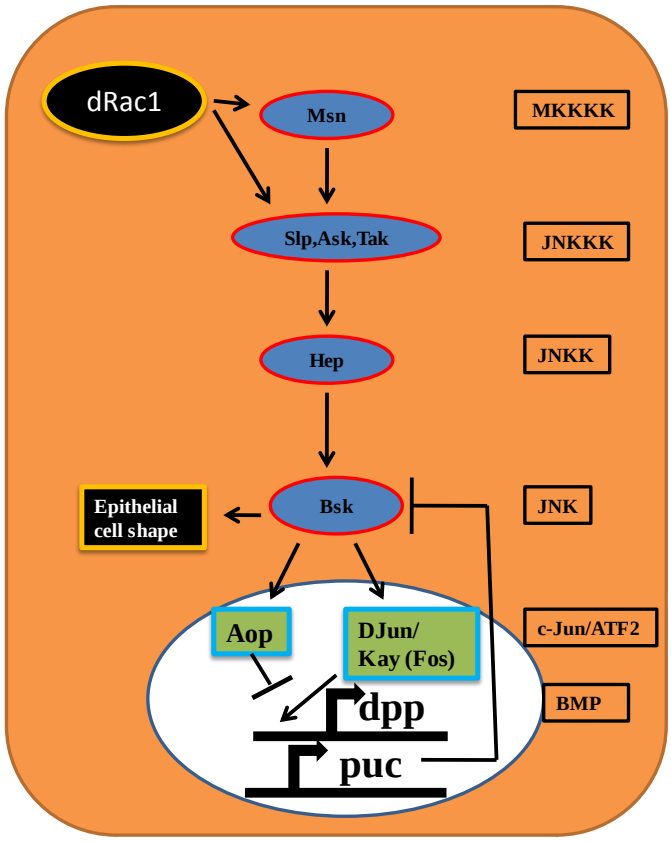

Figure5. JNK signaling is a Map Kinase signaling. Stress factors can activate this signaling cascade. Figure is modified after (Kathleen AG and Gary LJ in 2002).

1.7 Aim and significant of study

The major aim of this study was to elucidate the role of high fat diet and metabolic disorder utilizing the model organism *Drosophila melanogaster*. Metabolic imbalances cause pathological condition in the intestine. I choose high fat dieting as this very obvious type of metabolic imbalance. In this context I studied the effects of high fat feeding and the response of the intestinal epithelial layer. A major aim was to monitor the response of the intestine to these conditions. More precisely is to evaluate the responses of different cell types to this insult and to identify the underlying mechanisms as well as to elucidate the role of indigenous microbiota in this response.

Materials and Methods

2.1 Material

2.1.1 Devices

All listed necessary materials and use of different methods in lab for to study the effect of high fat diet on gut epithelium and its consequences.

Table 1: Name and source of laboratory devices

Heraeus Fresco 17 Centrifuge	Osterode, Germany
Heraeus Fresco 17 Centrifuge	Osterode, Germany
Unitek HB 130 thermo plate	scientific plastic, Great Britain.
Ika Vortex Genius 3	Staufen, Germany
Sensoquest Lab cycler	Goettingen Germany
Thermo Electric Corporation Incubator	Goettingen, Germany
Hybrid mini-oven, Biometra,	Goettingen, Germany
Molecular Imager, Bio-Rad	Munich, Germany
Microscope SZX12 + camera DP 71, Olympus,	Hamburg, Germany
My Cycler thermal cycler, Bio-Rad,	Munich, Germany
NanoDrop ND-1000 Spectrophotometer, Peqlab	Erlangen, Germany
Microwave	AFK,Hamburg Germany
Magna Rack	Invitrogen, Karlsruhe, Germany
Incubator	Thermo electron Cooperation, Germany
Thermo cycler Robocycler 96	Stratagene, Heidelberg, Germany
Blotting Paper	A.Hartenstein GmbH, Germany
Cover slips (24×40mm)	Roth, Karlsruhe, Germany
Vial Stoppers	Greiner Bio-One, Germany
Microscope slides	Roth,Karlsruhe, Germany
Cell Filter 30µm	Miltenyi Biotec, Germany
Dynabeads MyOne Streptavidin T1	Invitrogen, Oslo, Norway
Plastic Vials 22ml, 68ml, 178ml	Greiner Bio-One, Germany
Water bath (thermostat 2761)	Eppendorf, Hamburg, Germany
Thermo mixer HTMR-2-133, Haep laboratory Consult (HLC),	Bovenden, Germany

Micro centrifuge	Thermo Electron Corporation Dreieich, Germany

2.1.2 Microscopy

Table 2: Microscope

Stereo light microscope	WILD M3, Heerbrugg Germany
Stereo light microscope SMZ 745T	Nikon, Toyko, Japan.
Stereo microscope SZX12 with U-CMAD3 camera	Olympus GmbH,Hamburg
Inverted microscope Axiovert S 100	Zeiss, Oberkochen Germany.
Flourescence microscope Imager.Z1 with Apotome and AxioCam Mrmcamera also HXP 120 lamp	Zeiss Oberkochen Germany.

2.1.3 Chemicals

Table 3: Name and source of chemicals

Agar	Carl Roth, Karlsruhe, Germany
Agarose	Biozym, Oldendorf, Germany
Alexa Fluor (555/647) Molecular Probes	Invitrogen, Karlsruhe,Germany
Aminoallyl-UTP	Ambion, Applied Biosystems, Darmstadt, Germany
Boric acid	Carl Roth, Karlsruhe, Germany
Chloroform	AppliChem Darmstad, Germany
DIG Easy Hyb	Roche Diagnostics GmbH, Mannheim, Germany
DSS Dextrin sulfate sodium salt	MP Biomedicals , Ohio USA
DMSO	Sigma, Steinheim, Germany
dNTPs	Invitrogen, Karlsruhe, Germany
Dopamine HCl	Sigma Steinheim, Germany
EDTA disodium salt	AppliChem, Darmstadt, Germany
Ethanol	Carl Roth, Karlsruhe, Germany

Ethidium bromide	AppliChem, Darmstadt, Germany
Copper Chloride	Merck, Darmstadt, Germany
Glycerol	Carl Roth, Karlsruhe, Germany
Glucose	Carl Roth, Karlsruhe, Germany
Isopropanol	Merck, Darmstadt, Germany
Methyl-4-hydroxybenzoate	Sigma, Steinheim, Germany
Sodium citrate	Carl Roth, Karlsruhe, Germany
Sodium chloride	Carl Roth, Karlsruhe, Germany
Sodium acetate trihydrate	AppliChem, Darmstadt, Germany
Palm Fat	Palmin, Germany
Peptones	Becton Dickinson GmbH, Heidelberg, Germany
Phenol red	Sigma-Aldrich, Germany
RNAmagic	Bio budget, Krefeld, Germany
Sucrose	Carl Roth, Karlsruhe, Germany
Propionic acid	Sigma, Steinheim, Germany
Tris HCl	Carl Roth, Karlsruhe, Germany
Schneider's medium	Genaxxon eBioscien GmbH, Germany.
Fetal Bovine Serum	Biochrom, AG Berlin, Germany
LB agar medium	Invitrogen, Karlsruhe, Germany

2.1.4 Antibiotics

Table 4: Name and source of antibiotics and antifungal

Penicillin/Streptomycin	Biochrom, AG Berlin, Germany
Gentamycine sulfate	Biochrom, AG Berlin, Germany
Kenamycin sulphate	Sigma, Steinheim, Germany
Streptomycin sulphate	Sigma, Steinheim, Germany
Chloramphenicol	AppliChem GmbH, Darmstadt, Germany.
Tetracycline	Sigma, Steinheim, Germany
Amphoyericine B	Invitrogen, Karlsruhe, Germany

2.1.5 Reagent systems

Table 5: Name and source of reagents

Sure clean kit	Bio line GmbH, Luckenwalde, Germany.
MEGA script T7 Ambion	Applied Bio systems, Darmstadt, Germany.
NucleoSpin RNA II,	Macherey Nagel, Duren, Germany.
DNA isolation kit, Power Soil	Mo Bio Laboratories Ltd, Carlsbad, USA.
Super script ll	Invitrogen, Karlsruhe, Germany

2.1.6 Enzymes

Table 6: Name and source of enzymes

RiboLockTM ribonuclease inhibitor	Fermentas, GmbH, St. Leon-Rot
Prime Script reverse transcriptase	Takara Bio Europe/SAS, Saint-Germain-en-Laye, France.
LaTaq DNA polymerase	Invitrogen, Karlsruhe, Germany
Taq DNA polymerase	Fermantas, ST. Leon-Rot, Germany
Pwo DNA polymerase	Peqlab Biotech, Erlangen, Germany

2.1.7 Oligonucleotides

Table 7: Name and source of oligonucleotides

All oligonucleotides listed below were supplied by Invitrogen, Karlsruhe, Germany

Dm-RPL32, CG7939 F	5′-CCGCTTCAAGGGACAGTATC -3′
Dm-RPL32, CG7993 R	5′-GACAATCTCCTTGCGCTTCT-3′
Dm unpaired III F CG 5963	5′-GAGAACACCTGCAATCTGAA-3′
Dm unpaired III R CG 5963	3′-AGAGTCTTGGTGCTCACTGT-5′
Biot-ODT-T7	5'-GAG AGA GGA TCC AAG TAC TAA TAC GAC TCA CTA TAG G-3’

II	
SP6 adapter-PCR	5'-GAC GCC TGC AGG CGA TGA ATT TAG G-3’
OdTT7 I	5'-GAG AGA GGA TCC AAG TAC TAA TAC GAC TCA CTA TAG GGA GAT TTT TTT TTT TTT TTT TTT TTT TTT-3 '
CF SP6rG1	5'-CAG CGG CCG CAG ATT TAG GTG ACA CTA TAG GTG ACA CTA TAG-3’
V2 F	5′-AGAGTTTGAGCCTGGCTCAG-3′
V2 R	3′-TGCTGCCTCCCGTAGGAGT-5′
BskCG5680F	5′-GAGAGGATCCACTAGTGGTCGGAGTACTGTCCTCC-3′
Bsk CG5680 R	3′GAGATCTAGAACGCGTGCTAGCGCGGCCGCAAGATCTGTTAACG -5′
DM-ImmrEC Stat93E F	5′-TTTTGTGAAACGCCAAAACA-3′
DM-ImmrEC Stat93E R	3′-TGTCACAGACGAACACGTCA-5′
Dm domless CG 14226 F	5′-CGGCACGTCCTCTAAGATAC-3′
Dm domless CG 14226 R	3′-ATATGCGGCTGAAGATGAGT-5′
1086-12SBI F	5′-AAGAGCGACGGGCGATGTGT-3′
1086-12SBI R	3′-AAACTAGGATTAGATACCCTATTAT-5′

2.1.8 Buffers and stock solutions

Table 8: Name and stock solutions

10x TBE	108g Tris, 55 g boric acid and 40 ml of 0.5 M Na 2 EDTA (pH 8), lL and with ddH2O
10x PBS	80g NaCl, 2g KCl, 26.8 g Na2HPO4-7H2O and 2.4 g KH2PO4 add 1L with ddH2O pH adjusted to 7.4 with HCl, autoclaved
20x SSC	175.3 g NaCl and 88.2 g sodium citrate ad 1L with ddH 2 O, pH adjusted to 7 with HCl, autoclaved.
1%Sucerose	1g sucrose diluted in 99 ml ddH2O.

10%Glucose	10g glucose diluted in 90 ml ddH20.
HL3	Hemolymph-like 3-Saline (HL3): 70 mM NaCl, 5 mM KCl, 1.5 mM CaCl 2.2H 20, 20 mM MgCl 2.H 20, 10mM NaHCO3, 5mM Trehalose, 115mM Sucrose, 5mM HEPES(pH7.1).
PFA 4%	Paraformaldehyde (4%PFA): 4g in 100 ml of 1×PBS+0.3% Triton ×-100.

2.1.9 DNA Ladder

Table 9: Name and source of Gene Ruler

Ikb-Gene ruler	Fermentas GmbH,St, Leon-Rot
100bp Gene Ruler	Fermentas GmbH,St, Leon-Rot
50bp Gene Ruler	Fermentas GmbH,St, Leon-Rot

2.1.10 Primary Antibodies

Table 10: Name and source of primary antibodies

Rabbit α-delta	Developmental studies Hybridoma Bank.Iowa, USA.
Rabbit α-GFP	Invitrogen,Karlsruhe, Germany.
Rabbit α-Notch	Developmental studies Hybridoma Bank.Iowa USA.
Mouse α-Propero (MR1A)	Developmental studies Hybridoma Bank.Iowa, USA.
Mouse α-coracle	Developmental studies Hybridoma Bank.Iowa, USA

2.1.11 Secondary Antibodies

Table 11: Name and source of secondary antibodies

Goat α-rabbit Dylight 488	Jackson ImmunoResearch Europe Ltd, Suffolk, UK.
Goat α-mouse Dylight 549	Jackson ImmunoResearch Europe Ltd, Suffolk, UK.
Goat α-rabbit Dylight 549	Jackson ImmunoResearch Europe Ltd, Suffolk, UK.
Rat α-mouse CD8a Biotin	eBioscience, Frankfurt am Main Germany.

2.2. Fly Media

2.2.1 Fly medium

2.5 g of agar-agar, 16.75 g brewer's yeast, 16.75 g corn meal and 5 g glucose were mixed in 250 ml of cold tap water and brought to a boil under stirring. 7.5 g molasses and 7.5 g sugar syrup were added and the solution was boiled until it thickened, then autoclaved for 15 min and afterwards was cooled to approx. 60 °C in a water bath. 7.5 ml Nipagin (10% w / v) and 0.75 ml of Propionic acid (10 % v / v) were added and the medium was transferred to 68 ml culture vials.

2.2.2 High Fat medium

2.5 g of agar-agar, 16.75 g brewer's yeast, 16.75 g corn meal and 5 g glucose were mixed in 250 ml of cold tap water and brought to a boil under stirring. 7.5 g molasses and 7.5 g sugar syrup were added. Subsequently, 37.5g Palm fat was added to the medium and the solution was boiled until it thickened, then autoclaved for 15 min and afterwards was cooled to approx. 60 °C in a water bath. 7.5 ml Nipagin (10% w / v) and 0.75 ml of Propionic acid were (10 % v / v) added and the medium was transferred to 68 ml culture vials.

2.2.3 High Fat medium with Phenol red

Medium was prepared as described above (2.2.2) and supplemented with 0.5% phenol red prior to transferring to culture vials.

2.2.4 Normal medium with Phenol red

Medium was prepared as described above (2.2.1) and supplemented with 0.5% phenol red prior to transferring to culture vials.

2.2.5 Normal medium with Bromophenol blue

Medium was prepared as described above (2.2.1) and supplemented with 0.5% bromophenol blue prior to transferring to culture vials.

2.2.6 High Fat medium with Bromophenol blue

Medium was prepared as described above (2.2.2) and supplemented with 0.5% bromophenol blue prior to transferring to culture vials.

2.2.7 Normal medium with Copper chloride

Medium was prepared as described above (2.2.1) and supplemented with 1mM copper chloride prior to transferring to culture vials.

2.2.8 Apple Medium

2.5 g of agar-agar mixed with 100 ml of cold tap water and brought to boiling under magnetic stirring. Cooking proceeded for 10-15 minutes. Afterwards the medium was autoclaved for 15 minutes and to 60°C in a water bath with stirring. Subsequently, 30ml apple juice was added and the medium transferred into petri dishes.

2.2.9 LB medium

Dissolve 10 g tryptone, 5 g yeast extract, 10 g NaCl and 15gm agar in 950 ml deionized water. Adjust the pH of the medium to 7.0 using 1N NaOH and bring volume up to 1 liter. Autoclave on liquid cycle for 20 min. allow solution to cool to 55°C, and pour into petridishes and store at +4°C in the dark.

2.2.10 Flies

Fly lines

The following lines of flies were used in the experiments.

Table 12: Name, function and source of fly lines

Name	Function	Source
Intestine Copper Cell Gal4	Expresses GAL4 in Copper Cells.	DGRC Japan 113192
amon-Gal4	Drives expression in enteroendocrine cell in intestine.	Gift from C. Wegner, Marburg Germany
NP1-Gal4	Drives expression in enterocytes in intestine.	Gift from D. Ferrandon STRASBOURG, France
Su(H)GBE-Gal4	Promotor for labeling enteroblasts in the intestine	Gift from S. Hou, Boston USA.
Su(H)GBE-Gal4	Promotor for labeling enteroblasts in the intestine	Gift from S. Hou Boston USA.
Dl-Gal4	promotor for labeling stem cells in the intestine	Gift from S. Hou, Boston USA.
puckered reporter-Gal4	Expresses GAL4 in pattern of puckered gene expression.	Bloomington 6762
Drosomycin-GFP	Expression of antimicrobial peptide Drosomycin.	AG Roeder Lab
Defensin-GFP	Expression of antimicrobial peptide Defencin.	AG Roeder Lab

Drosocin-GFP	Expression of antimicrobial peptide Drosocin.	AG Roeder Lab
Attacin-GFP	Expression of antimicrobial peptide Attacin.	AG Roeder Lab
Metchnikowin-GFP	Expression of antimicrobial peptide Metchnikowin.	AG Roeder Lab
Diptericin-GFP	Expression of antimicrobial peptide Diptericin.	Lemaitre Lab Lausanne, Switzerland. Lab
2x STAT-GFP	w: 2x STAT-GFP 3rd	Gift from Erika A. Bach
10x STAT-GFP 2nd	w: 10x STAT-GFP 2nd	Gift from Erika A. Bach
10x STAT-GFP 3rd	w: 10x STAT-GFP 3rd	Gift from Erika A. Bach
10x STAT-DGFP 2nd	w: 10x STAT-DGFP 2nd	Gift from Erika A. Bach
upd3-Gal4;UAS-GFP	unpaired-3	Gift from Perrimon
GST D, Nrf2	GSTD-Gal4 UAS-GFP	Gift from Dirk Bohmann, Rochester
Wnt-ERFP	fz3-RFP/CyO	Gift from DasGupta NY University
Wt Canton S	Wild type	Bloomington *Drosophila* stock center
Wt Oregon	Wild type	Bloomington *Drosophila* stock center.
w^{1118}	Wild type	Bloomington *Drosophila* stock center 5905
UAS.GFP	Cameleon GFP 2.1	Bloomington *Drosophila* stock center 6901
UAS-basket	Expresses dominant negative bsk protein	Bloomington *Drosophila* stock center 9311
UAS-basket	Expresses dominant negative bsk protein	Bloomington *Drosophila* stock center 6409
pUAST foxo GFP	pUAST foxo-GFP St mme 2-5, 10 Localisation.	BestGene OrderNr: 3154-2
UAS-GFP	Expresses mCD8-tagged GFP under the control of 20 UAS sequences with an intron (IVS) interposed between the UAS and coding sequences, B.P.	Bloomington *Drosophila* stock center 32194
UAS-PLC-ß-mRFP	Visualization of PLC-ß activation (translocation) from the cytoplasm to the membrane	Gift from HW Lee
Dome-RNAi KK	Expresses dsRNA for RNAi of Domeless under UAS control.	VDRC 106071
Dome-RNAi DG	Expresses dsRNA for RNAi of Domeless under UAS control.	VDRC 36356
STAT92E-RNAi	Expresses dsRNA for RNAi of STAT92E under UAS control.	VDRC 106980

2.3 Methods

2.3.1 Performing crosses

Virgin females (how many) from the corresponding responder line were crossed with 6 – 8 males from the different promoter lines in conventional culture tubes. Crosses were kept for more than a week at room temperature.

Unless otherwise stated, flies were reared on a standard *Drososphila* medium at room temperature (RT, between 20°C and 23°C). Flies were transferred into new vials before emergence of F1 adults. In case of breeding, flies were maintained in a controlled incubator with a 12h/12h light/dark cycle at 29 ºC. Adult progenies were maintained at 25ºC for 5 days before subjected to different experiments.

2.3.2 Manual dissection of the midgut

Flies were placed at the center of a sylgard coated 35mm petri dish plate. Petri dishes contained ice cold HL-3 buffer. The posterior part of the fly has to be cut. The fly head was grabbed with forceps and pulled outward together with the whole intestine. It has to be secured that the whole intestine is prepared. Subsequently, the head is detached from the intestine and removed together with the crop. The midgut has to be placed into a 1.5 ml eppendorf tube containing ice cold HL-3 buffer.

2.3.3 RNA isolation

Isolation of RNA from the midgut of the *Drosophila* adult was performed manually. The extracted tissue was transferred to 1ml RNAmagic and initially frozen in liquid nitrogen. (NO REAL PHYSICAL SEPARATION?) After thawing, the samples were again frozen in liquid nitrogen. After thawing 250 µl of pure chloroform were added, vortexed and incubated for 10 min on ice in order to achieve a better phase separation. The samples were centrifuged at 4° C and 15.000g for 5min. The upper aqueous phase was then transferred into a 1.5 ml Eppendorf tube and mixed with an equal volume of isopropanol. The samples were precipitated overnight at -20 °C or for a minimum for 30 minutes. This was followed by centrifugation at 4 °C (15.000g) for about 30-60min. Subsequently, the resulting pellet was washed twice with EtOH (70%). The pellet was resuspended after drying in 5-10µl RNase-free H_2O. To verify the successful isolation 1µl of the obtained RNA was run on a 1% agarose gel.

2.3.4 cDNA synthesis

The synthesis of cDNA was performed using the Prime Script RT (0.5µl per batch = 100U). The reaction contained in a final volume of 10ul; 2µl of the first-strand buffer (Prime 5xBuffer script), 0.25µl $MnCl_2$ (40 mM), 0.25µl RiboLock^{TM}RNase inhibitor, 1µl dNTPs (10 mM), 0.5µl Cap Finder primer SP6rG1 (100pmol), 0.5µl I-ODT T7 primer (10pmol), 1µl of the corresponding RNA. The synthesis was carried out for 60min at 42 °C in an incubator. As a primer for RNA-binding, the oligo dT-T7 I (see Section 2.1.5) was used.

2.3.5 Amplification of the cDNA by PCR

To conduct further experiments with the sample, it is recommended to amplify the cDNA by PCR (polymerase chain reaction). Since the cDNA-PCR is to increase the total DNA material, LaTaq DNA polymerase was used. For the first PCR I used 1µl cDNA, 5µl La PCR buffer, 2µl dNTPs (10 mM), 1µl adapter-Sp6 PCR primer (10pmol), 1µl oligo-dT primer T7 II (10pmol) and 0.5 µl of LaTaq polymerase mixture together, filled with 50µl ddH_2O and amplified under the following conditions. Initial denaturation at 95°C for 1 min 1 cycle and then again denaturation at 95°C for 20 sec 28 cycles. Annealing is at 58°C for 20 sec 28 cycles, extension is at 72°C for 2 min 30 sec 28 cycle, elongation at 72°C for 5 min 1 cycle and finally hold on at 4°C.

2.3.6 Gel electrophoresis

By means of agarose gel electrophoresis, nucleic acids can be separated according to their size. The agarose is cooked in a fitting volume TBE buffer (1x) in the microwave oven. For separation of nucleic acids, the samples to be tested are mixed with loading buffer (6x) and placed in the pockets of the agarose gel. In the experiments described here, the agarose gel electrophoresis was used only for determining the quality of DNA and RNA. Therefore, for 1% agarose gel combined with ethidium bromide staining were used.

2.3.7 Purification of the amplified cDNA

The cleaning of the amplified cDNA was performed using the Sure clean PCR Purification Kit . Here, according to the protocol, the PCR product was transferred into an eppendorf tube and the same volume of sure clean was added and incubated for 10 minutes. Then, the sample was centrifuged at 21,000× g for 10 minutes and the supernatant discarded. Subsequently, the same volume of ethanol (70%) was added. After vortexing for 10 second and centrifugation, this step was repeated, the pellet dried and taken into 10µl of RNase free ddH_2O. The concentration and quality of cDNA was checked.

2.3.8 Reverse Transcriptase PCR (RT-PCR)

For RT-PCR 0.5µl dNTPs were mixed with 2.5 µl F101 buffer. Forward and reverse primers (0.5 µl each) and amplified cDNA in a concentration of 100ng/µl were used. After adding 25µl ddH_2O and 0.25 µl Taq-polymerase the PCR was run with the following program. Cycling parameters were as follows: Initial denaturation at 95°C for 1 min 1 cycle, denaturation at 95°C for 30 sec 28 cycles. Annealing is at 58°C for 20 sec 28 cycles, extension is at 72°C for 1 min 28 cycle, elongation at 72°C for 5 min 1 cycle and finally hold on at 4°C.

2.3.9 q-RT-PCR

Materials for q-RT PCR were treated under the UV light for 30 min. The cDNA required for each reaction was 20ng/µl and primers were used at a 1:20 dilution from a 5 µM solution. For each reaction 0.25µl ROX and 5µl Dynamo Flash Master Mix were added into each valve. Then, 10 µl HPLC-water was added, the reaction mixed and used for q-RT-PCR:

A fold change of expression of a gene was calculated according to Pfaffl (2001) that put the primer efficiencies of the both target and reference genes into consideration. The primer efficiencies were obtained by using (1:2) serial dilutions of cDNA from 50 ng to 3.125 ng. After runs of primer efficiency the corresponding program of the StepOne gives the standard

curve and the slope. Then the slope was used to calculate the efficiency with the following formula,

$E = 10 - 1/slope$

From this the relative expression ratio of the target gene to reference gene (Rpl32) was calculated as follow,

$\Delta CT = CT\ target - CT\ reference$

Where ΔCT is change of cycle threshold (CT) calculated by the StepOne program during amplification.

2.3.10 qPCR for gDNA

The gDNA required for each reaction is 20ng/µl and primers were used at a 1:20 dilution from a 5 µM solution. For each reaction 0.25µl ROX and 5µl Dynamo Flash Master Mix were added into each valve. Then, 10 µl HPLC-water was added to the reaction mix and used for q-RT-PCR. Initial denaturation at 95°C for 10 min 1 cycle and then again denaturation at 95°C for 10 second 40 cycles. Annealing is at 60°C for 20 sec 40 cycles, extension is at 72°C for 2 min 35 sec 40 cycle, melting curve at 95°C for 15 sec, melting curve 60°C + 0.3°C until 95°C.

2.3.11 qPCR analysis

The analysis of the q-RT-PCR results is used to verify the results obtained from the Microarray analyses. The analysis is based upon the mean CT values. These values are calculated with an inherent program of the StepOne. Mean values are calculated with Microsoft Excel .

2.4. Immunohistochemistery

After dissection, the gut of the fly was fixed in PFA (4% paraformaldehyde in PBS) for 30 minutes at room temperature. The fixed intestine was washed three times with PBT (0.3% triton in PBS) for 5-10 minutes each. Subsequently, the tissue was blocked with 10% NGS

(in PBT) at room temperature for 30 minutes. Then, the blocking buffer was removed and primary antibodies were added. Incubation with primary antibodies was overnight at 4°C. After removal of the primary antibodies the tissue was washed five times with PBT, they were incubated with a secondary antibody in PBT over night at 4°C or 4 hrs at RT. Washing was done six time 10 mins each with PBT. The following antibodies were used, Primary antibodies were used as described in section 2.1.10 and 2.1.11 above. Primary antibodies: Rabbit α-delta (1:100), Mouse α-prospero (1:10), Rabbit α-notch (1:10), Rabbit α-GPF (1:400), Mouse α-coracle (1:100) and secondary antibodies were: Dylight 488 conjugated Goat α-Rabbit (1:500), Dylight 549 conjugated Goat α-Mouse (1:200), Dylight 549 conjugated Goat α-Rabbit (1:500). Mounting was done in RotiMount containing DAPI for nuclei staining and glass slides and cover slips with Rapi clear. Fluorescent z-series images were acquired by Zeiss Axio Imager Z1 with Apotome. Next, images were processed with AxioVision Rel.4.8 and corrections for brightness.

2.5. Dechoroination method

Eggs were washed off from the medium using a soft brush and tap water and filtered using a fine sterile nylon gaze disc (mesh size 50µm, diameter 55mm). The gaze disc bearing the eggs was placed for 10 minutes into a beaker containing 50% sodium hypochlorite solution. Most of the eggs will float on the surface of the solution. Then, the eggs were filtered again through a second sterile gaze disc. Subsequently, the eggs were rinsed in tap water and transferred with a soft and sterile brush onto a Petri dish (diameter 55mm) with Nipagin-Agar medium.

2.6 Fat staining

2.6.1 Oil red staining

Dissected guts were fixed it with 4%PFA (Paraformaldehyde). Fixed intestines were briefly washed with running tap water for 1-10 min followed by a rinse with 60% isopropanol. Then, the intestines were stained with freshly prepared Oil Red O working solution for 15 min and rinsed again with 60% isopropanol. After washing with tap water and spreading on a glass slide they were mounted using Roti-mount (contains DAPI).

2.6.2 Nile red staining

Dissected and fixed intestines were washed with tap water 3 times and placed on glass slide together with one drop of Nile red (concentration?) and viewed under the microscope.

2.6.3 BODIPY staining

Dissected intestines were fixed with 4%PFA (paraformaldehyde) and washed with 1×PBS for 3 times. After removal of PBS 20µl BODIPY working solution and incubate for 1 h in the dark at RT. After removal of the dye and washing with 1×PBS for 3 times intestines were viewed under the microscope.

2.7. gDNA isolation for microbiota analysis

Dissected guts from the fly were placed into power bead tube and placed in the BioRupture to completely homogenized and follow the further step as below,

1. Vortex the power bead tube containing gut for complete mixing.
2. Add 60 µl Solution C1 + 20 µl Proteinase into power bead tube and short vortex.
3. Incubate the power bead tube for 2 hours at 50°C and 750 rpm shaker.
4. After incubation vortex for 10 min at high speed
5. Centrifuge the power bead tube at 10.000 x g for 30 sec at RT.
6. Carefully move the supernatant into a fresh 2 ml collecting tube.
7. Add 250 µl C2 into the 2 ml collecting tube, vortex for 5 sec and incubate for 5 min at 4°C.
8. Centrifuge the tube at 10.000 x g for 60 sec at RT.
9. Transfer only 550 µl in a fresh collecting tube.
10. Add 200 µl C3 solution into the 550 µl collecting tube, vortex shortly and incubate for 5 min at 4°C.

11. Centrifuge the tube containing 550 µl +C3 solution at10.000 x g for 60 sec at RT.
12. Transfer only 600 µl from collecting tube into a fresh collecting tube
13. Add C4 approximately 1200 µl to the 600 µl collecting tune and vortex for 5 sec.
14. Add 675 µl of the mixture into a filter tube each time.
15. Centrifuge the filter tube at 10.000 x g for 60 sec at RT.
16. Repeat step 14 & 15 until all solution being filtered through Spin Filter column.
17. To clean the filters from any contamination add 500 µl C5 solution to the Spin Filter column.
18. Centrifuge the filter column at 10.000 x g for 30 sec at RT.
19. Discharge the flow through centrifugation at 10.000 x g for 60 sec at RT.
20. Place this Spin Filter column into a fresh collecting tube.
21. Add 30 µl H_2O (sterile HPLC 65°C) on the middle of the Spin filter column and keep it for 1 min at 65 °C.
22. Centrifuge the collecting tube containing the Spin filter at10.000 x g for 30 sec at RT.
23. Dispose of Spin filter and the collecting tube containing gDNA in solution now (keep preserve at -20°C or -80°C)

2.7.1 Midgut microbiota culture

Approximately 10 guts from males and females from animals held under different conditions were homogenized in approximately 100µl HL-3 and spread on to petri dishes containing LB medium. Plates were incubated at 29º C for 24 h or 48 hours.

3.0 Results

Different diets have a great impact on our health. High fat diet (HFD) is a major reason for the epidemic development of various metabolic disorders. Manifestation of metabolic disorder in the gut may be causally associated with several chronic diseases such as IBD, IBS, insulin resistance and ultimately cancer. HFD are well-known to modulate the metabolisms of lipids and carbohydrates being a major cause of obesity. In contrast, the effects of HFD on the intestine itself, the first organ that is confronted with this nutritional intervention, much less is known. Thus, the effects of HFD on various aspects of the gut structure and physiology were studied using the fruit fly *Drosophila melanogaster* as a model.

3.1. Effect of HFD on fat deposition in enterocytes (ECs) of the midgut.

3.1.1. Visulization the fat using BODIPY staining to assess the effect of HFD in flies.

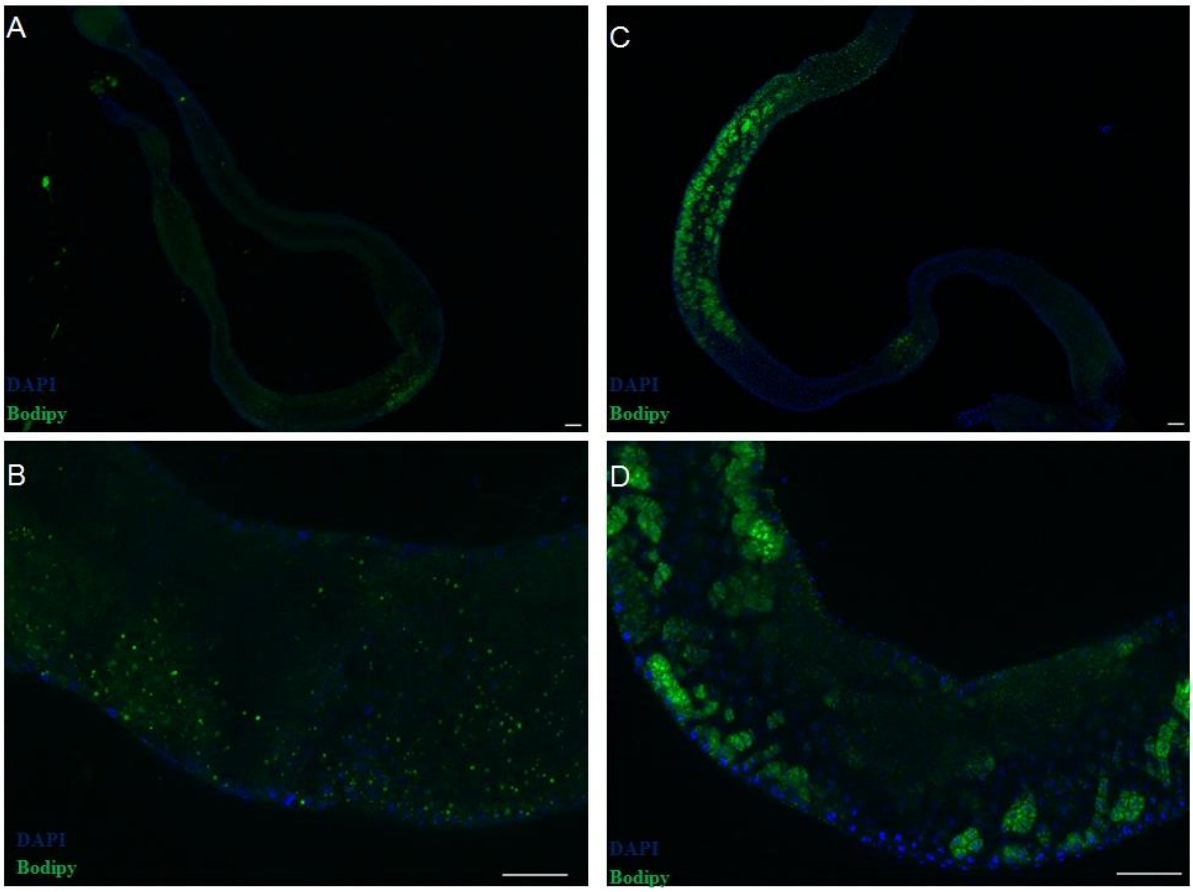

Figure 6. **A** is the overview merged picture of DAPI and bodipy staining (GFP) under control medium. **B** higher magnification of expression level of fat droplets after staining with bodipy (GFP) in the midgut under normal medium while as the **C** is the overview of merged picture of DAPI and bodipy staining (GFP) under high fat medium. **D,** higher magnification of expression level of fat droplets after staining with bodipy (GFP) in the midgut under high fat medium.

Fig. 6 and 7 shows the effects of HFD in comparison to feeding on a normal diet for the fat deposition in enterocytes. For both males (Fig. 6) and females (Fig. 7) HFD led to dramatic increases in the deposition of fat droplests in the intestine, more specifically in the enterocytes. While under normal nutritional conditioans, almost no fat droplets could be identified, the majority of enterocytes of both sexes contained a huge amount of fat droplets.

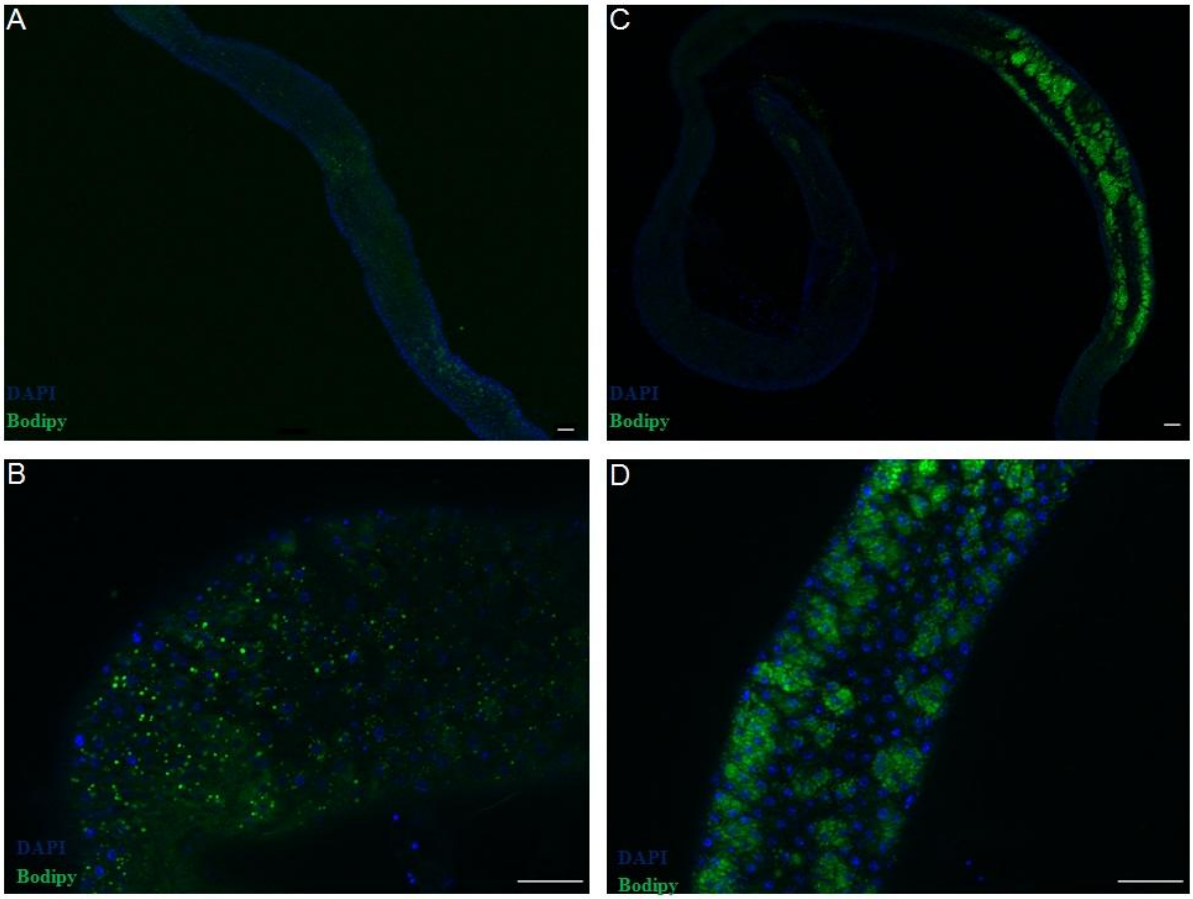

Figure 7. **A** is the overview merged picture of DAPI and bodipy staining (GFP) under control medium. **B** higher magnification of expression level of fat droplets after staining with bodipy (GFP) in the midgut under normal medium while as the **C** is the overview of merged picture of DAPI and bodipy staining (GFP) under high fat medium. **D** higher magnification of expression level of fat droplets after staining with bodipy (GFP) in the midgut under high fat medium.

3.2. Effect of HFD on the regenerative potential of the intestine

3.2.1. Using esg-Gal4 to assess the effects of HFD.

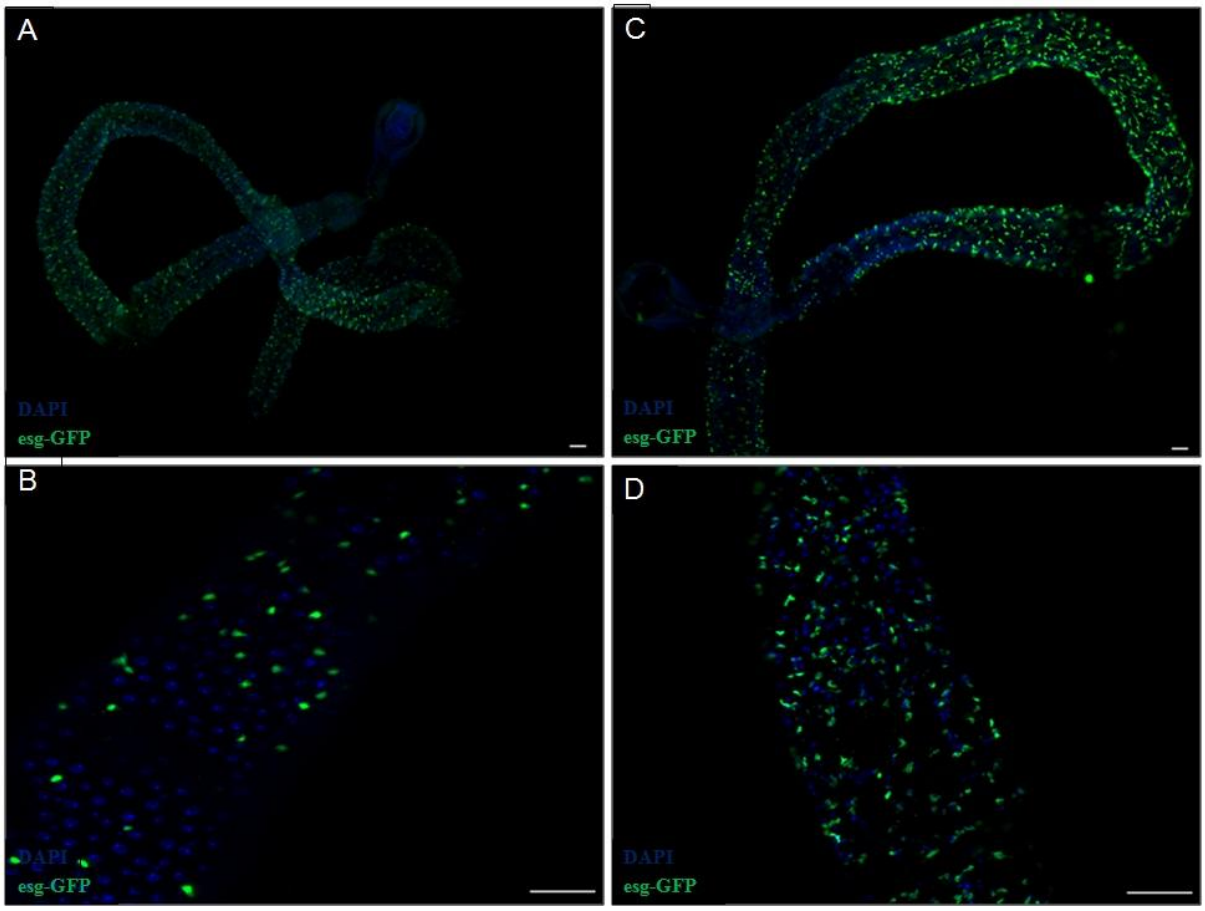

Figure 8. **A** is the overview merged picture of DAPI and anti GFP (Green) positive ISC and EBs **B** higher magnification of expression level of ISC and EBs after using anti GFP (Green) positive ISC and EBs s in the midgut under normal medium while as the **C** is the overview merged picture of DAPI and anti GFP (Green) positive ISC and EBs **D** higher magnification of expression level of ISC and EBs after using anti GFP (Green) positive ISC and EBs in the midgut under high fat medium.

The F1-generation of the cross esg-Gal4 (Rachael LS et al., 2010; Amcheslavsky A et al., 2014) X UAS-gfp labels ISCs and enteroblasts in the midgut of the fly. Challenge with HFD compared to confrontation with normal medium induced a significant increase in the number of GFP-positive cells. Figure 8 gives an overview of the entire midgut (A, B), and a close up at higher magnification (C, D). In contrast to controls, where usually single stem cells are visible, HFD induced the generation of groups of GFP-positive cells, presumably consisting of an ISC and newly produced enteroblasts.

3.2.2. Using esg-GFP labelling (ISC and EBs) to assess the effects under different conditions.

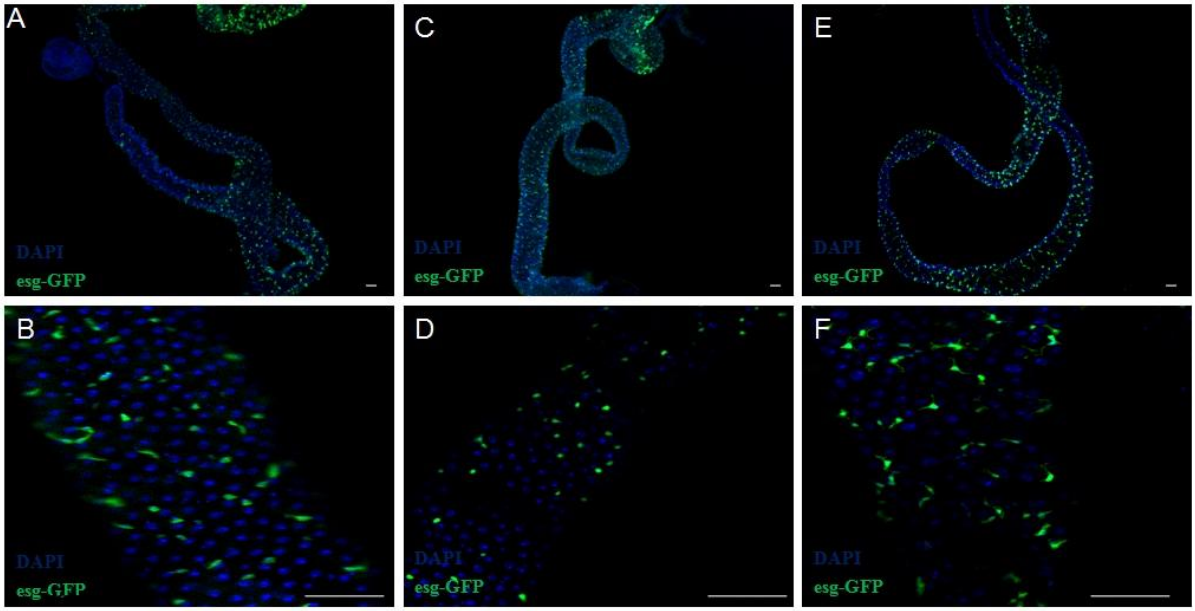

Figure 9. **A** is the overview merged picture of DAPI and anti GFP (Green) positive ISC and EBs **B** higher magnification of expression level of ISC and EBs after using anti GFP (Green) positive ISC and EBs s in the midgut under normal medium while as the **C** is the overview merged picture of DAPI and anti GFP (Green) positive ISC and EBs**. D** higher magnification of expression level of ISC and EBs after using anti GFP (Green) positive ISC and EBs in the midgut after bleaching **E** is the overview merged picture of DAPI and anti GFP (Green) positive ISC and EBs. **F** higher magnification of expression level of ISC and EBs after using anti GFP (Green) positive ISC and EBs in the midgut after bleaching and treated medium with antibiotic. Scale bar is 50 µm.

Expression level of esg-GFP positive ISCs and EBs cells in the midgut epithelium. Control flies are kept on normal medium and in comparison there is two other group design to rate the expression level of esg-GFP. In B group all the flies are bleached and F1 generation kept on normal medium while in the third group after bleaching if eggs and F1 generation kept on normal medium containing antibiotic. Observe the effect of antibiotic and effect of bleaching. The rate of expression of esg-GFP positive cell in over view of the entire midgut epithelium is almost equal. Use of anti GFP (Green) protein for esg-GFP positive cells and measuring bar is 50µM. Results prove that bleaching or antibiotic has not significant effect on the entire gut epithelium. Closer view of the midgut for the esg-GFP positive cells expression level under 3 conditions. The level of expression under control in comparison to flies after bleaching and F1 generation kept on normal medium and control in comparison the bleaching

and treated with antibiotic in the medium. By close view the expression level in the all 3 different condition express no significant different in between them. Use of anti-GFP (Green) protein for esg-GFP positive cells.

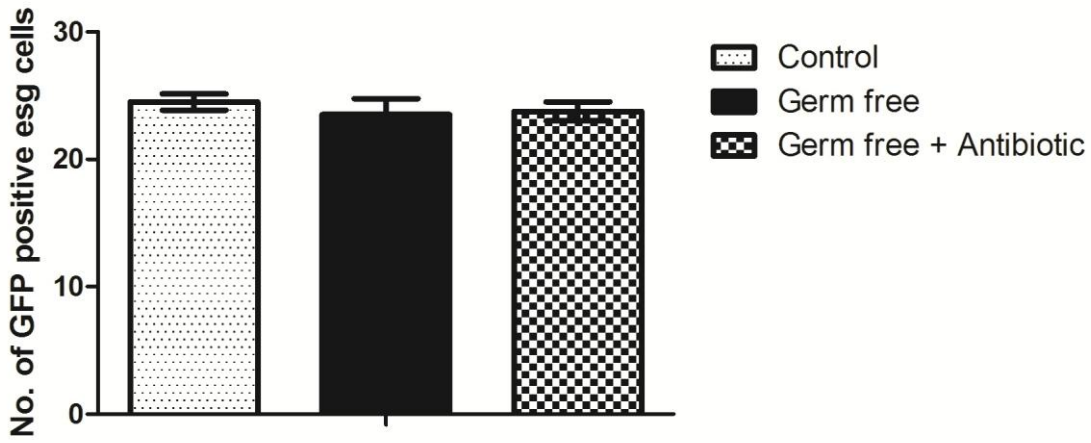

Figure 10. A counting of GFP positive cells in the midgut normal medium **B** counting the GFP positive cells after dechorionized in normal medium **C** Counting the GFP postive cells after dechorionized and kept under medium containing antibiotic.

In the following graph express the true picture of the esg-GPF positive cells rate after counting in the midgut epithelium. After 7 biological replicates the esg-GPF positive cells in the all three condition show no significant difference. Results elaborate, as the rate of expression under normal medium as compared to bleaching or after bleaching treatment with the antibiotics has no significant role to cause destruction on the gut epithelium to increase the rate of intestinal stem cell proliferation and differentiation.

3.3. Effect of HFD on ISCs number in the midgut.

3.3.1. Effect of HFD on the number of stem cells (ISCs) in the midgut

To assess if the increase in esg positive cells following HFD is due to an increase in ISCs or enteroblasts, specific driver for either cell type were analysed. Dl-Gal4 selectively labelling the ISCs were used and crossed to UAS-gfp.,

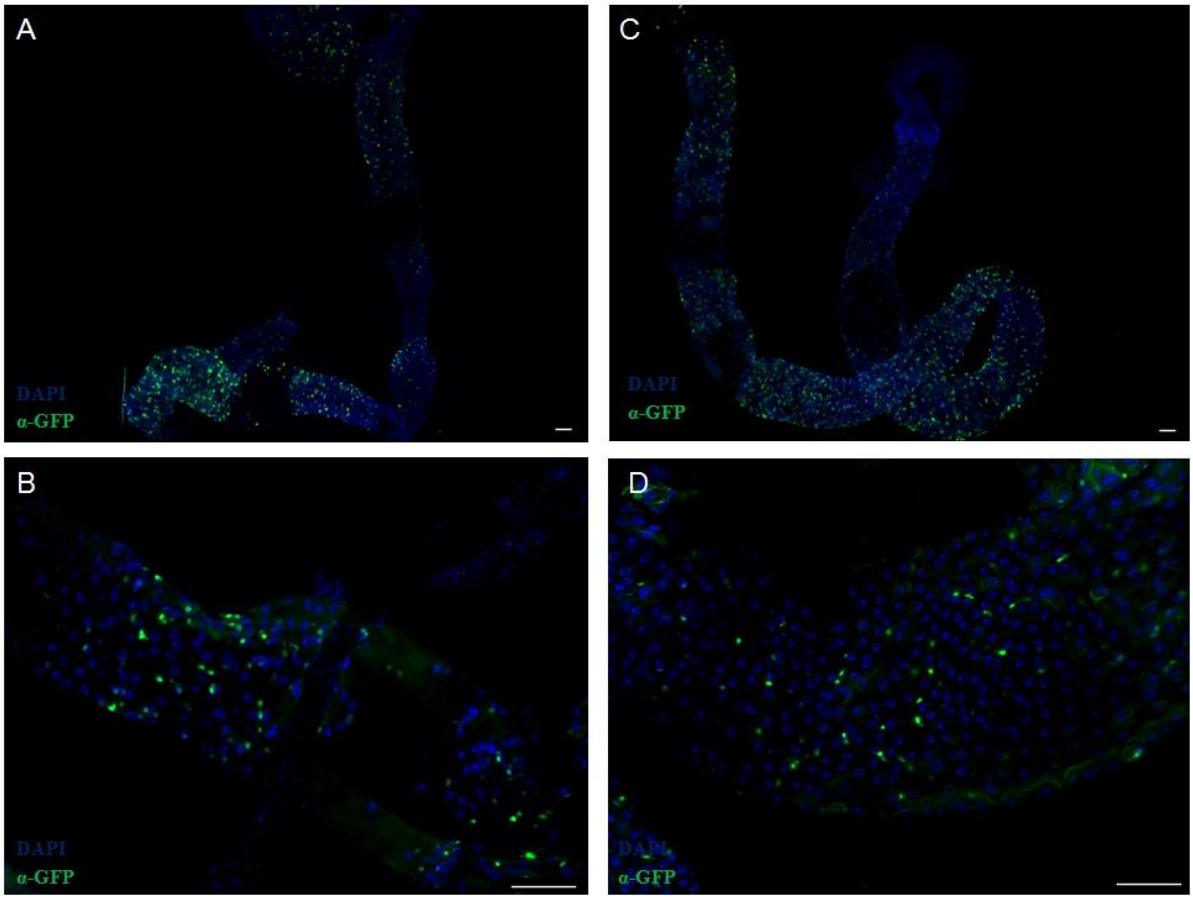

Figure 11. A Over view of the DAPI stain the nuclei and anti GFP (Green) protein against the GFP positive Delta-Gal4::UAS-GFP (labelling the ISCs) under normal medium while as, **C** Over view of the DAPI stain the nuclei and anti GFP (Green) protein against the GFP positive Delta-Gal4::UAS-GFP (labelling the ISCs) under HFD. **B and D** are the closer view of DAPI stain the nuclei and anti GFP (Green) protein against the GFP positive Delta-Gal4::UAS-GFP (labelling the ISCs) under normal and HFD respectively. Scale bar is 50µm.

Delta-Gal4 positive cells (F1 generation of the cross between delta-Gal4 (Zeng X et al., 2010) and UAS-gfp are shown in the midgut from flies held on control medium or on HFD. In A, expression of Dl-GPF positive cells in normal medium, while in B Dl-GPF positive cells following HFD are shown. Gross observation revealed very similar numbers of cells. At higher magnification, it became apparent that the number of Dl-Gal4 positive cells (ISCs) is indeed not different between both experimental groups indicating that the increase in esg-positive cells is not due to an increase in intestinal stem cell numbers.

Next, I evaluated if the increased number of esg-positive cells following HFD is due to an increased number of enteroblasts.

3.3.2. Effect of HFD on the number of enteroblasts (EBs) in the midgut

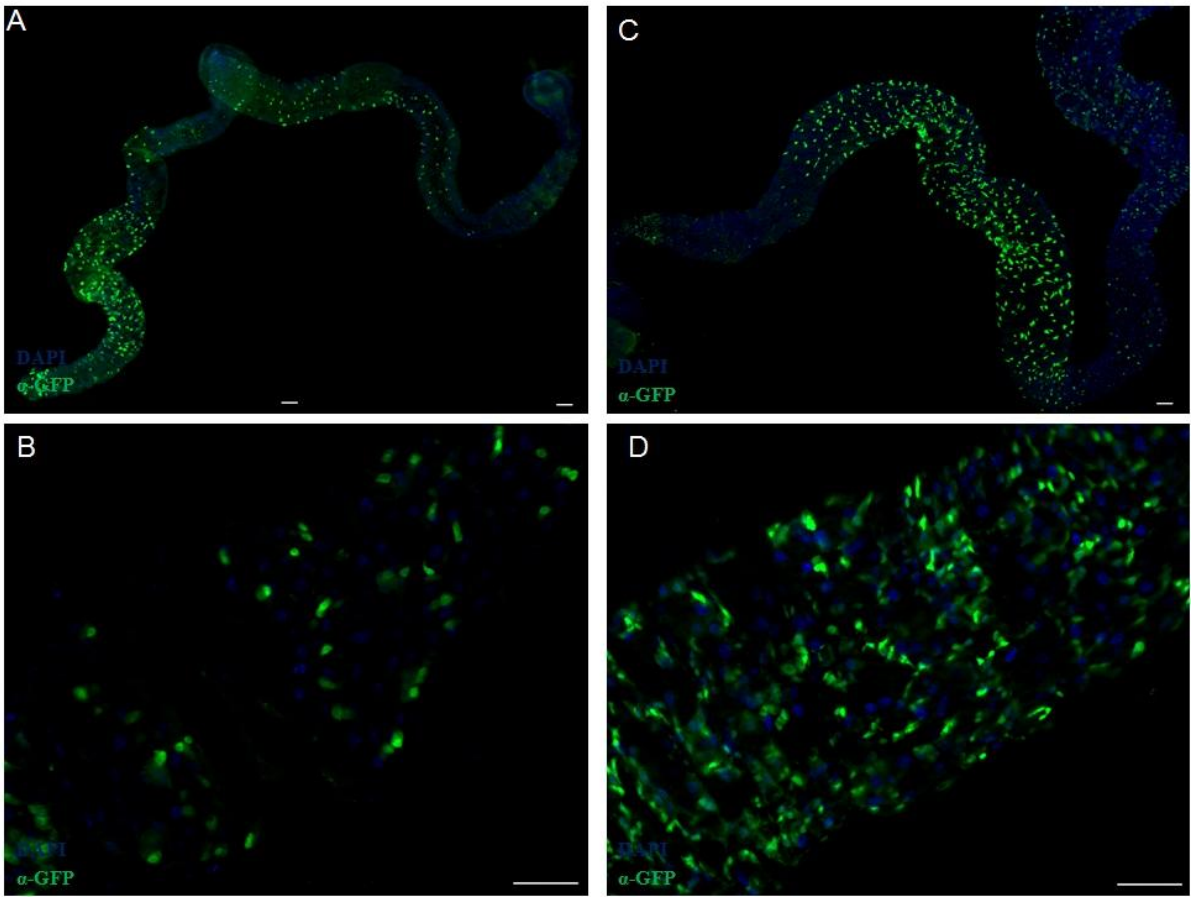

Figure 12. A Over view of the DAPI stain the nuclei and anti GFP (Green) protein against the GFP positive Su(H)GBE-Gal4::UAS-GFP (labelling the EBs) under normal medium while as, **C** Over view of the DAPI stain the nuclei and anti GFP (Green) protein against the GFP positive Su(H)GBE-Gal4::UAS-GFP (labelling the EBs) under HFD. **B and D** are the closer view of DAPI stain the nuclei and anti GFP (Green) protein against the GFP positive Su(H)GBE-Gal4::UAS-GFP (labelling the EBs) under normal and HFD respectively. Scale bar is 50µm.

To label enteroblasts specifically, the Su(H)GBE-Gal4 (Zeng X et al., 2010) was used and crossed to UAS-gfp. At low magnification, it became apparent that the number of EB-positive cells increased in response to HFD. This is seen throughout the entire intestine. At higher magnification, this difference became apparent, meaning that the number of enteroblasts (EBs) in HFD treated animals is much higher than in matching controls.

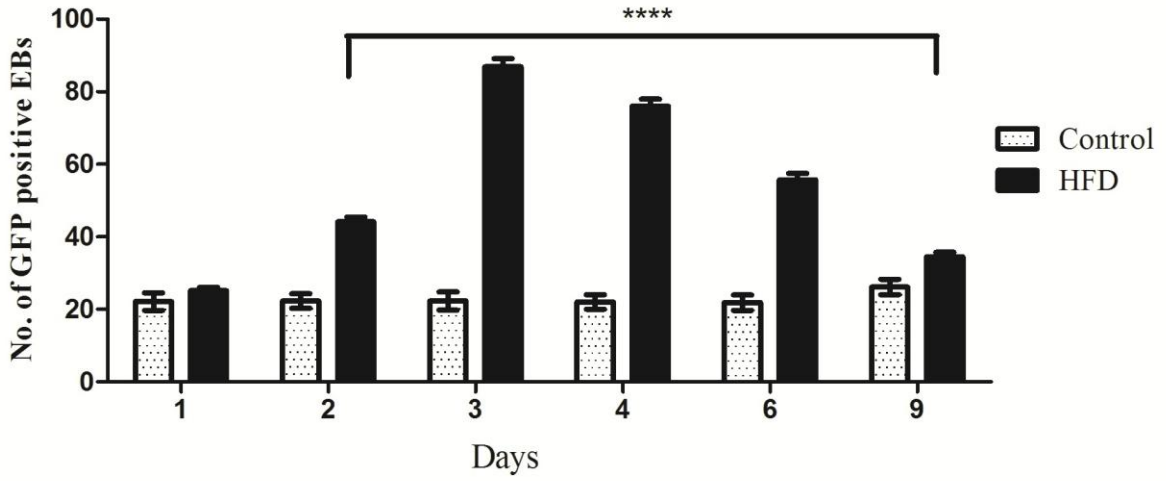

Figure 13. GPF positiveEBs cell counting on different days under normal miedium in comparison with the high fat medium.

To quantify this response and to learn more about the temporal component of this response, I counted GFP positive EBs in control treated anmimals and those subjected to HFD. As shown in the graph, the number of GFP-positive cells started to increase from the second day on HFD. The increase peaked on the 3rd day. From the 4th day onwards, the differences in numbers between HFD treated and control treated animals dropped to roughly 1.3 fold on the 9th day.

3.3.3. Effect of a short term (1d) HFD on cell proliferation in the intestine.

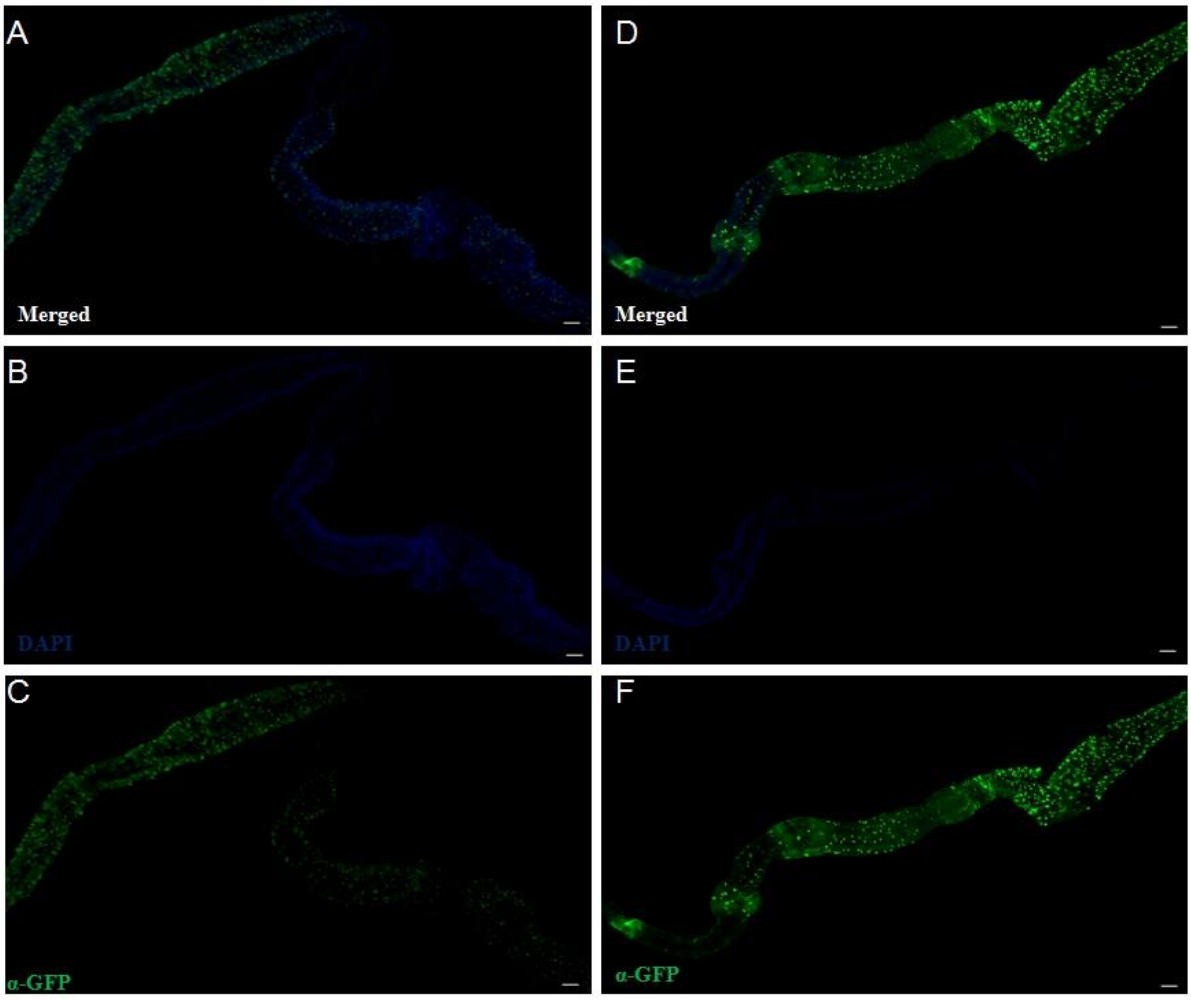

Figure 14. A Over view of the DAPI stain the nuclei and anti GFP (Green) protein against the GFP positive Su(H)GBE-Gal4::UAS-GFP (labelling the EBs) under normal medium while as, **C** Over view of the DAPI stain the nuclei and anti GFP (Green) protein against the GFP positive Su(H)GBE-Gal4::UAS-GFP (labelling the EBs) under HFD. **B and D** are the closer view of DAPI stain the nuclei and anti GFP (Green) protein against the GFP positive Su(H)GBE-Gal4::UAS-GFP (labelling the EBs) under normal and HFD respectively. Scale bar is 50µm.

Even a high fat diet for a short period (24 hours) followed by a transfer to normal medium in comparison to control medium induced an increase in the number of enteroblasts. Using the (Su(H)GBE-Gal4) driver line (Zeng X et al., 2010) crossed to UAS-gfp, this increase became apparent (Fig 14).

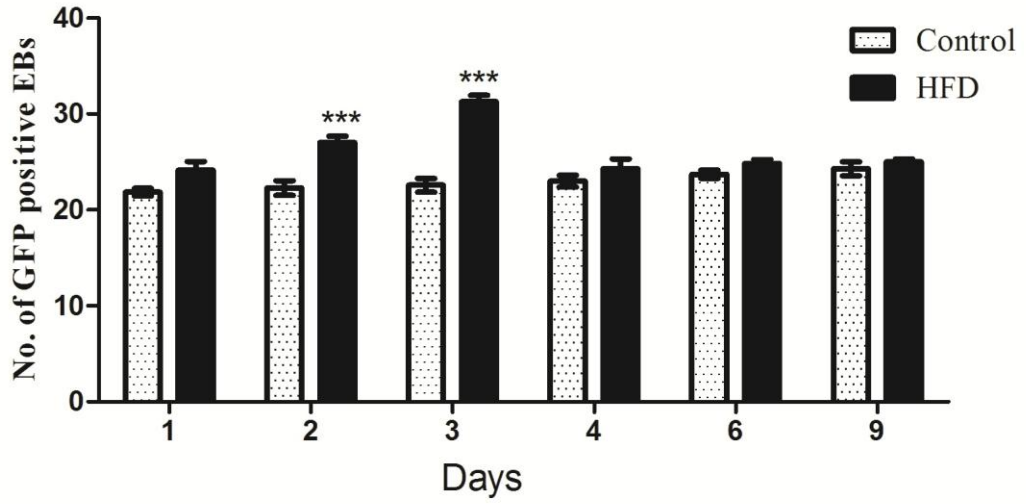

Figure 15. GPF positiveEBs cell counting on different days under normal miedium in comparison with the high fat medium.

A quantitative evaluation of the number of GFP-posistive cells revealed a similar kinetic as seen for chronic HFD. For the second and third day a significant increase compared to matching controls could be seen. From the 4th day onwards, this increase was not detectable anymore.

3.3.4. Labeling ECs (Enterocytes) in control and HFD treated animals.

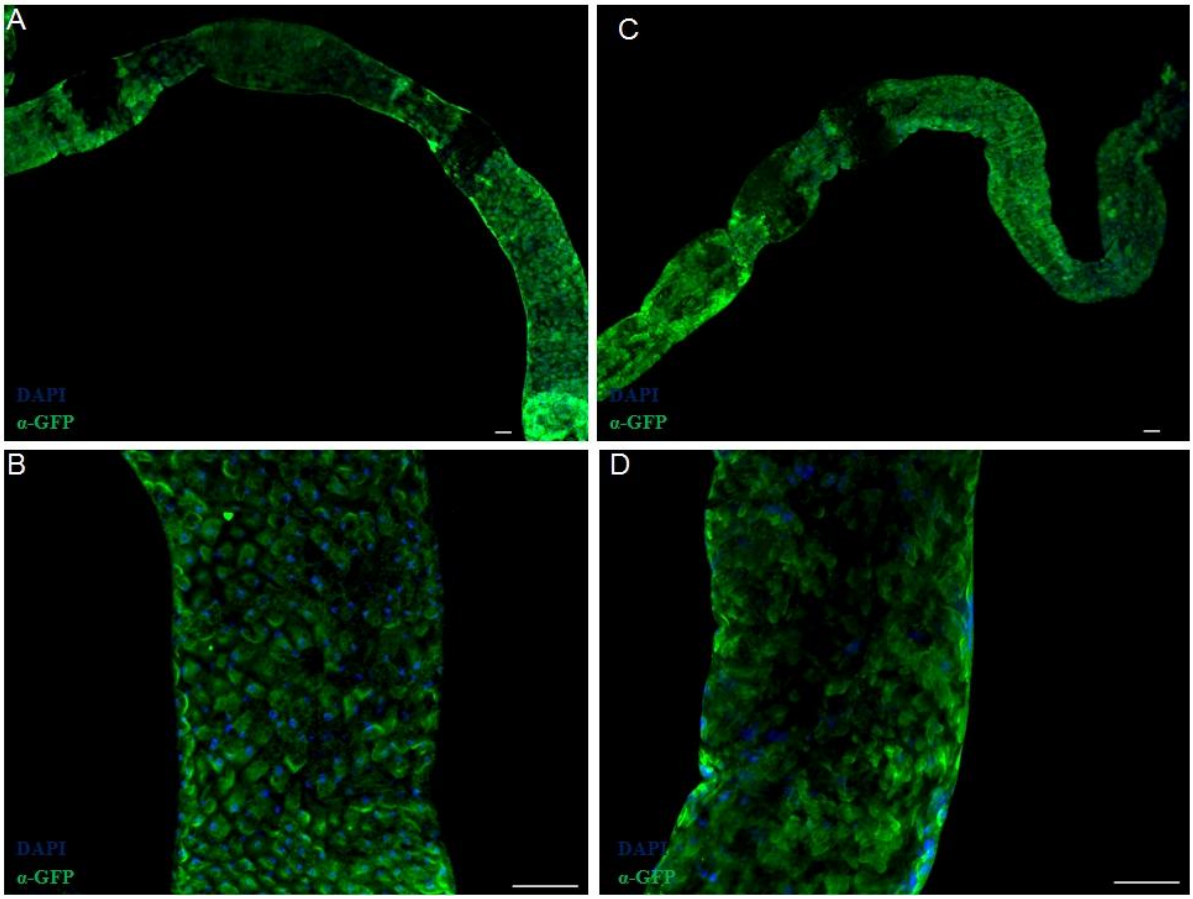

Figure 16. **A** Over view of the DAPI stain the nuclei and anti GFP (Green) protein against the GFP positive NP1-Gal4::UAS-GFP (labelling the ECs) under normal medium while as, **C** Over view of the DAPI stain the nuclei and anti GFP (Green) protein against the GFP positive NP1-Gal4::UAS-GFP (labelling the ECs) under HFD. **B and D** are the closer view of DAPI stain the nuclei and anti GFP (Green) protein against the GFP positive NP1-Gal4::UAS-GFP (labelling the ECs) under normal and HFD respectively. Scale bar is 50µm.

The use of NP1-Gal4 (Nicolson S et al., 2012) line, which specifically labels intestinal ECs (enterocytes), allowed visualizing effects of HFD on this cell population. ECs are larger in size and are equipped with larger nuclei if compared with all other classes of cells in the intestine. They occupy the majority of the intestinal epithelium (Jensen J et al., 2000). It is almost impossible to quantify if more EC are made in response to HFD as they make the vast majority of all cells in the intestinal epithelium. Although a quantification of ECs is almost

impossible, it has to be mentioned that the structure of the intestine is different following HFD, indicative for structural changes of this cell compartment.

3.3.5. Effect of HFD on the number of EEs (Enteroendocrine).

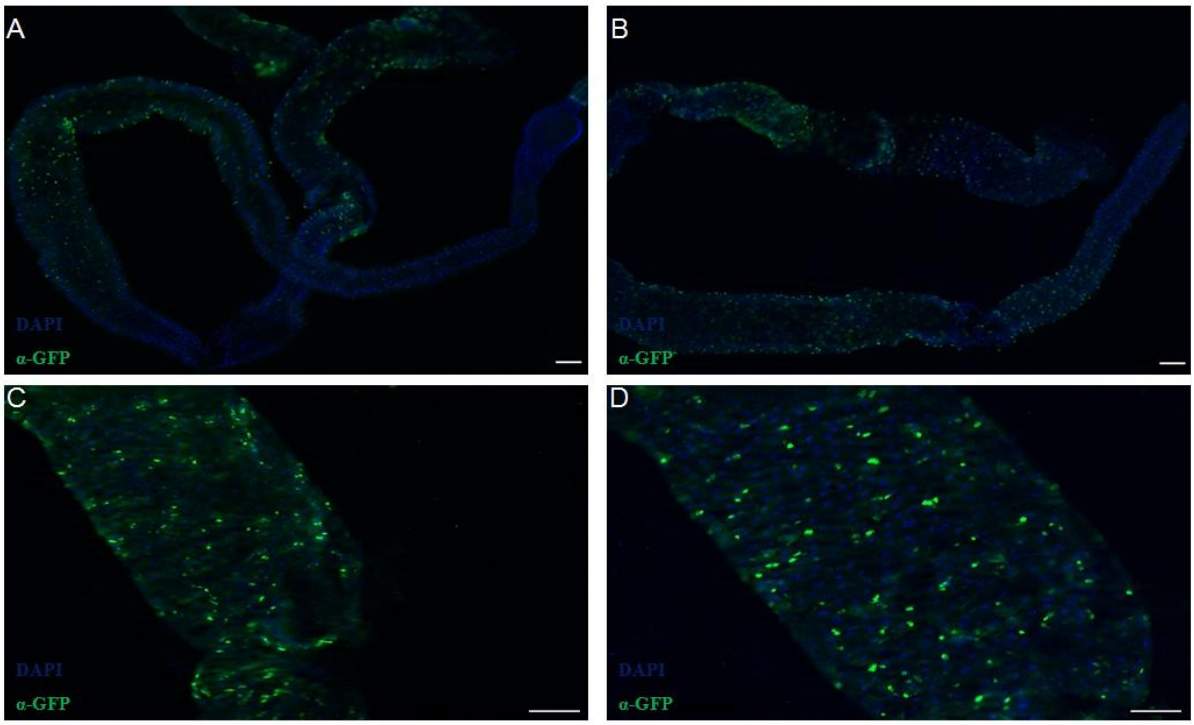

Figure 17. A Over view of the DAPI stain the nuclei and anti GFP (Green) protein against the GFP positive amon-Gal4::UAS-GFP (labelling the EEs) under normal medium while as, **B** Over view of the DAPI stain the nuclei and anti GFP (Green) protein against the GFP positive amon-Gal4::UAS-GFP (labelling the EEs) under HFD. **C and D** are the closer view of DAPI stain the nuclei and anti GFP (Green) protein against the GFP positive amon-Gal4: UAS-GFP (labelling the EEs) under normal and HFD respectively. Scale bar is 50µm.

EEs represent only a small proportion (1%) of all intestinal cells (Schonohoff SE et al., 2004). Using the EE-specific amon-Gal4-driver (Jeanne MR et al., 2010), this cell population was unequivocally labelled. The number of EEs was higher following HFD as compared to animals held on control medium. At low magnification, it is obvious that this effect of increasing the number of EEs is not restricted to a certain region of the intestine, but seen

throughout the entire midgut. This difference becomes more visible if higher magnifications were used for analysis.

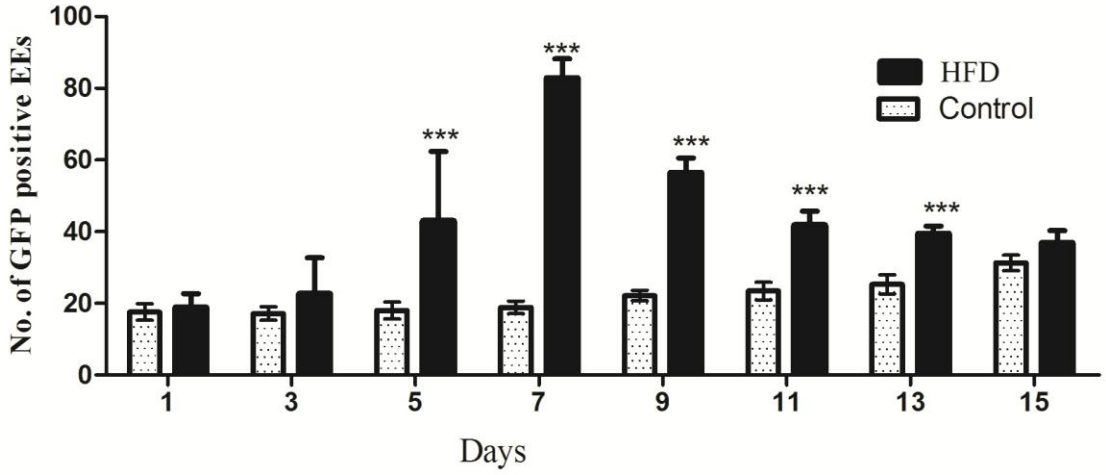

Figure 18. GPF positive EEs cell counting on different days under normal miedium in comparison with the high fat medium.

Counting the number of GFP positive EEs in the intestinal epithelium after HFD challenge revealed an increased number showing a maximal difference at day 7 with almost 4 times the number of cells if compared to matching controls. The increase was significant from day 5 onwards and even after 15 days slightly more EEs are seen if compared to matching controls.

3.3.6. Short term HFD affects the number of EECs.

The same experimental approach as outlined before was used and HFD was applied for only 24h. A quantitative evaluation of the data revealed a comparable kinetic with a much shallower increase reaching a maximal difference at day 7 with roughly 20% more EECs than the matching controls. From day 9 onwards, these differences were not detectable anymore.

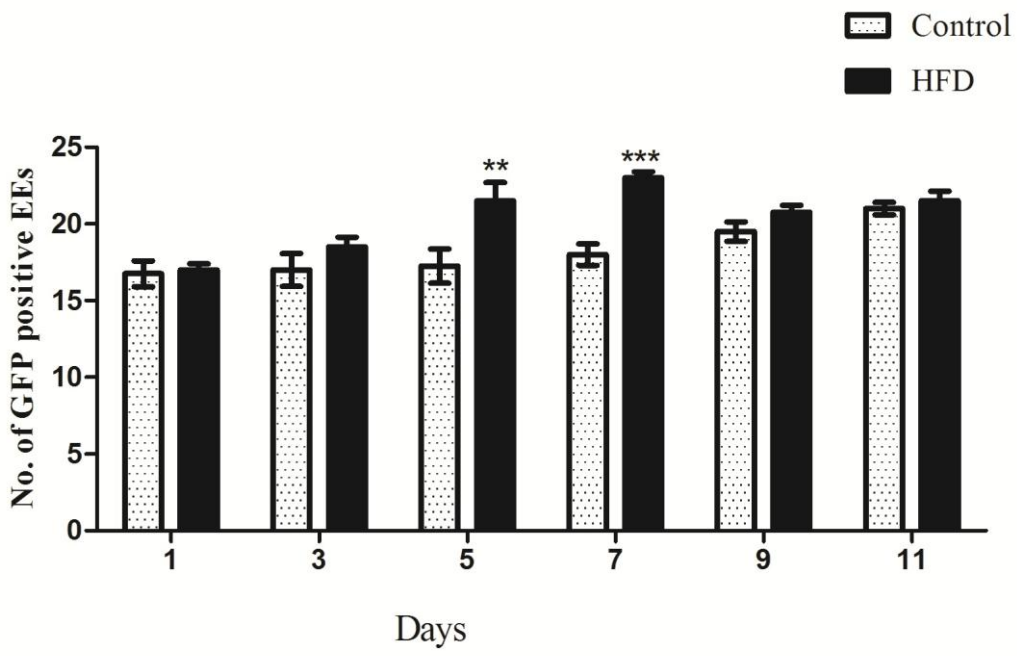

Figure 19. GPF positive EEs cell counting on different days under normal miedium in comparison with the high fat medium.

A quantitative evaluation of the number of GFP-posistive cells revealed a similar kinetic as seen for chronic HFD. For the third and fifth day a significant increase compared to matching controls could be seen. From the 7th day onwards, this increase not seen anymore. But here is significant different as expression pattern is similar but after attaining the peak there is sharp declining. This sharp declining equalizer to control on day 10.

3.4. Activation of signalling pathways in the fly's intestine following HFD

3.4.1. Using the CalexA system to monitor the effects of HFD on Ca^{2+}-signalling

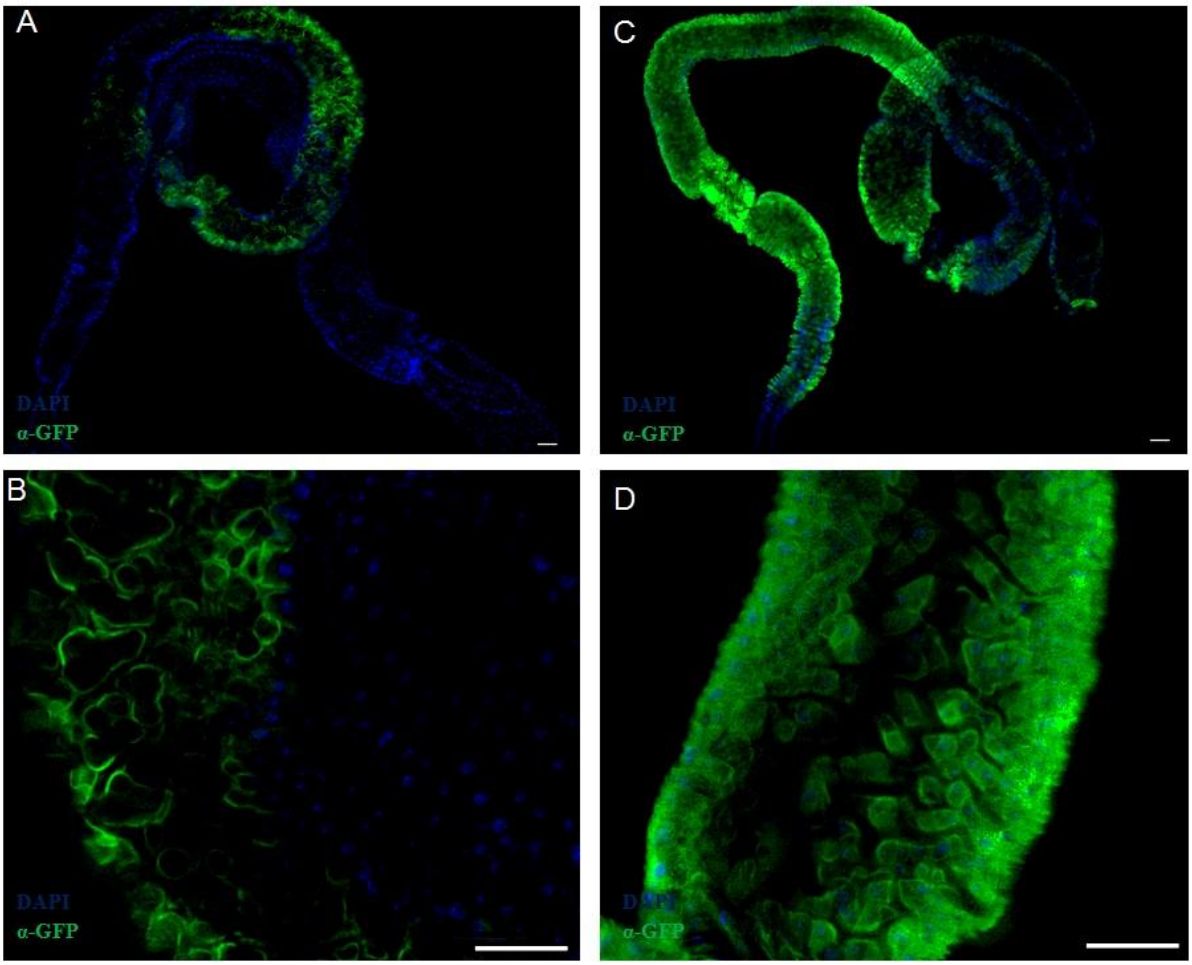

Figure 20. A is the over view where DAPI stain blue the nuclei and anti GFP (Green) protein specific for the GPF positive NP1-GAL4:: CaLexA UAS-GFP under normal medium while as, **C** over view where DAPI stain the nuclei blue and anti GFP (Green) protein specific for the GPF positive NP1-GAL4:: CaLexA UAS-GFP under HFD. **B and D** are the closer view to visualize, DAPI stain the nuclei blue and anti GFP (Green) protein specific for the GPF positive NP1-GAL4:: CaLexA UAS-GFP under normal and HFD respectively. Scale bar is 50 µm.

.CaLexA (Calcium-dependent nuclear import of LaxA) is a system that allows to monitor long-lasting increases in the Ca^{2+}-level of the corresponding cell (Masuyama K et al., 2001). Ca^{2+} signaling pathways are known to be activated via PLCβ (Phospolipase C β). The CaLexA line consists of (NFAT and LexA operator). Targeting this construct to enterocytes

only allowed to evaluate the effects of HFD on intestinal Ca^{2+}-signaling. HFD induced a strong CaLexA signal throughout the entire intestinal epithelium (Fig.20). A closer view revealed that single enterocytes express GFP, indicative for a mosaic like activation of the CaLexA system following HFD.

3.4.2. Dopamine activates $Ca2^{+}$-signalling in enterocytes

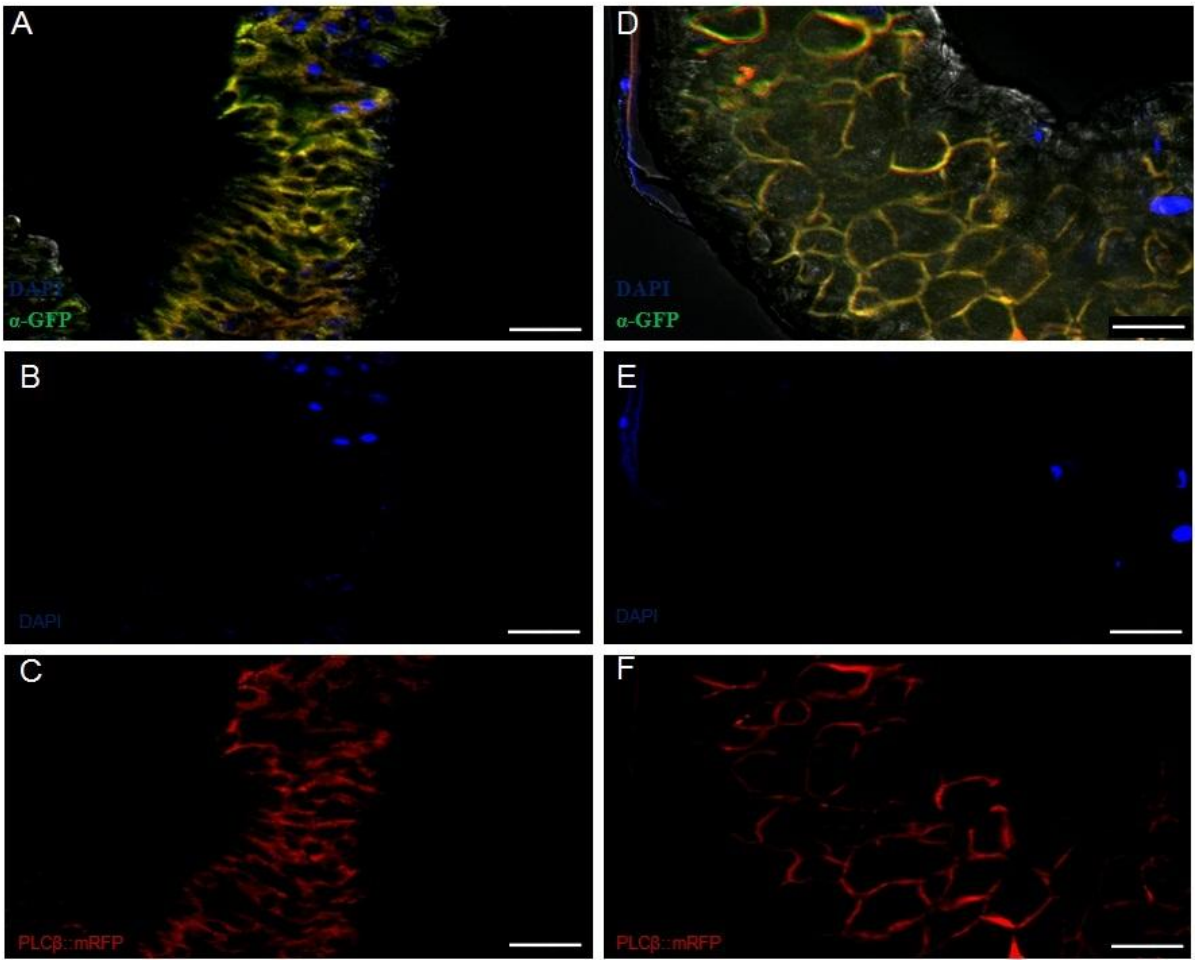

Figure 21. A, where DAPI stain the nuclei to blue and GPF and PLC-ß-mRFP (Red) under control whereas, **D** where DAPI stain the nuclei to blue and GPF and PLC-ß-mRFP (Red) under treated with dopamine. **B** and **E,** Dapi stain the nucleus to blue. **C** PLC-ß-mRFP (Red) translocation in the cytoplasm under control condition. **F** PLC-ß-mRFP (Red) translocation in the cytoplasm under dopamine treatment.

Targeting the expression of a fusion protein consisting of PLC-ß and mRFP to the enterocytes allowed to identify signals that hold the potential to induce Ca^{2+}-signalling in these(Lee SH et al 2009) cells. Translocation of PLC-ß from the cytoplasm to the cell membrane monitors

activation and subsequent Ca^{2+}-signalling. At 10^{-6} mol/l dopamine a clear translocation is unequivocally visible

3.4.3. Involvement of the Nrf2 pathway in the midgut under normal medium and HFD.

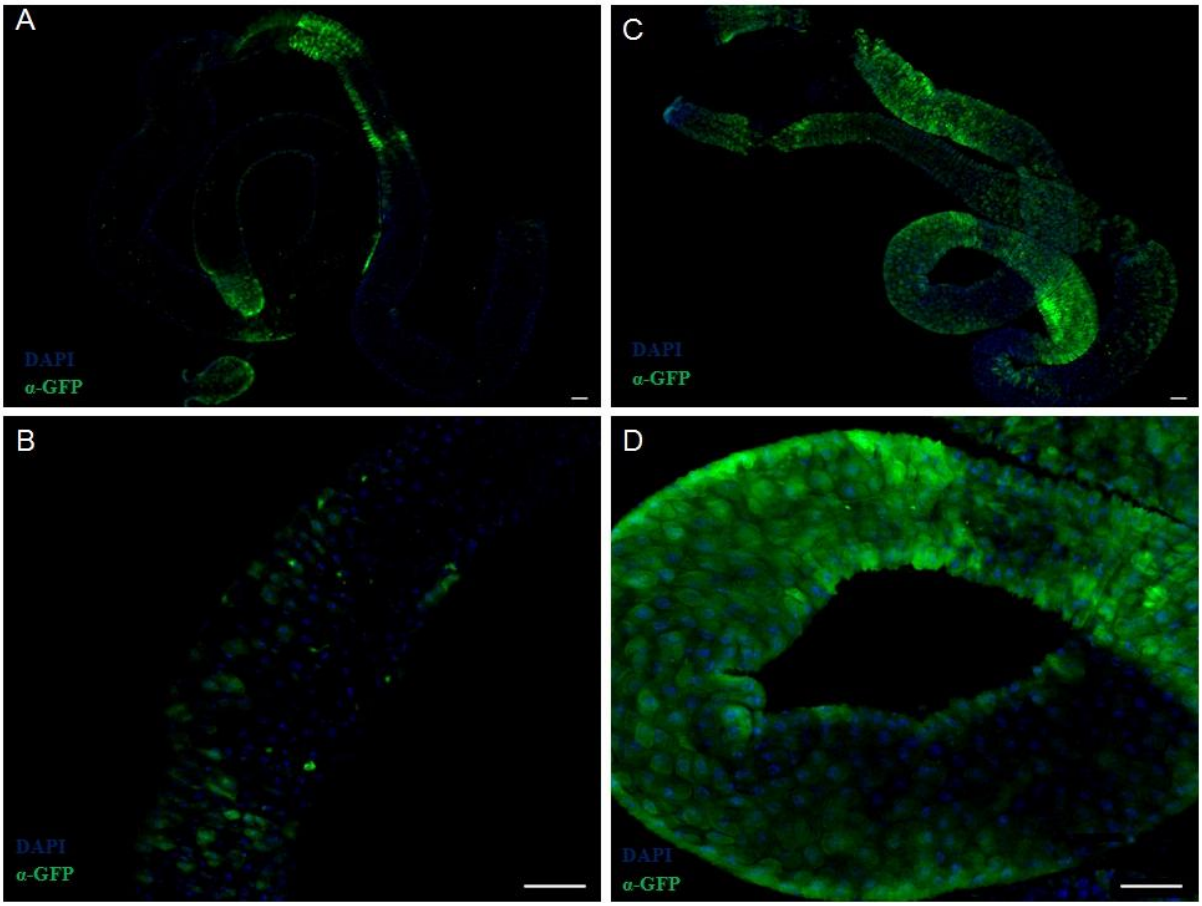

Figure 22. A is the over view where DAPI stain blue the nuclei and anti GFP (Green) protein specific for the GPF positive GSTD-GAL4::UAS-GFP under normal medium while as, **C** over view where DAPI stain the nuclei blue and anti GFP (Green) protein specific for the GPF positive GSTD-GAL4::UAS-GFP under HFD. **B and D** are the closer view to visualize, DAPI stain the nuclei blue and anti GFP (Green) protein specific for the GPF positive GSTD-GAL4::UAS-GFP under normal and HFD respectively. Scale bar is 50 µm.

Nrf2 pathways activation is monitored using a GST-D reporter Gal4 (Geranimos and Bohmann, 2008) line that is typically activated following different stressors. Thus, I used the GSTD-Gal4::UAS-GFP crossing. HFD activates expression of the marker, indicative for activation of Nrf2 signalling. A closer evaluation of the expression site revealed that enterocytes in the intestinal epithelium are the cells that activate expression of the indicator.

3.4.4. JNK activation in the midgut induced by HFD

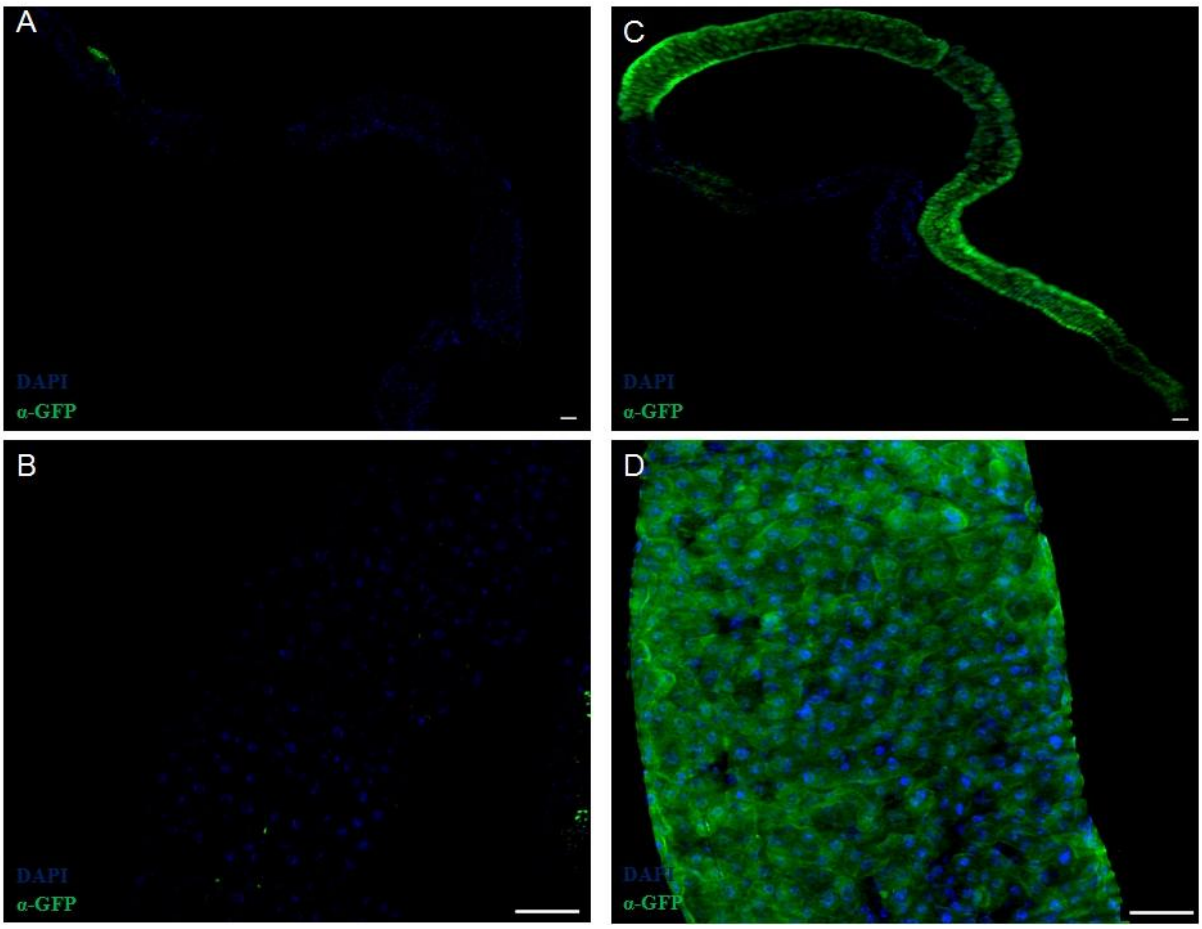

Figure 23. A is the over view where DAPI stain blue the nuclei and anti GFP (Green) protein specific for the GPF positive puckered reporter-Gal4::UAS-GFP under normal medium while as, **C** over view where DAPI stain the nuclei blue and anti GFP (Green) protein specific for the GPF positive puckered reporter-Gal4::UAS-GFP under HFD. **B and D** are the closer view to visualize, DAPI stain the nuclei blue and anti GFP (Green) protein specific for the GPF positive puckered reporter-Gal4::UAS-GFP under normal and HFD respectively. Scale bar is 50 µm.

To monitor activation of the JNK, a specific puckered reporter-Gal4 (Takashi AY, 2002) line was crossed to UAS-gfp. High fat medium obviously activates the JNK signalling pathways in the gut epithelium as compared to control medium, which is seen in (Fig 23). Under normal medium conditions, no activation of JNK signalling is visible. A closer view revealed that the response to HFD is carried by the ECs.

3.4.5. Notch-signalling pathway activation in the midgut

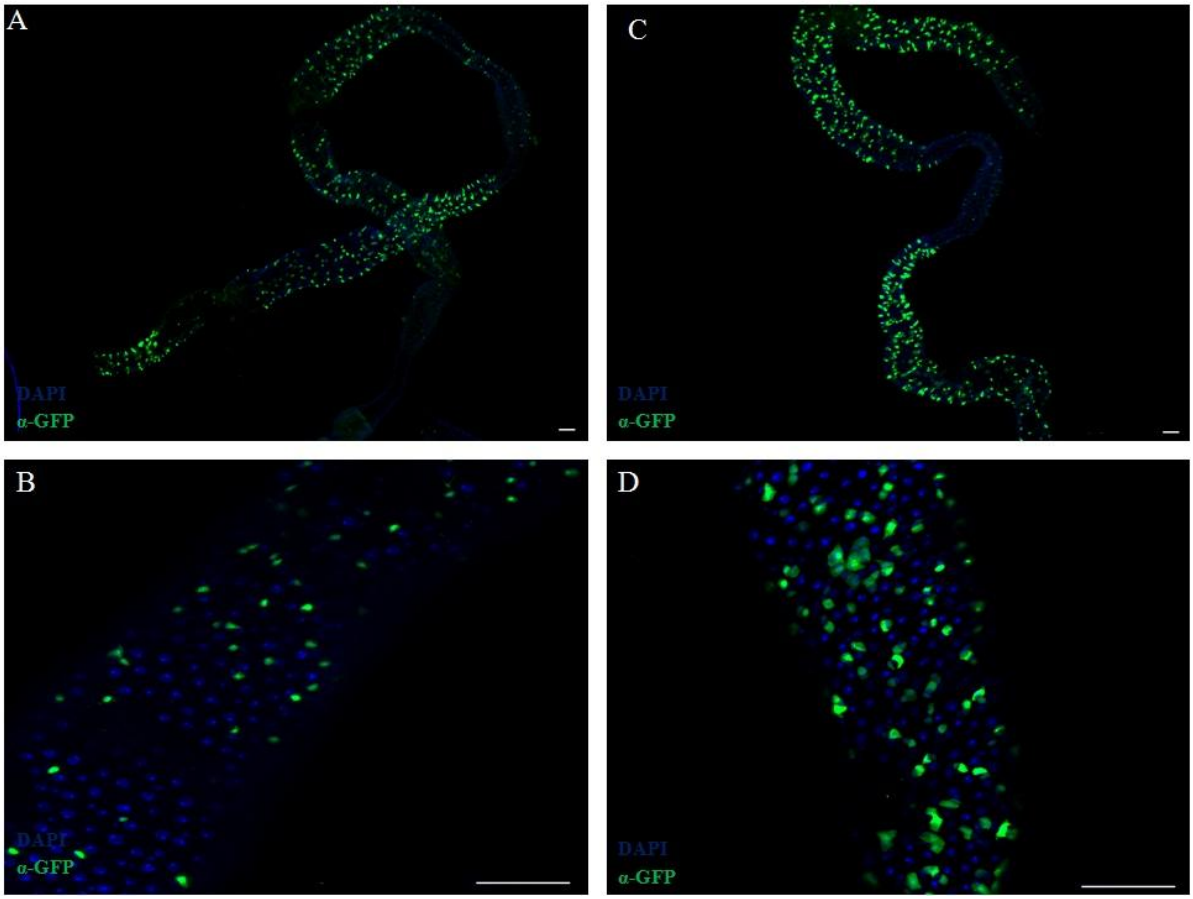

Figure 24. A is the over view where DAPI stain blue the nuclei and anti GFP (Green) protein specific for the GPF positive NRE-GAL4::UAS-GFP under normal medium while as, **C** over view where DAPI stain the nuclei blue and anti GFP (Green) protein specific for the GPF positive NRE-GAL4::UAS-GFP under HFD. **B and D** are the closer view to visualize, DAPI stain the nuclei blue and anti GFP (Green) protein specific for the GPF positive NRE-GAL4::UAS-GFP under normal and HFD respectively. Scale bar is 50 µm.

The fly line that allows monitoring of Notch-signalling contains a Notch Response Element (NRE) NRE:EGFP (Zacharioudaki and Sarah in 2014; Zeynep AS et al., 2010). GFP expression is under control of these promoter elements. Even under control conditions, a relatively high level of expression is seen in the midgut (Fig 24). HFD increased this number of cells. They are single, relatively small cells scattered throughout the entire structure.

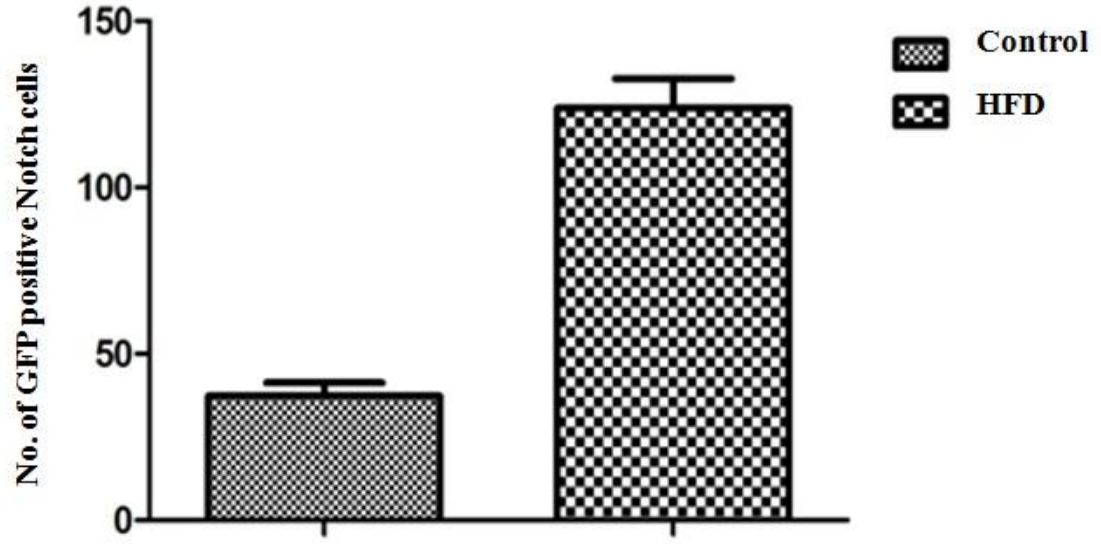

Figure 25. Number of GFP positive cells under normal medium in comparison to HFD. Expression level of GFP positive cells the Notch signalling pathways.

To quantify this response and to learn more about the temporal component of this response, I counted GFP positive cells in control anmimals and those subjected to HFD. As shown in the graph (Fig 25), the number of GFP-positive cells under HFD as compared to control is approximately 3 folds increased..

3.4.6 Expression of UPD3 in the midgut epithelium under control and high fat conditions

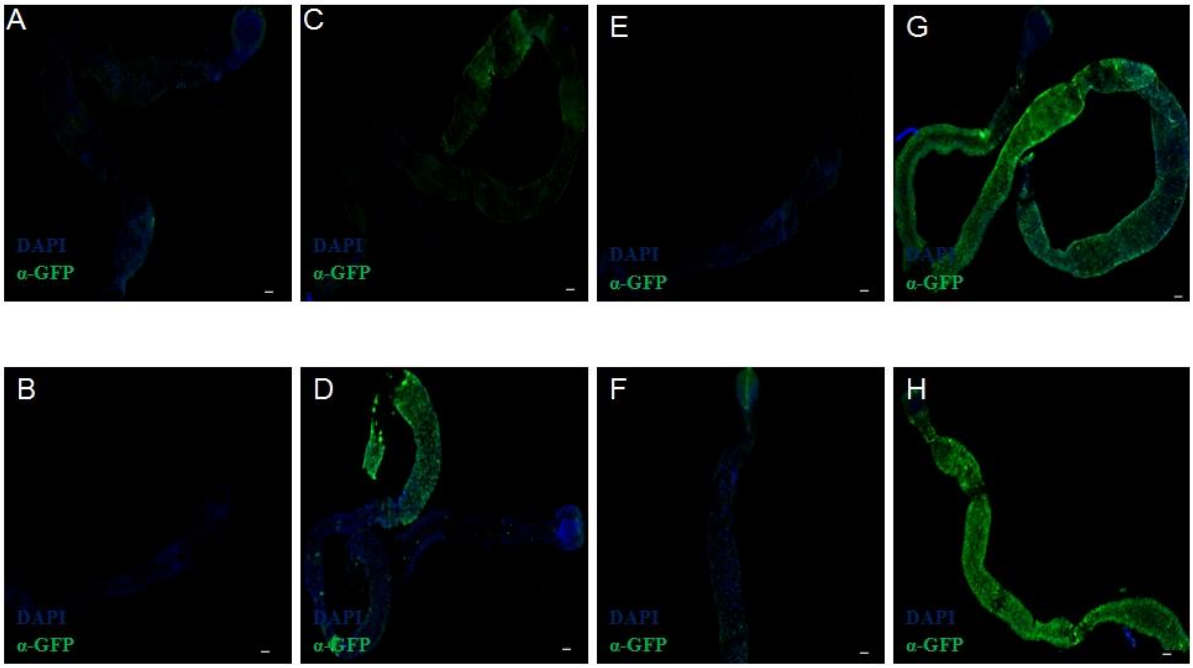

Figure 26. A, where DAPI stain the nuclei to blue and anti GFP (Green) protein bind specific to GFP positive UPD3-Gal4::UAS-GFP expressing cells under control medium after 18 hour. **B,** where DAPI stain the nuclei to blue and anti GFP (Green) protein bind specific to GFP positive UPD3-Gal4::UAS-GFP expressing cells under control medium after 18 hour after dechorionized . **C,** where DAPI stain the nuclei to blue and anti GFP (Green) protein bind specific to GFP positive UPD3-Gal4::UAS-GFP expressing cells under HFD after 18 hour. **D,** DAPI stain the nuclei to blue and anti GFP (Green) protein bind specific to GFP positive UPD3-Gal4::UAS-GFP expressing cells under HFD after 18 hour after dechorionized**. E,** DAPI stain the nuclei to blue and anti GFP (Green) protein bind specific to GFP positive UPD3-Gal4::UAS-GFP expressing cells under control medium after 48 hour. **F,** DAPI stain the nuclei to blue and anti GFP (Green) protein bind specific to GFP positive UPD3-Gal4::UAS-GFP expressing cells under control medium after 48 hour after dechorionized. **G** DAPI stain the nuclei to blue and anti GFP (Green) protein bind specific to GFP positive UPD3-Gal4::UAS-GFP expressing cells under HFD after 48 hour. **H,** DAPI stain the nuclei to blue and anti GFP (Green) protein bind specific to GFP positive UPD3-Gal4::UAS-GFP expressing cells under HFD after 48 hour after dechorionized**.** Scale bar is 50 µm.

UPD3 expression was monitored using upd3-Gal4 (Zheng G et al., 2013) reporter line. For this, the promoter upd3-Gal4 was crossed to UAS-GFP. Upd3 positive cells are present at

Low levels under control conditions, and increase dramatically following HFD. The response started after 18 hours and maximum expression level was seen after 48 hours.

3.5. Quantitative Real Time PCR

3.5.1. UPD3 gene expression level of upd3-gfp and wild type under normal and hight fat medium.

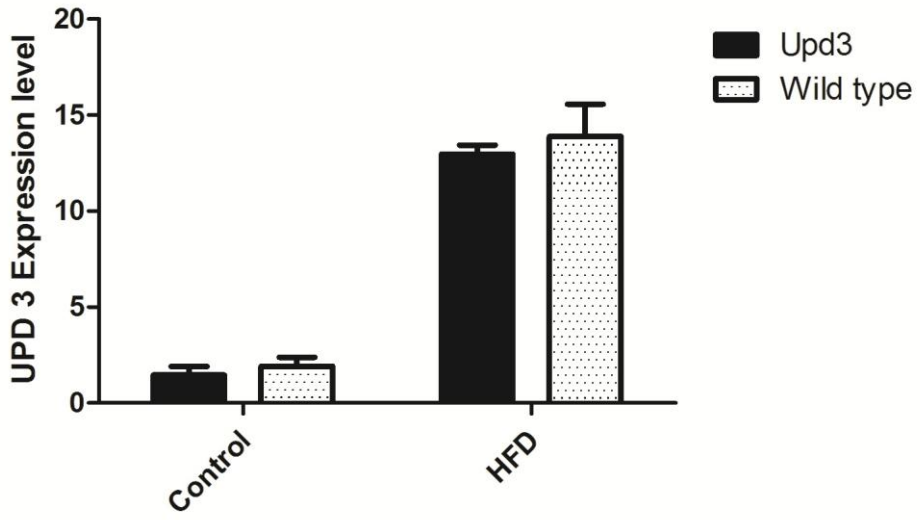

Figure 27. UPD3gene expression level in UPD3 line and in comparison with wild type under normal medium as well as high fat medium.

To quantify the effects of HFD on upd3 expression, two different *Drosophila* lines (the upd3-gfp reporter line and the matching wildtype w^{1118}) were used. For both lines, the upd3 expression was increased up to tenfold in response to HFD if manually isolated intestines were used for analyses. This increase was statitically significant in both lines. By using the both control medium and high fat medium.

3.5.2. UPD3 gene expression level of Domless RNAi and Sata92E RNAi in comparison with UPD3 line under normal and hight fat medium.

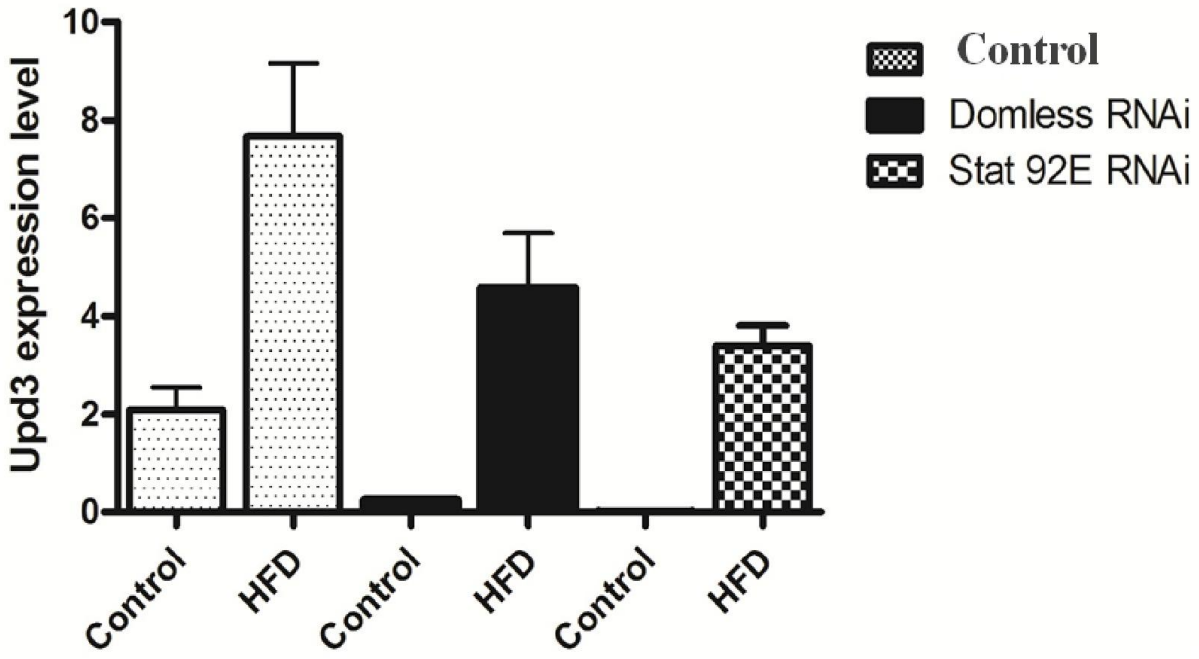

Figure 28. Expression level of UPD3 in UPD3 line ,Domless RNAi and Stat92E RNAi line under normal medium in comparison with high fat medium.

Using RNAi targeted to enterocytes by crossing the corresponding RNAi line to the NP1-driver, I studied if components of the JAK/STAT pathway are relevant for the induction of upd3 expression. Nor downregulation of domeless neiter that of STAT92e abolished the HFD induced increase in upd3 expression, indicating that the JAK/STAT pathway is not part of the upd3 induction pathway.

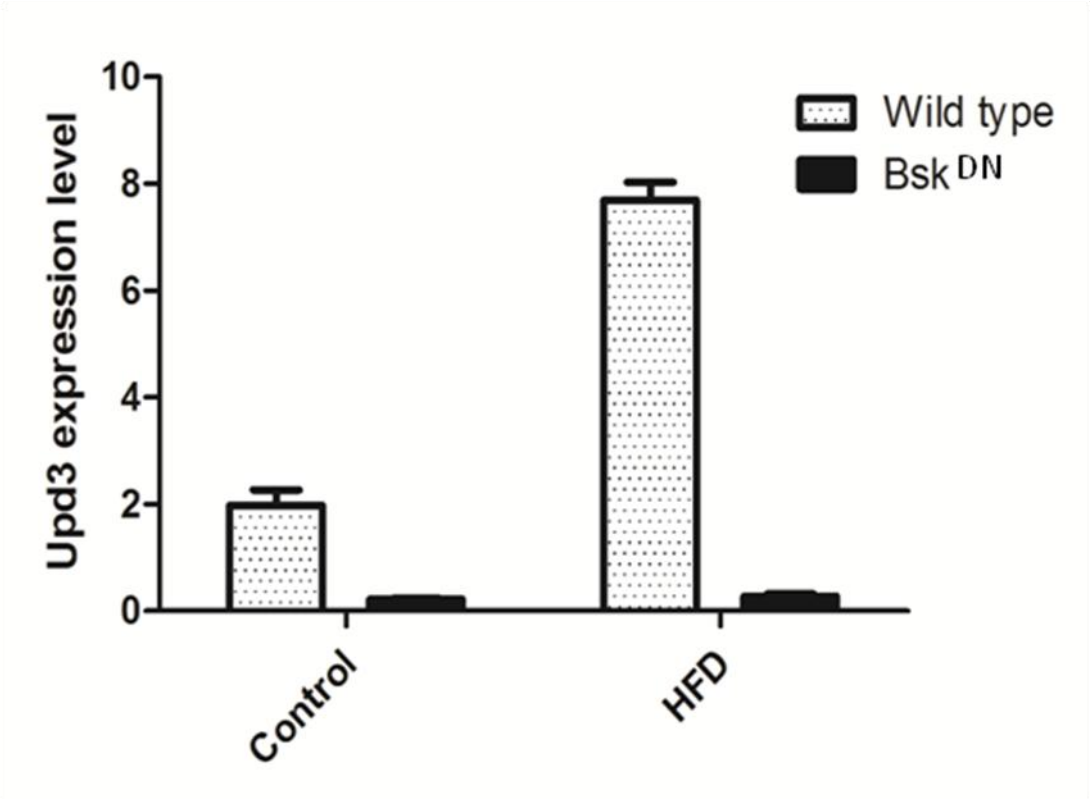

Figure 29. UPD3gene expression level in UPD3 line ,two Bsk dominant negative lines under normal medium in comparison with high fat medium.

Moreover, I tested a different pathway regarding the induction of upd3 expression. For this I used dominant negative basket lines (UAS-basket^{DN}) driven in the enterocytes. HFD induced increased upd3 expression, while in animals with a blocked JNK-pathway no difference to control levels could be observed (Fig 29). This result indicates that the JNK-pathway is essential for HFD induced increase in upd3 signalling.

3.6. Expression of antimicrobial peptides in response to HFD

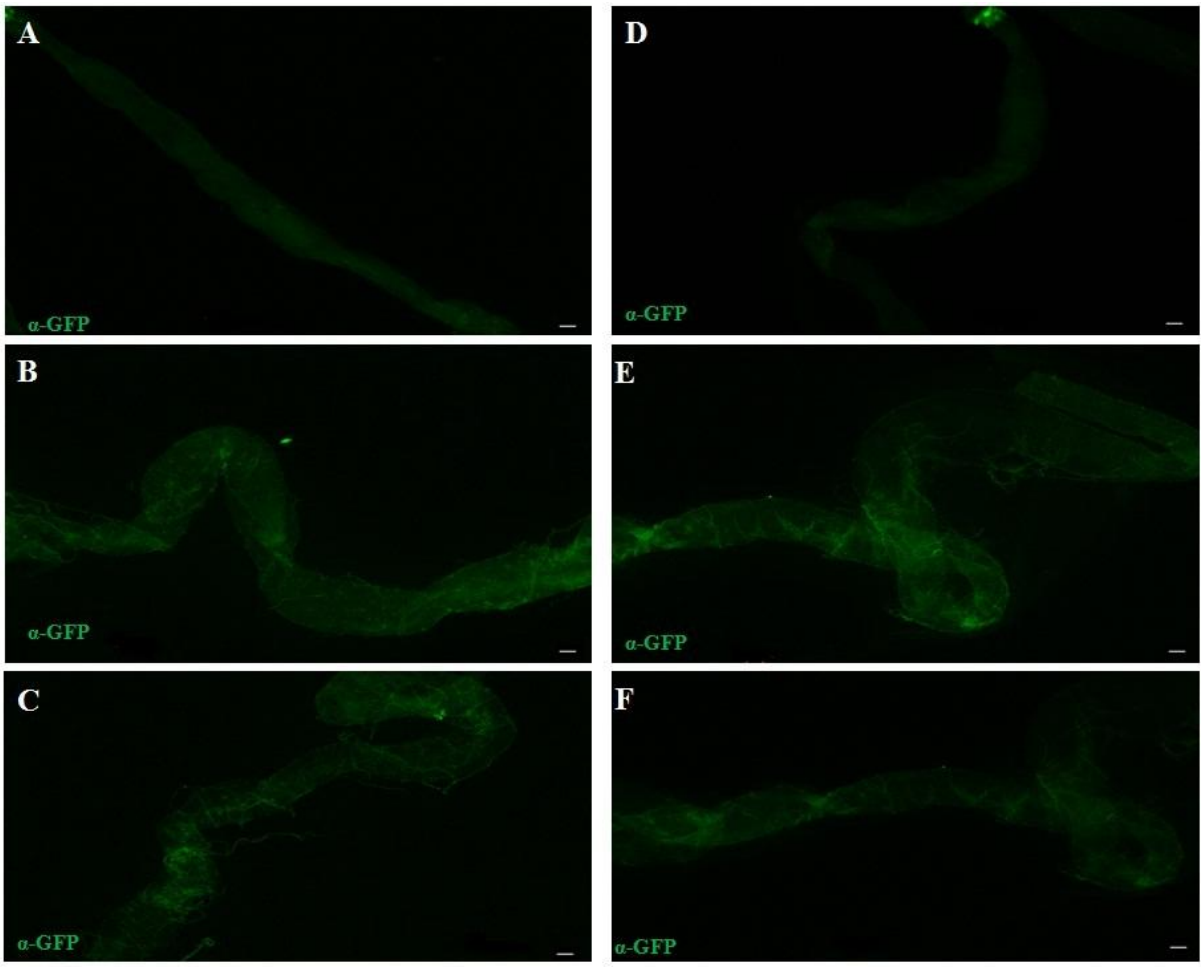

Figure 30. **A** Drosomycin under control medium. **D** Drosomycin under HFD. **B** Defencin under control medium while as, **E** Defensin under HFD. **C** Drosocin under control medium. **F** Drosocin under HFD. Scale bar is 50µm.

To visualize expression of antimicrobial peptide genes in response to HFD, I used reporter lines specifically monitoring expression of specific genes (Anne-Marie et al., 2004; Kiri LT et al., 2014: Mathilde G et al., 2009). Following HFD, no increase in the expression of drosmycin (A, B), defensin (C, D) and drosocin (E, F) could be seen (Fig 30).

3.7. Effect of HFD of the gut microbiota

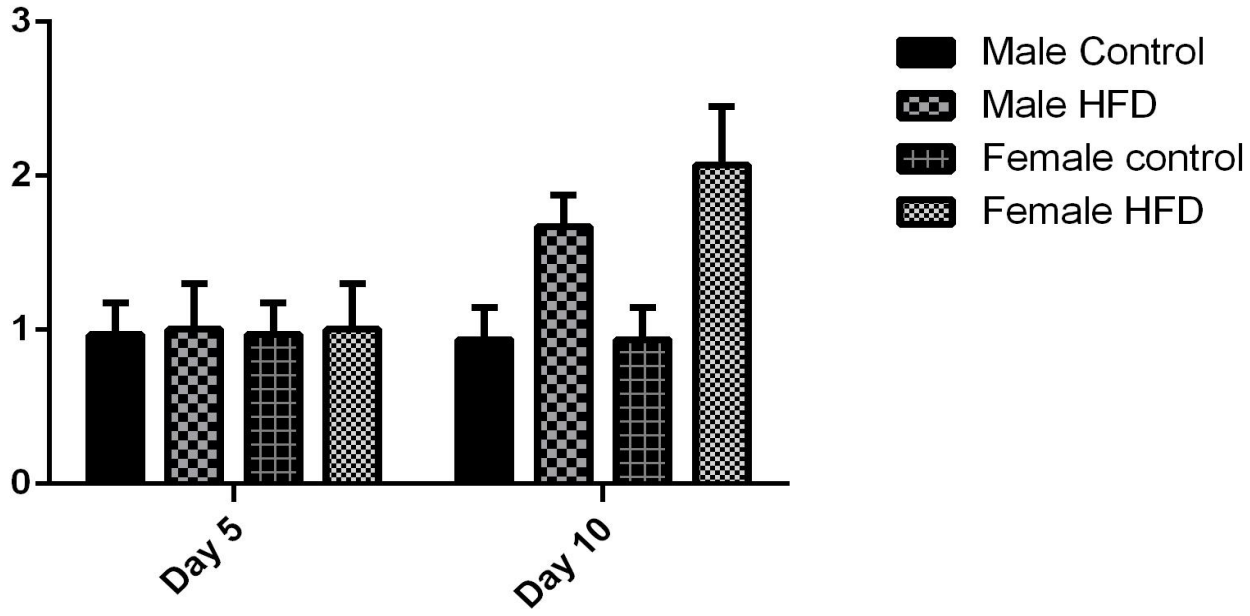

Figure 31. Expression level of gut microbiota under normal and high medium after day 5 and day 10.

HFD has an effect on the intestinal microbiota of the fly. Quantitative Real time PCR employing primers specific for eubacteria and isolated DNA from the intestine was used to quantify total bacteria amounts in the midgut of the *Drosophila melanogaster*. While after 5 days on HFD, the numbers of bacteria increased males and felames significantly, this effect was not seen anymore after 10 d on HF (Fig 31).

3.7.1. Dependency of induced upd3 expression on the presence of microbiota

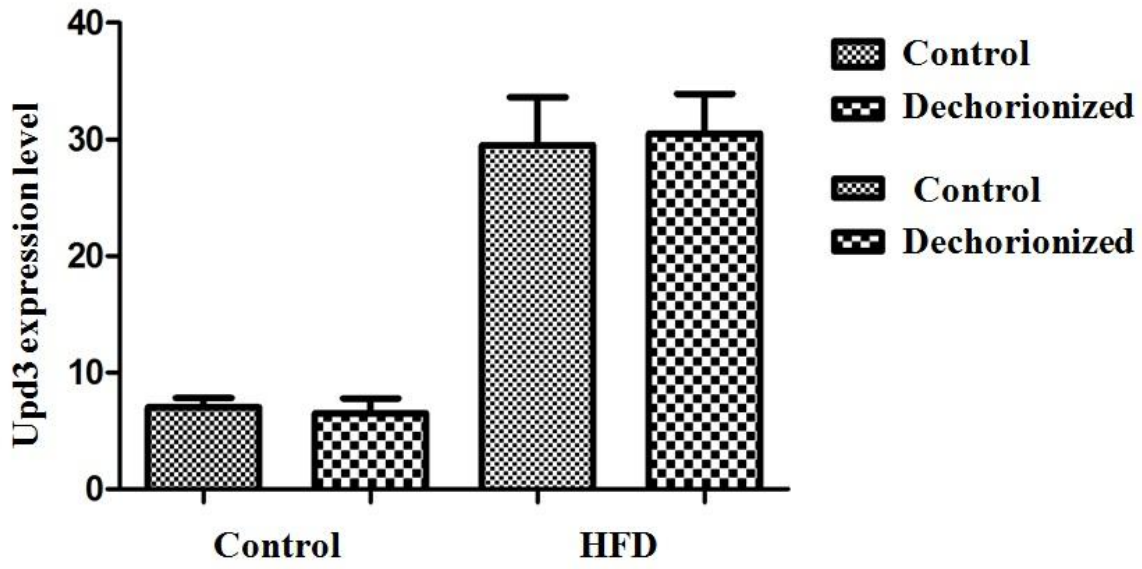

Figure 32. UPD3 gene expression level in UPD3 control in comparison UPD3 dechroinated line under normal medium as well as high fat medium.

Dechorionization is a good method to produce germ-free animals, meaning that the larvae are free of microbiota. Quantitative real time PCR as performed above revealed that dechorionization, meaning germ-freeness, had no effect on the HFD induced increase in upd3 expression (Fig 32).

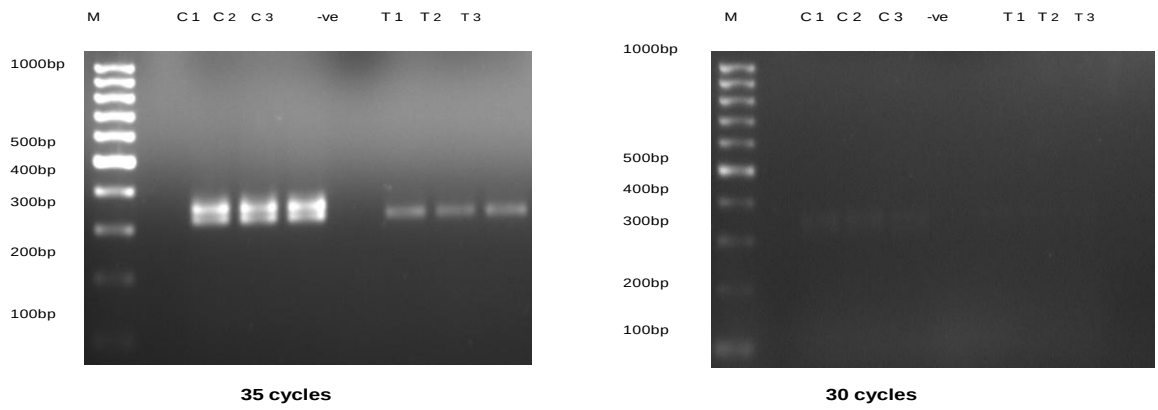

Figure 33. A, amplification of the gut microbioa after 32 cycles, **B,** amplification of the gut microbiota after 28cycles in between control and treated.

To evaluate if the process of dechorinization together with the use of antibiotics is sufficient to eliminate the inteatinal microbiota, gDNA was isolated from the corresponding animals and quantified using gPCR. After 35 cycles of amplification, the control shos a strong band, indicative for the presence of microbiota, while in the dechoronized samples, a much less intesne band could be amplified, indicating that a small amount of microbiota was still present in these animals. To confirm the results and the effects of dechorinization and treatment after antibiotics, I also cultured bacteria on nutirent agar medium.

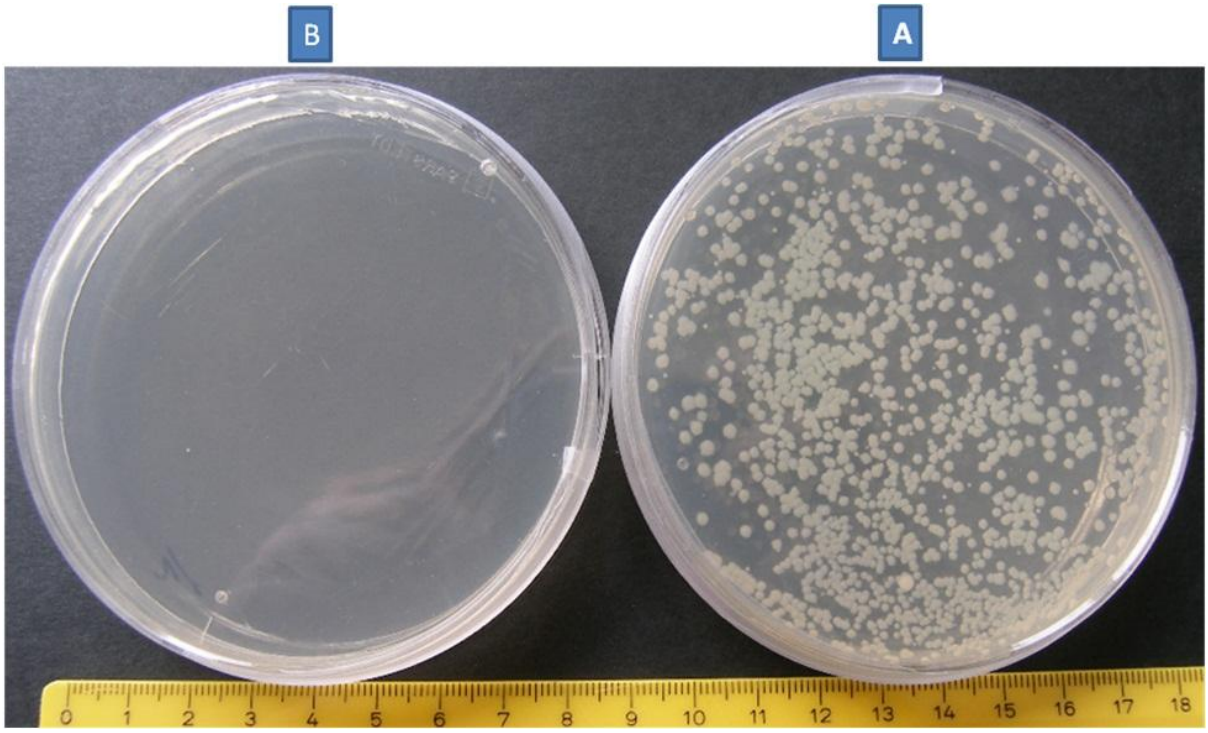

Figure 34. A control culture witout dechroination and control medium. **B** culture the gut microbiota after dechorionized and medium treated with antibiotic.

Although some material could be amplified in seemingly germ-free animals, the bacterial culture revelaed that the difference between control and dechorionated and antibiotics treated animals is more obvious. Shown in A is a sample from control animals and in B frrom those treated to become germ-free.

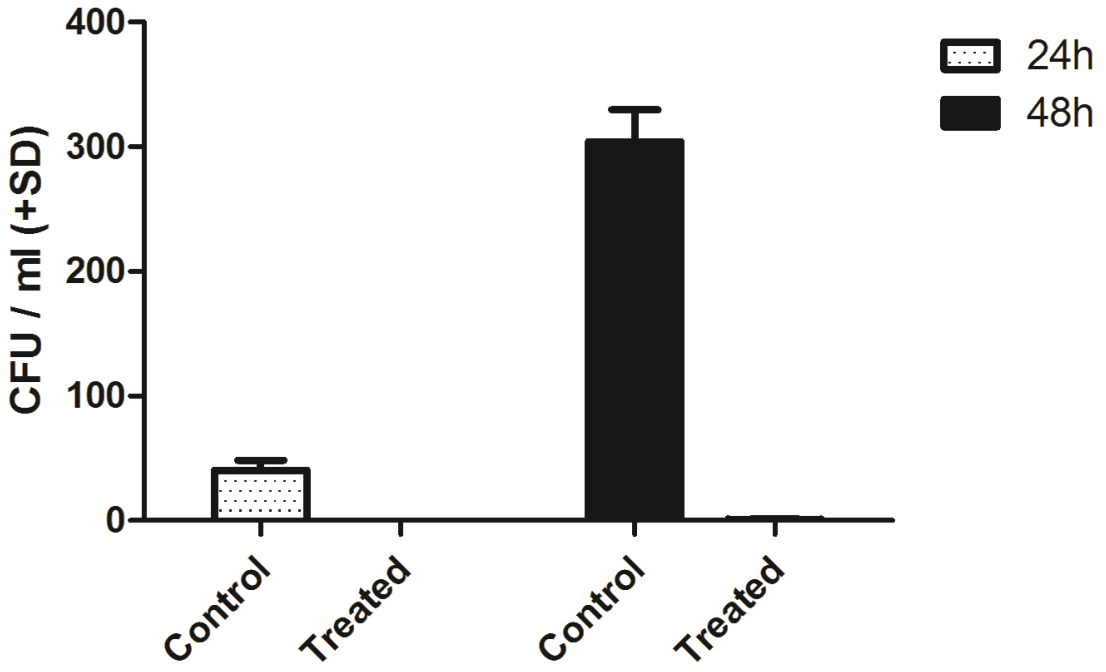

Figure 35. Control, gut microbiota culture colonies count after 24 and 48 hours. Treated, gut microbiota after dechorionized and treated with antibiotic containing medium counting culture colonies afer 24 and 48hours.

Counting the colonies after 24hours and after 48 hours revealed almost no colonies in the treated group, indicative for a very effective removal . The number of colonies on the control sample after 24 hours are approximately 50-65 colonies while in the treated samples no colonies could be seen. After 48 hours number of colonies on the control plates are between 295-315. Only 3 colonies were seen in the treated group.

3.8. Defecation

3.8.1. Use of bromophenole blue to assess the effect of HFD on defecation

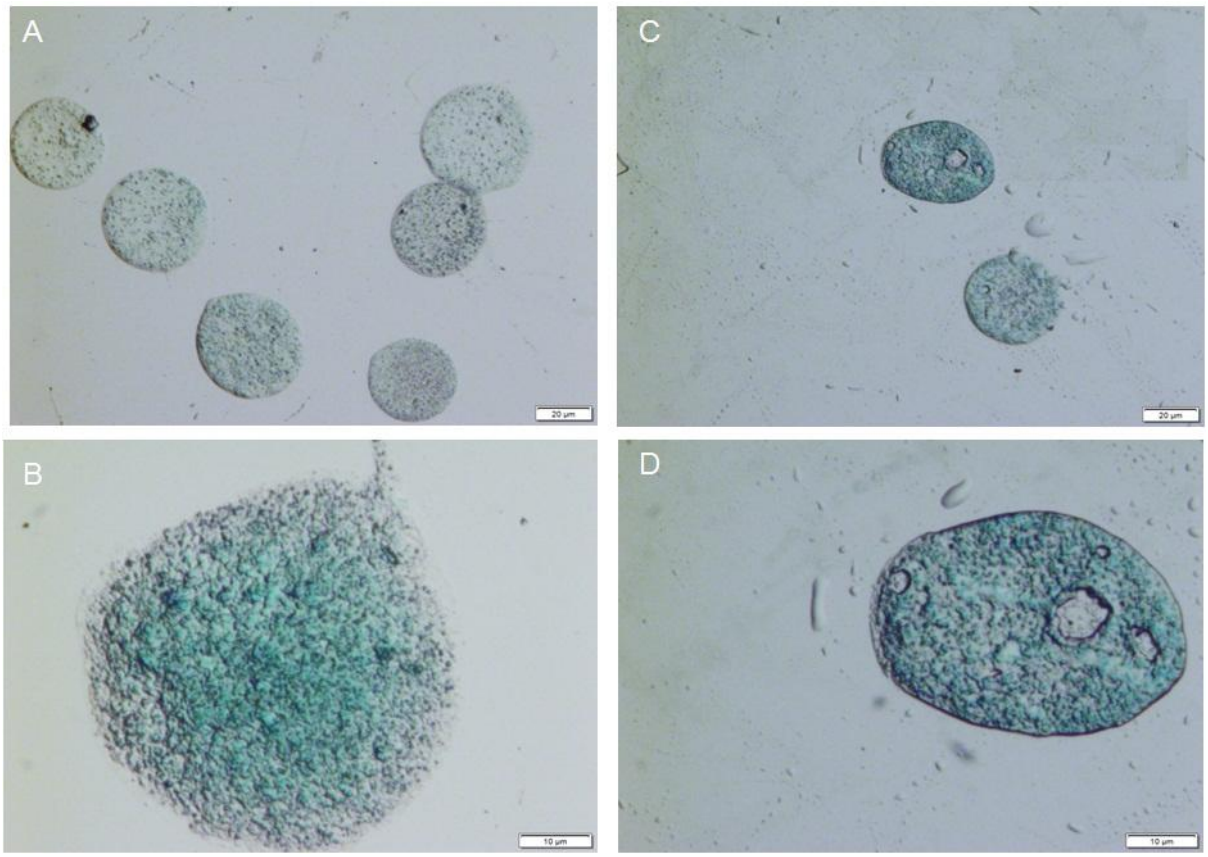

Figure 36. A and **B** is the defectaion under normal medium while as **C** and **D** is defication under hig fat medium.scale bar is 10 and 20mm.

The consistency, amount and rate of the defecation of *Drosophila melanogaster* kept on control medium was compared with that of those kept on high fat medium. The consistency is changed with high fat medium. It is evident that the defecation on high fat medium is oily, small in amount, compact and less watery. In comparison defecation on the control medium is watery, higher in amount and scattered (Fig 36).

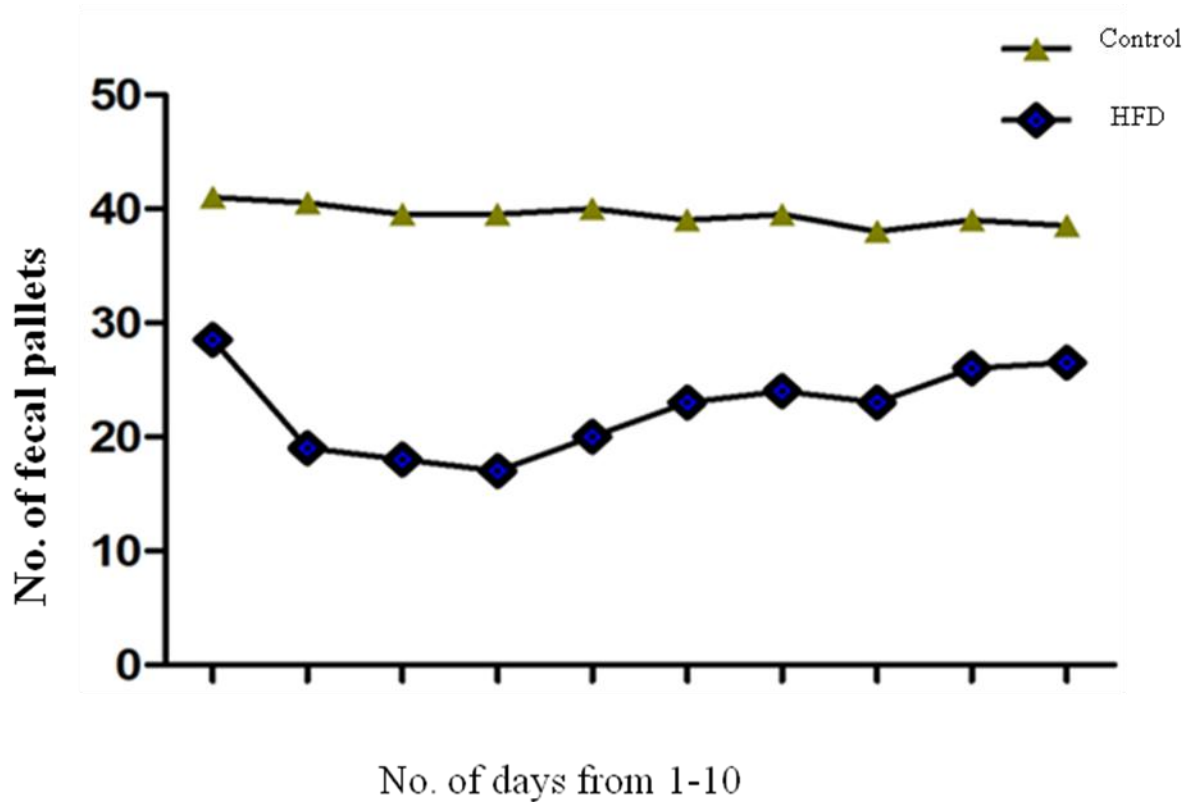

Figure 37. Counting of the defecation from day one to day 10 under normal and as well as under hig fat medium.

Moreover, I counted the number of defecation pellets per day. While the number of pellets remained almost constabt at 40, following HFD the value was between 20 and 30 indicative for a reduced defecation activity.

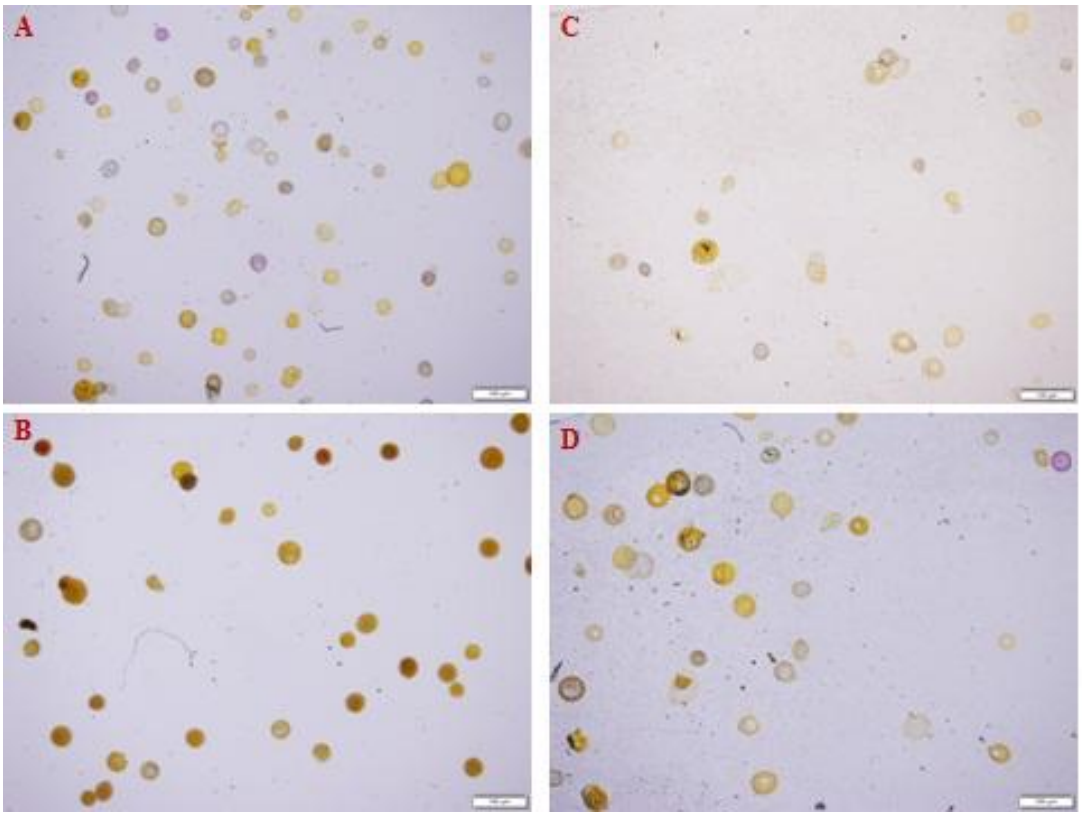

Figure 38. A male defacation under norma medium, **C** is male defecation on HFD. **B** is female defecation on control medium ,**D** is female defecation on HFD. Scale bar is 100mm.

Additional differences became apparent using phenol red as a dye. This dye allows to evaluate the effect of HFD on the pH.

3.8.5 Assesing the pH of defecation on HFD in females.

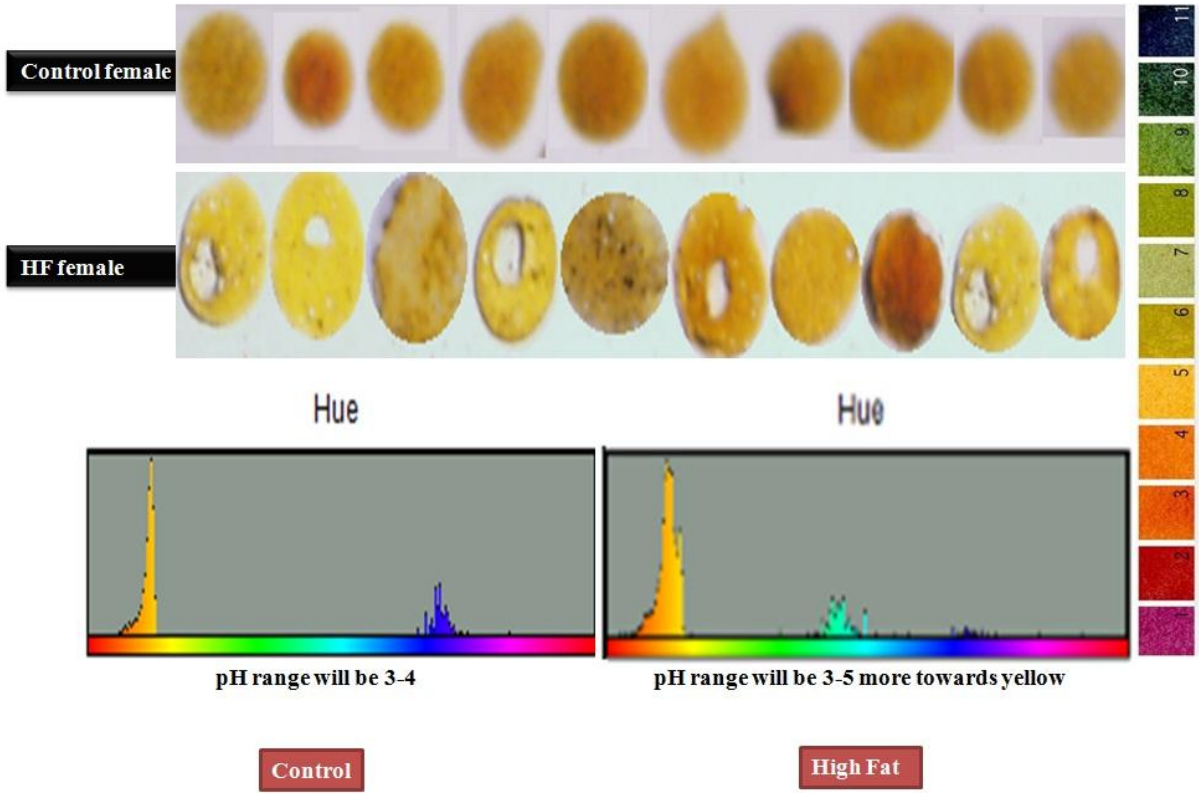

Figure 39. A pH calculation through Hu analysis for male on control medium, **B** is pH calculation through Hu analysis for male under high fat diet.

An in-depth analysis of the pH of defecation spots was performed to analyse the pH (Paola C et al., 2011) for males held on either control or high fat medium give different ranges of the pH. pH range for the control medium is between 3-5, while as the pH range for animals on HFD is between 4-5. This indicates that on HFD the pH of the defecation products is shifted slightly to the neutral region.

3.8.6 Assesing the pH of defecation on HFD in males.

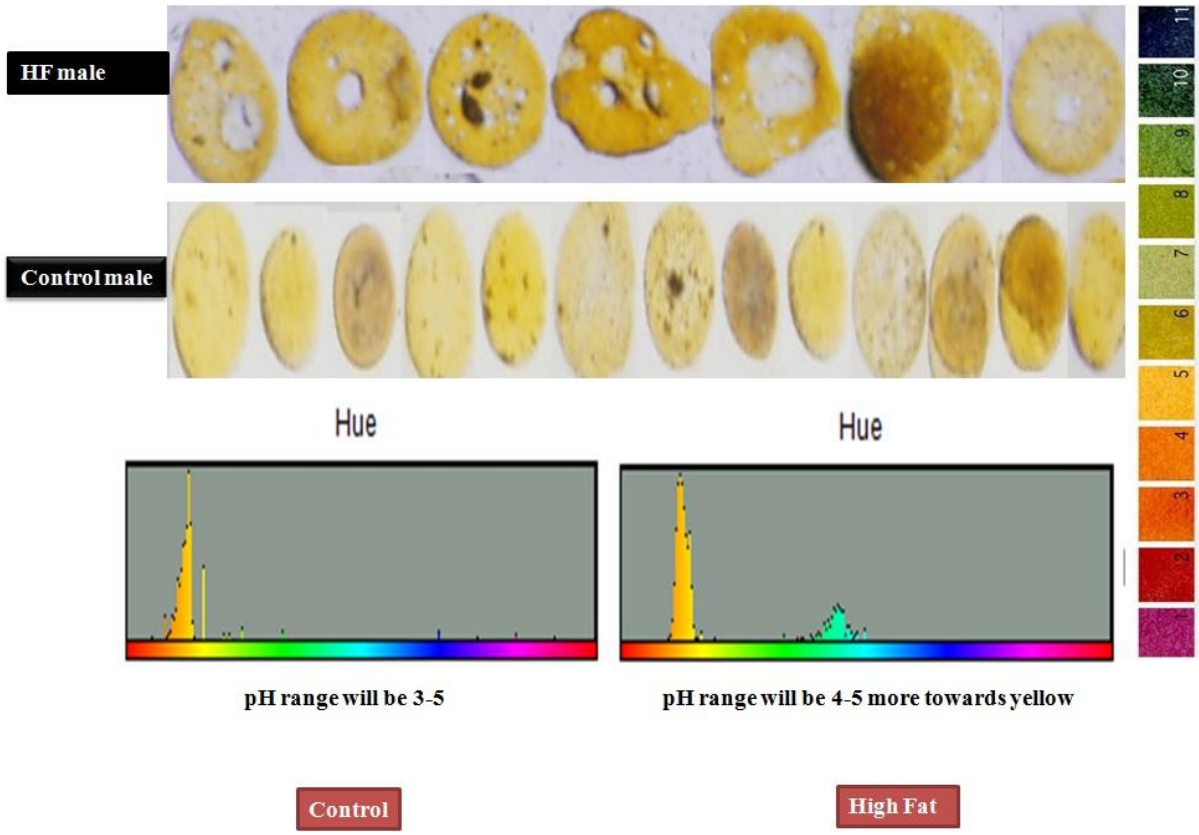

Figure 40. A pH calculation through Hu analysis for female on control medium, **B** is pH calculation through Hu analysis for female under high fat diet

A similar result was observed for defecatio products from females confronted either with normal meidum or high fat medium. Here, also a shift to the more neutral pH region became apparent (Fig 40)

3.8.3. Visualizing the effect on the Copper cell region using the phenol red dye as indicator on normal medium in comparison with high fat medium.

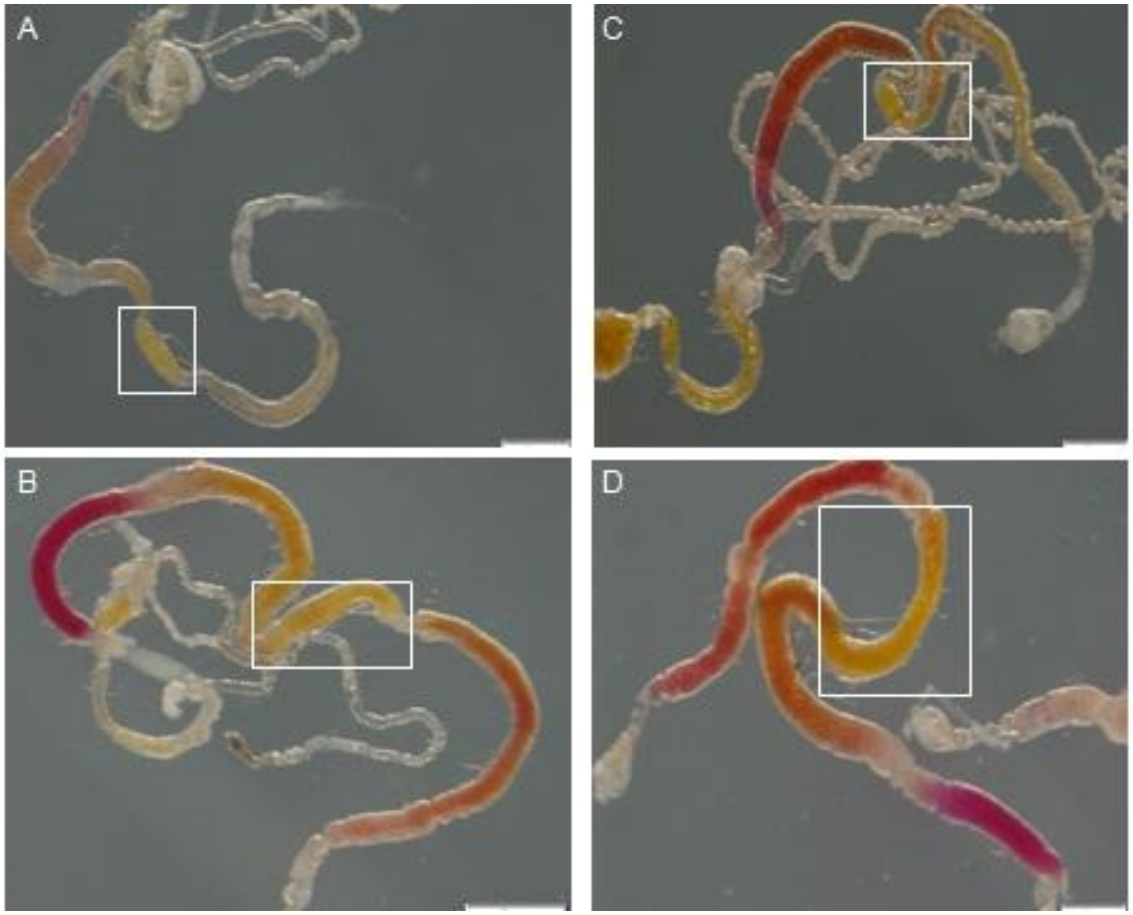

Figure 41. **A and B** marks the copper cell region under normal medium male and female respectively. **C and D** marks the copper cell region under high fat medium male and female respectively. Scale bar is 1mm.

The copper cell region, which is the most acidic part of the intestine, is also changed following HFD. Here in both male and female under normal and high fat medium, the pH is shown. The marked region in both male from normal and high fat medium while as it marked in female.

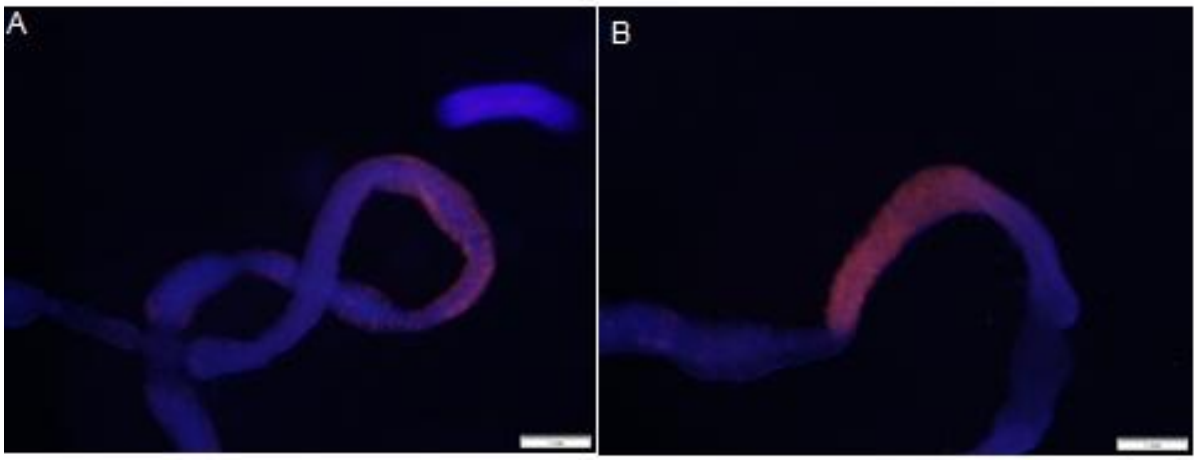

Figure 42. A marks the Copper cell region under normal medium. **B** marks the copper cell region under high fat medium. Scale bar is 1mm.

Alternatively, the copper cell region can be labelled with copper, as it is known to accumulate this ion at high levels. Copper emits a reddish fluorescence if activated with blue light. In HFD treated animals the copper cell region appears to be enlarged (Fig 42).

4.0. Discussion

In the current study, I evaluated the effects of high fat dieting (HFD) on various parameters of the intestinal system using the fruit fly *Drosophila melanogaster* as a model. HFD changed various parameters of the defecation process including the consistency of the fecal products. Moreover, defecation following HFD is slow and shows constipation like symptoms. The pH range of fecal products under control conditions is in between 3-5, while those of animals held on HFD is in between 4-5. HFD induced dramatic increases in the deposition of fat droplets not only in the fat body but also in in the intestine, more specifically in the enterocytes. In addition, the amount of indigenous bacteria making the microbiota was in response to HFD.

A number of different signaling systems operative in the intestine are activated following HFD. Among them are strong and prolonged activation of Ca^{2+}-signals monitored using the CaLexA system. In addition, strong Notch- and Nrf2-signaling could be observed throughout the entire intestinal epithelium. Very impressive is the strongly induced upd3 expression presumably activated via JNK signaling. Activation of these various signaling pathways appears to activate the epithelium proliferation and differentiation even after only 2h of HFD.

In humans, HFD is a major factor causing metabolic disorders in developed countries. Beside the effects of this metabolic intervention on fat storage organs, which is decisive for the development of diseases such as type-2 diabetes, the intestinal epithelium is the first tissue coming into contact with these nutrients. Intestinal cells are activated by duodenal lipids, causing impairments of the tight junction between them. This effect may also contribute to the metabolic syndrome that reacts to lipopolysaccharide transported into fat tissues via this route. Moreover, alteration of the gut microbiota may occur, directly associated with this dietary shift or indirectly as a consequence of the inflammatory response. High fat in the diet is a major source to cause molecular and physiological changes in the gut epithelium (Choo YL in 2013).

Function	Mammals	*Drosophila*
Digestion and nutrient absorption	Stomach, small intestine	Midgut
Lipid storage	Adipose tissue	Fat body
Lipid mobilization	Adipose tissue, liver	Fat body, oenocytes
Glycogen storage	Liver	Fat body
Carbohydrate homeostasis	Pancreatic α and β cells	Neurosecretory neurons, corpora cardiaca

Table 13. Metabolic tissue comparison in between mammals and *Drosophila* (Trinh and Boulianne in 2013).

Metabolic functions in both *Drosophila* and in vertebrates are highly similar (Perrimon and Leopold in 2007). Fat is stored in the fat body, oenocytes can function as hepatocytes and the intestine has a very similar architecture in either system (Table 1, Gutierrez et al., 2007; Perrimon and Leopold 2007; Thummel and Baker 2007).

In *Drosophila*, excessive fat in the diet is stored in fat body as triglycerides (Gutierrez et al., 2007; Perrimon and Leopold in 2007; Thummel and Baker in 2007). The fat content influences the mechanism through which the secretion of DILPs from the IPCs is regulated (Geminard et al., 2009; Colombani et al., 2003). Induction of the cytokine unpaired 2 (Upd2) in the fat body after feeding induced a JAK-STAT-dependent response in different parts of the body (Rajan and Perrimon in 2012). Upd2 regulates secretion of DILPs from the brain (IPCs) making a negative feedback-loop.

Taken together, high fat diet is a causative agent for metabolic disorders, changes in the physiology of the gut, feeding behaviour, obesity, immune response in the gut epithelium and cancer. Effect of high fat diet to triggers slow rate of defecation, inflammation, increased permeability of the epithelium, activation of various signaling pathways after release of cytokines, fat droplets in ECs and renewal of epithelium to protect against the deleterious effect of HFD.

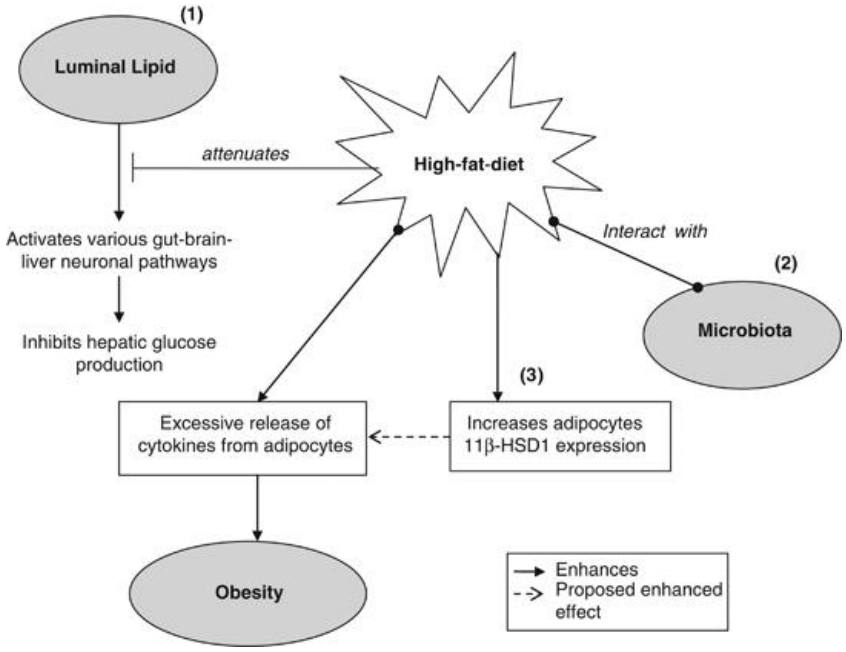

Figure 43: High fat interact with luminal lipid, microbiota and increases adipocytes 11β-HSD1 expression (Choo YL in 2013).

It is established through most recent studies that HFD is the sole causative agent for CRC in mice but the exact mechanism behind is still not clear. The expansion in the colon crypt in the mice is developing toward the onset of cancer in humans and other animals. HFD plays a central role towards induced expansion of the colon proliferative zone and the higher rate of proliferation is interlinked with innate inflammatory markers. HFD induced expression of TLR2/4, various TLR-4 responsible genes, COX-2, TNF-α and NF-κB in comparison to the normal diet. Moreover, a higher rate of macrophages infiltration, oxidative stress and inflammation at the site of distal colon become proliferative as well leading towards conversion into cancer after chronic consumption of HFD (Vanamala J et al., 2014).

4.1. Feeding behaviour

Regulation in feeding behaviour has a key role in keeping metabolic homeostasis. Diet in the gut stimulates various neural and endocrine hormones in a continuing position for the regulation of the feeding behaviour in animals. In *Drosophila*, various peptides play their role for controlling the feeding behaviour (Poon et al., 2005; Tschop et al., 2000; Wren et al., 2001a; Wren et al., 2001b; Nassel and Winther in 2010). sNPF over expression leads to the over consumption of diets, while lower expression results in reduced food intake. The release of sNPF is under the control of insulin. Moreover, sNPF is a key regulator of DILP release from the IPCs (Lee et al., 2004). Increase or decrease in food intake results in energy dependent activation of allatostatin expressing neurons, which also plays a major role in food consumption (Hergarden et al., 2012). Likewise, various other peptides such as PTTH have their roles in feeding behaviour. This is in agreement with those of the current study, where chronic high fat dieting has an impact on the structure of the intestine, especially regarding the enteroendocrine cells that are present at much higher levels following this intervention, indicative for an increased load of hormonal signalling emanating from the intestine. In the gut, high fat dieting affects various traits including the epithelium itself, but also the indigenous microbiota. It is the place where both pathogenic and commensal bacteria interact with the immune system. Diets containing high concentrations of fat content are able to cause "metabolic endotoximia'' and other inflammatory changes of the gut epithelium (Ghanim H et al., 2009). High fat diet has a major role in the translocation of the PAMPs from the lumen of the gastrointestinal tract into the circulation through the promotion of the microbiota and the functional decline of the tight junction functions (Cani PD et al., 2008). High fat diet will thus leads to the activation of NF-κB via TLR4 inducing an inflammatory response (Deopurkar R et al., 2010). Different levels of intestinal inflammation after HFD are major causes that change the composition of the microbiota being predictive for the development of obesity. The inflammation itself results in increased permeability of the gut epithelium (Ding S et al., 2010; de La Serre et al., 2010). Thus, HFD can cause oxidative stress, reduced glucose tolerance, body weight gaining, visceral fat deposition and inflammation after modulation of the gut microbiota (Cani PD et al., 2008; Membrez M et al., 2008).

The gut microbiota is very important for the digestion and absorption of the gut content. Microbes within the microbiota use the fiber content of the diet for energy absorption after fermentation as well as the production of short chain fatty acids (Backhed F in 2011).

Following HFD the modulation in the colonic gastrointestinal microbiota alters its role for the control of obesity and metabolic diseases (Wanders AJ et al., 2011; Spreadbury I in 2012). Fat has inhibitory effects on the gastric emptying. Feedback signals are arising from the intestine especially if fat is in the diet (Lin HC et al., 1990). These feedback signals are mediated by release of e.g. PYY and GLP1 (Couce ME et al., 2006). High fat diet initiates hypertrophy of the intestinal epithelium and increased fat digestion capability. High fat can affect the length, the gut functioning and energy intake. Increase transit times in the intestine after exposing it to the high fat diet (Palm oil) could be observed (Brown NJ et al 1994). High fat also alters the motility of the intestine (Boyd KA et al., 2003). Thus, intestinal motility, gastric emptying time and intestinal transit time is dependent upon the fat concentration, the higher the fat concentration the lower the gastric emptying time, the higher the transit time (Castiglione KE et al., 2002). These results are very similar to those seen in the fly, where I observed also changes in the transit time and the load of the intestine following HFD.

In mammals, the CCK concentration is elevated after consumption of high fat diets (French SJ et al., 1995). Higher intestinal contents cause local excessive release of CCK. Moreover, high fat can alter the CCK concentration in plasma indirectly (Boyd KA et al., 2003; Cunningham KM et al., 1991).

4.2. Dysbiosis (Intestinal microbiota)

Numerous types and species of intestinal microbes are residing in the gut. The diversity and composition of microbiota depends upon various factors including diet, host genetics, environment, inflammation and other composite disease condition (Hansen et al., 2010; Sangild and Buddington in 2011; Musso et al., 2010; Cref-Bensussan and Gaboriau-Routhiau in 2010). The relation between host and microbiota is close and the result of a coevolution (Ley et al., 2008). The change in the composition of the microbiota is named dysbiosis and is elaborated in different diseases. Normal or healthy microbiota composition can be defined as that of healthy individuals. Dysbiosis of the gut microbiota has been correlated with various diseases such as obesity, irritable bowel syndrome and inflammatory bowel disease (Gerritsen J et al., 2011). In humans as well as in flies, microbiota colonisation in the intestine starts straight after the birth by contact with the mother (humans) and the environment (flies) (Adlerberth and Wold in 2009; Mackie et al., 1999). Use of high fat diet

affects the composition of the intestinal microbiota. This is also seen in the experiments presented in the current study (Mariat et al., 2009; Mueller et al., 2006; Zweielehner et al., 2009; Bartosch et al., 2004). Diet in general is the main influencing source for changing the composition of the intestinal microbiota (Osterdahl M et al., 2008). High fat diet in animals and as well as in human have significant effects on the quantity and composition of the microbiota as well as on the level of endotoxin (Erridge C et al., 2007; Amar J et al., 2008). Endotoximia leads towards a low grade of inflammation, adipocyte hyperplasia, insulin resistance as well as reduced levels of β-cell function leading towards the metabolic syndrome (DiBaise JK et al., 2007).

Activation of JNK signaling has been demonstrated in the current work. Comparable results have been obtained in mammalian systems. JNK signaling plays a pivotal role to mediate metabolic stress after HFD (Vernia S et al., 2013). JNK1 also regulate body weight and energy expenditure (Belgardt BF et al., 2010). JNK1 also plays its role to maintain the metabolic homeostasis, to induce inflammation without altering the adipose tissue under HFD (Solinas G et al., 2007; Vallerie SN et al., 2008).

4.3. Diseases associated with the microbiota

The onset of IBS (irritable bowel syndrome) is under the control of impaired intestinal motility, inflammation, hypersensitivity as well as due to dietary factors (Chang and Telley in 2011; Longstreth et al., 2006; Karantanos et al., 2010). Studies established the relationship of IBS and dysbiosis. Both, the intestinal epithelium and the residing microbiota are exposed to the diet (in my case the HFD) and agents derived from the diet (Kristy B et al., 2012). It is established that certain dietary factors are involved in shaping the host reaction and determining the host susceptibility (Kristy B et al., 2012). This is outlined in Fig 44.

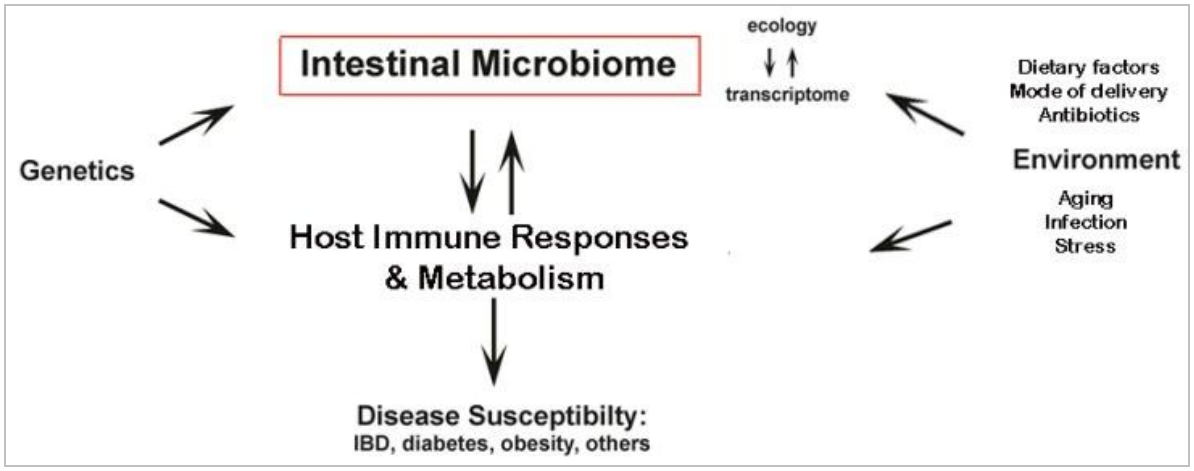

Figure 44: Dietary factors induced dysbiosis affects disease susceptibility of the host. IBD, obesity and diabetes are outcomes of the diet. Diet has a specific role in regulating the gut immune system and the host metabolism. Diet also has its role to in microbial modulation, host immunity, metabolism and ultimately susceptible to various diseases. (Kristy B et al., 2012).

Taken together, gut microbiota are involved in metabolism, inflammation, energy balancing, obesity and other metabolic disorders. Moreover, a very close relationship between obesity and dysbiosis has been established.

4.4. T2D (Type 2 Diabetes)

Microbiota changes are correlated with insulin resistance T2D (Type 2 diabetes) presumably acting through the metabolic syndrome. In humans, the interlinked relationship between the microbiota and T2D is based on the ratio of the titre of Bacteriodetes/Firmicutes. Metabolic syndrome, T2D and obesity are also linked with inflammation leading to the assumption that microbes are able to induce obesity, metabolic syndrome as well as T2D. Endotoxemia is based upon increased level of LPS in the circulation and induced inflammation locally and systemically (Cani PD et al., 2007; Pendyala S et al., 2012). Studies on human suggested that high fat diet can cause 71% more plasma level of endotoxins if applied for more than one month (Pendyala S et al., 2012). T2D patients often have high titres of plasma LPS (Creely SJ et al., 2007) implying that bacteria are the main causative agent for inducing inflammation, insulin resistance and metabolic syndrome (Cani PD et al., 2007).

It is established that the microbiota is the key factor provoking the immune system and spreading of bacteria into various active metabolic tissues. It will lead into chronic

inflammation, insulin resistance, metabolic syndrome, hepatic fat deposition and impaired development of the adipose tissue. Recovery or treatment with dysbiosis will leads to decrease or prevention of metabolic diseases (Amar J et al., 2011).

4.6. IBD (Inflammatory bowel disease)

Crohn's disease and ulcerative colitis collectively known as IBD are characterized by disrupted epithelial integrity in the gut. Microbes can easily penetrate the epithelial barrier and provoke a local immune response. Continuously provoked immune reactions in the gut epithelium convert the tissue into a chronically inflamed one. The microbiota is very important to keep the homeostasis in the gut lumen and reduce provoking the innate immune system while retaining the epithelial integrity (Rakoff-Nahoum S et al., 2004; Garrett WS et al., 2007). The role of dysbiosis in the etiology of IBD is still not clear. Evidence point to be associated in between increased number of bacteria and a decreased population of preventive microbes in IBD (Ghosh S et al., 2011).

It is established that HFD is a critical factor for the etiology of IBD. Studied using a Danish population revealed that HFD triggers IBD and ulcerative colitis at an incidence that is up to 30 % higher than in populations on normal diet (Chapkin RS et al., 2007; Asakaura H et al 2008; Tjonneland A et al., 2009; Uchiyama K et al., 2010; Wallace DF et al., 2011; Ma X et al., 2008). Studies revealed that fatty acids directly impair the host gut immune response and thus increase the IBD risk.

Conclusion

Different diets have a great impact on our health. HFD has adverse effects on the metabolism and the structure and physiology of the gastrointestinal tract. High fat diet (HFD) is a major reason for the epidemic development of various metabolic disorders. In *Drosophila melanogaster* HFD triggers the proliferation and differentiation of the intestinal epithelium leading to renewal of the epithelial layer. HFD and microflora trigger inflammation and permeability through disruption of tight junctions within the epithelium. In the fly, proliferation and differentiation of the gut epithelium results from activation of various signalling pathways including stress responses within the ECs finally leading to release of upd3. This triggers ISC proliferation and differentiation. The interplay role of HFD behind the activation of JNK, Nrf2, notch and Ca^{2+}-signaling pathways are remains to be elucidated.

Moreover, HFD affects gastric emptying time and slows down the defecation rate. HFD modulates the metabolisms of lipids being a major cause of metabolic disorder increasing the number of microbiota community. Manifestation of metabolic disorder in the gut may be causally associated with several chronic diseases such as IBD, IBS, insulin resistance and ultimately with cancer.

References

Abil Saj Zeynep Arziman Denise Stempfle Werner van Belle Ursula Sauder Thomas Horn Markus Dürrenberger Renato Paro Michael Boutros[2], Gunter Merdes. A Combined Ex Vivo and In Vivo RNAi Screen for Notch Regulators in *Drosophila* Reveals an Extensive Notch Interaction Network. *Developmental Cell* (2010) 18:(5);Pages 862–876.

Abraham C, Cho J. Interleukin-23/Th17 pathways and inflammatory bowel disease. *Inflamm Bowel Dis* (2009)

Adlerberth I, Wold AE. Establishment of the gut microbiota in Western infants. *Acta Paediatr* (2009) 98(2):229–238.

Alla Amcheslavsky, Wei Song,, Qi Li, Yingchao Nie, Ivan Bragatto, Dominique Ferrandon, Norbert Perrimon, and Y. Tony Ip. Enteroendocrine Cells Support Intestinal Stem-Cell-Mediated Homeostasis in Drosophila. *Cell* (2014) 9: 32–39.

Amar J, Burcelin R, Ruidavets JB *et al*. Energy intake is associated with endotoxemia in apparently healthy men. *Am J Clin Nutr* (2008) 87:1219–1223.

Amar J., Chabo C., Waget A., Klopp P., Vachoux C., Bermudez-Humaran L.G., Smirnova N., Berge M., Sulpice T., Lahtinen S., et al. Intestinal mucosal adherence and translocation of commensal bacteria at the early onset of type 2 diabetes: Molecular mechanisms and probiotic treatment. *EMBO Mol. Med* (2011) 3:559–572.

Amcheslavsky A., Jiang J., Ip Y.T. Tissue damage-induced intestinal stem cell division in Drosophila. *Cell Stem Cell* (2009) 4, 49–61.

Amsen D, Antov A, Jankovic D et al. Direct regulation of GATA 3 expression determines the T helper differentiation potential of Notch. *Immunity* (2007) 27(1):89-99.

Anne-Marie Alarco Anne Marcil, Jian Chen, Beat Suter, David Thomas and Malcolm Whiteway. Immune-Deficient *Drosophila melanogaster*: A Model for the Innate Immune Response to Human Fungal Pathogens. *J Immunol* (2004) 172:5622-5628.

Apidianakis Y., Mindrinos M.N., Xiao W., Lau G.W., Baldini R.L., Davis R.W., Rahme L.G. Profiling early infection responses: Pseudomonas aeruginosa eludes host defenses by

suppressing antimicrobial peptide gene expression. *Proc. Natl. Acad. Sci* (2005) 102, 2573–2578

Apidianakis Y., Mindrinos M.N., Xiao W., Tegos G.P., Papisov M.I., Hamblin M.R., Davis R.W., Tompkins R.G., Rahme L.G. Involvement of skeletal muscle gene regulatory network in susceptibility to wound infection following trauma. *PLoS ONE* (2007) 2, e1356.

Apidianakis Y., Rahme L.G. Drosophila melanogaster as a model host for studying Pseudomonas aeruginosa infection. *Nat. Protoc* (2009) 4, 1285–1294.

Asakura H., Suzuki K., Kitahora T., Morizane T. Is there a link between food and intestinal microbes and the occurrence of Crohn's disease and ulcerative colitis? J. Gastroenterol. *Hepatol* (2008) 23:1794–1801.

Aw TY. Determinants of intestinal detoxication of lipid hydroperoxides. *Free Radic Res* (1998) 1925:637–646.

Backhed F. Programming of host metabolism by the gut microbiota. *Ann Nutr Metab* (2011) 58(Suppl 2):44–52.

Baker KD, Thummel CS. Diabetic larvae and obese flies-emerging studies of metabolism in *Drosophila*. *Cell Metab.* (2007) 6(4):257-66.

Bartosch S, Fite A, Macfarlane GT, McMurdo ME. Characterization of bacterial communities in feces from healthy elderly volunteers and hospitalized elderly patients by using real-time PCR and effects of antibiotic treatment on the fecal microbiota. *Appl Environ Microbiol* (2004) 70(6):3575–3581.

Bastide P, Darido C, Pannequin J, Kist R, Robine S, et al. Sox9 regulates cell proliferation and is required for Paneth cell differentiation in the intestinal epithelium. *J. Cell Biol* (2007)178:635–48.

Baumann O. Posterior midgut epithelial cells differ in their organization of the membrane skeleton from other Drosophila epithelia. *Exp. Cell Res* (2001) 270, 176–187.

Becam, I., Rafel, N., Hong, X., Cohen, S.M., Milán, M. Notch-mediated repression of bantam miRNA contributes to boundary formation in the Drosophila wing. *Development* (2011) 138(17): 3781--3789.

Belgardt BF, Mauer J, Wunderlich FT, Ernst MB, Pal M, Spohn G, Bronneke HS,Brodesser S, Hampel B, Schauss AC, et al. 2010. Hypothalamic and pituitary c-Jun N-terminal kinase 1 signaling coordinately regulates glucose metabolism. *Proc Natl Acad Sci* (2011) 107: 6028–6033.

Bellen HJ, Tong C, Tsuda. 100 years of Drosophila research and its impact on vertebrates neuroscience: a history lesson for the future. *Nat Rev Neurosci* (2010) 11:514-522.

Berkey C.D., Blow N., Watnick P.I. Genetic analysis of Drosophila melanogaster susceptibility to intestinal Vibrio cholerae infection. *Cell Microbiol* (2009) 11, 461–474

Biccas BN, Lemme EM, Abrahão LJ Jr, et al. Higher prevalence of obesity in erosive gastroesophageal reflux disease. *Arq Gastroenterol* (2009) 46:15-9.

Bier E (2005). *Drosophila* , the golden bug,emerges as a tool for human genetics.Nat Rev Genet 6:9-23.

Biteau B., Hochmuth C.E., Jasper H. JNK activity in somatic stem cells causes loss of tissue homeostasis in the aging Drosophila gut. *Cell Stem Cell* (2008) 3, 442–455.

Bjerknes M, Cheng H. Intestinal epithelial stem cells and progenitors. *Methods Enzymol* (2006) 419:337–83.

Boyd KA, O'Donovan DG, Doran S, et al. High-fat diet effects on gut motility, hormone, and appetite responses to duodenal lipid in healthy men. *Am J Physiol Gastrointest Liver Physiol* (2003) 285:G188–96.

Brown ED, Morris VC, Rhodes DG, et al. Urinary malondialdehyde equivalents during ingestion of meat cooked at high or low temperatures. *Lipids* (1995) 30:1053–1056.

Brown KA, Carpenter EP, Watson KA, Coggins JR, Hawkins AR, Koch MHJ, Svergun DIet al.Twists and turns: a tale of two shikimate-pathway enzymes, *BIOCHEMICAL SOCIETY TRANSACTIONS*, (2003) 31, 543-547.

Brown NJ, Rumsey RD, Read NW. Gastrointestinal adaptation to enhanced small intestinal lipid exposure. *Gut* (1994) 35:1409–12.

Buddington RK, Sangild PT. Companion animals symposium: Development of the mammalian gastrointestinal tract, the resident microbiota, and the role of diet in early life. *J Anim Sci* (2011) 89:1506–1519.

Buchon N., Broderick N.A., Poidevin M., Pradervand S., Lemaitre B. Drosophila intestinal response to bacterial infection: activation of host defense and stem cell proliferation. *Cell Host Microbe* (2009b) 5, 200–211.

Camilleri M. Peripheral mechanisms in the control of appetite and related experimental therapies in obesity. *Regul Pept* (2009) 156:24-7.

Cani P.D., Amar J., Iglesias M.A., Poggi M., Knauf C., Bastelica D., Neyrinck A.M., Fava F., Tuohy K.M., Chabo C., et al. Metabolic endotoxemia initiates obesity and insulin resistance. *Diabetes* (2007) 56:1761–1772.

Cani PD, Bibiloni R, Knauf C, et al. Changes in gut microbiota control metabolic endotoxemia-induced inflammation in high-fat diet-induced obesity and diabetes in mice. *Diabetes* (2008) 57(6):1470–1481.

Cani PD, Bibiloni R, Knauf C, et al. Changes in gut microbiota control metabolic endotoxemia-induced inflammation in high-fat diet-induced obesity and diabetes in mice. *Diabetes* (2008) 57(6):1470–1481.

Castiglione KE, Read NW, French SJ. Adaptation to high-fat diet accelerates emptying of fat but not carbohydrate test meals in humans. *Am J Physiol Regul Integr Comp Physiol* (2002) 282:R366–71.

Cavassani KA, Ishii M, Wen H, et al. TLR3 is an endogenous sensor of tissue necrosis during acute inflammatory events. *J Exp Med* (2008) 205:2609–2621.

Cerf-Bensussan N, Gaboriau-Routhiau V. The immune system and the gut microbiota: friends or foes? *Nat Rev Immunol* (2010) 10(10):735–744.

Chamulitrat W. Activation of the superoxide-generating NADPH oxidase of intestinal lymphocytes produces highly reactive free radicals from sulfite. *Free Radic Biol Med* (1999) 27:411–421.

Chang JY, Talley NJ. An update on irritable bowel syndrome: from diagnosis to emerging therapies. *Curr Opin Gastroenterol* (2011) 27(1):72–78.

Chapkin R.S., Davidson L.A., Ly L., Weeks B.R., Lupton J.R., McMurray D.N. Immunomodulatory effects of (*n*-3) fatty acids: Putative link to inflammation and colon cancer. *J. Nutr* (2007) 137:200S–204S.

Chatterjee M., Ip Y.T. Pathogenic stimulation of intestinal stem cell response in *Drosophila. J. Cell. Physiol* (2009) 220, 664–671.

Choi N.H., Kim J.G., Yang D.J., Kim Y.S., Yoo M.A. Age-related changes in Drosophila midgut are associated with PVF2, a PDGF/VEGF-like growth factor. *Aging Cell* (200ba) 7, 318–334.

Choi PM, Zelig MP. Similarity of colorectal cancer in CD and UC. Implications for carcinogenesis and prevention. *Gut* (1994) 35:950–4.

Chooi Y Lee The Effect of High-Fat Diet-Induced Pathophysiological Changes in the Gut on Obesity: What Should be the Ideal Treatment? Clinical and Translational Gastroenterology *(2013) 4, e39; doi:10.1038/ctg.2013.1.*

Choi Y.J., Hwang M.S., Park J.S., Bae S.K., Kim Y.S., Yoo M.A. Age-related upregulation of Drosophila caudal gene via NF-kappaB in the adult posterior midgut. Biochim. *Biophys. Acta* (2008b) 1780, 1093–1100.

Colombani J, Raisin S, Pantalacci S, Radimerski t, Montagne J, Leopold P. A nutrient sensor mechanism controls Drosophila growth. *Cell* (2003) 114: 739-749.

Cordero, J., Vidal, M., Sansom, O. APC as a master regulator of intestinal homeostasis and transformation: from flies to vertebrates. *Cell Cycle* (2009) 8(18): 2926--2931.

Couce ME, Cottam D, Esplen J, Schauer P, Burguera B. Is ghrelin the culprit for weight loss after gastric bypass surgery? *A negative answer. Obes Surg (*2006) 16:870–8.

Creely S.J., McTernan P.G., Kusminski C.M., Fisher M., Da Silva N.F., Khanolkar M., Evans M., Harte A.L., Kumar S. Lipopolysaccharide activates an innate immune system response in human adipose tissue in obesity and type 2 diabetes. *Am. J. Physiol. Endocrinol. Metab* (2007) 292:E740–E747.

Crosnier C., Stamataki D., Lewis J. Organizing cell renewal in the intestine: stem cells, signals and combinatorial control. *Nat. Rev. Genet* (2006) 7, 349–359.

Crosnier C, Vargesson N, Gschmeissner S, Ariza-McNaughton L, Morrison A, Lewis J. Delta-Notch signalling controls commitment to a secretory fate in the zebrafish intestine. *Development* (2005)132:1093–104.

Cronin S.J., Nehme N.T., Limmer S., Liegeois S., Pospisilik J.A., Schramek D., Leibbrandt A., Simoes Rde M., Gruber S., Puc U., et al. Genome-wide RNAi screen identifies genes involved in intestinal pathogenic bacterial infection. *Science* (2009) 325, 340–343.

Cunningham KM, Daly J, Horowitz M, Read NW. Gastrointestinal adaptation to diets of differing fat composition in human volunteers. *Gut* (1991)32:483–6.

D Denton , T-K Chang , S Nicolson , B Shravage , R Simin , E H Baehrecke and S Kumar. Relationship between growth arrest and autophagy in midgut programmed cell death in Drosophila. Cell Death and Differentiation *(2012) 19, 1299–1307.*

de La Serre CB, Ellis CL, Lee J, Hartman AL, Rutledge JC, Raybould HE. Propensity to high-fat diet-induced obesity in rats is associated with changes in the gut microbiota and gut inflammation. *Am J Physiol Gastrointest Liver Physiol* (2010) 299(2) G440–G448.

Delgado-Aros S, Kim DY, Burton DD, et al. Effect of GLP-1 on gastric volume, emptying, maximum volume ingested, and postprandial symptoms in humans. *Am J Physiol Gastrointest Liver Physiol* (2002) 282:G424-31.

Deopurkar R, Ghanim H, Friedman J, et al. Differential effects of cream, glucose, and orange juice on inflammation, endotoxin, and the expression of Toll-like receptor-4 and suppressor of cytokine signaling-3. *Diabetes Care* (2010) 33(5):991–997.

De Gregorio E., Spellman P.T., Rubin G.M., Lemaitre B. Genome-wide analysis of the Drosophila immune response by using oligonucleotide microarrays. *Proc. Natl. Acad. Sci* (2001) 98, 12590–12595.

Deretic V, Levine B. Autophagy, immunity, and microbial adaptations. Cell Host Microbe *(2009) 5:527–549.*

Desai S, Loomis Z, Pugh-Bernard A, Schrunk J, Doyle MJ, et al. Nkx2.2 regulates cell fate choice in the enteroendocrine cell lineages of the intestine. *Dev. Biol* (2008) 313:58–66.

Dessens J.T., Mendoza J., Claudianos C., Vinetz J.M., Khater E., Hassard S., Ranawaka G.R., Sinden R.E. Knockout of the rodent malaria parasite chitinase pbCHT1 reduces infectivity to mosquitoes. *Infect. Immunol* (2001) 69, 4041–4047.

Ding S, Chi MM, Scull BP, et al. High-fat diet: bacteria interactions promote intestinal inflammation which precedes and correlates with obesity and insulin resistance in mouse. *PLoS One* (2010) 5(8):e12191.

Djärv T, Wikman A, Nordenstedt H, et al. Physical activity, obesity and gastroesophageal reflux disease in the general population. *World J Gastroenterol* (2012) 18:3710-4.

Eaden JA, Abrams KR, Mayberry JF. The risk of colorectal cancer in ulcerative colitis: a meta-analysis. *Gut* (2001) 48: 526–35.

Ekbom A, Helmick C, Zack M, *et al*. Increased risk of large bowel cancer in Crohn's disease with colonic involvement. *Lancet* (1990) 336: 357–9.

Enteric Neurons and Systemic Signals Couple Nutritional and Reproductive Status with Intestinal Homeostasis. Paola Cognigni, Andrew P. Bailey and Irene Miguel-Aliaga. *Cell Metabolism* (2011) 13, 92–104.

Erridge C, Attina T, Spickett CM *et al*. A high-fat meal induces low-grade endotoxemia: evidence of a novel mechanism of postprandial inflammation. *Am J Clin Nutr* (2007) 86:1286–1292.

Eun-Mi Ha ,Kyung-Ah Lee Seon Hwa Park, Sung-Hee Kim, Hyuck-Jin Nam Hyo-Young Lee Dongmin Kang Won-Jae Lee. Regulation of DUOX by the Gαq-Phospholipase Cβ-Ca^{2+}Pathway in *Drosophila* Gut Immunity . *Developmental Cell* (2009) 386–397, 17.

Evanthia Zacharioudaki and Sarah J. Bray. Tools and methods for studying Notch signaling in *Drosophila melanogaster*. *Methods* (2014) 68(1): 173–182.

Ferrero-Miliani L, O H Nielsen, P S Andersen, and S E Girardin in Chronic inflammation: importance of NOD2 and NALP3 in interleukin-1β generation. *Clin Exp Immunol* (2007) 147(2): 227–235.

Fornari F, Callegari-Jacques SM, Dantas RO, et al. Obese patients have stronger peristalsis and increased acid exposure in the esophagus. *Dig Dis Sci* (2011) 56:1420-6.

French SJ, Murray B, Rumsey RD, Fadzlin R, Read NW. Adaptation to high-fat diets: effects on eating behaviour and plasma cholecystokinin. *Br J Nutr* (1995) 73:179–89.

Friedenberg FK, Xanthopoulos M, Foster GD, et al. The association between gastroesophageal reflux disease and obesity. *Am J Gastroenterol* (2008)103:2111-22.

Garrett W.S., Lord G.M., Punit S., Lugo-Villarino G., Mazmanian S.K., Ito S., Glickman J.N., Glimcher L.H. Communicable ulcerative colitis induced by T-bet deficiency in the innate immune system. *Cell* (2007) 131:33–45.

Garrett W.S., Gordon J.I., Glimcher L.H. Homeostasis and inflammation in the intestine. *Cell* (2010) 140, 859–870.

Geminard, C., Rulifson, E. J. and Leopold, P. Remote control of insulin secretion by fat cells in *Drosophila. Cell* Metab (2009) 10, 199-207.

Gerasimos P. Sykiotis and Dirk Bohmann. Keap1/Nrf2 signaling regulates oxidative stress tolerance and lifespan in *Drosophila. Dev Cell* (2008) 14(1): 76–85.

Girardin S.E., Philpott D.J. Mini-review: the role of peptidoglycan recognition in innate immunity. *Eur. J. Immunol (*2004) 34, 1777–1782.

Ghanim H, Abuaysheh S, Sia CL, et al. Increase in plasma endotoxin concentrations and the expression of Toll-like receptors and suppressor of cytokine signaling-3 in mononuclear cells after a high-fat, high-carbohydrate meal: implications for insulin resistance. *Diabetes Care* (2009) 32(12):2281–2287.

Ghosh S., Dai C., Brown K., Rajendiran E., Makarenko S., Baker J., Ma C., Halder S., Montero M., Ionescu V.A., et al. Colonic microbiota alters host susceptibility to infectious colitis by modulating inflammation, redox status, and ion transporter gene expression. Am. J. Physiol. Gastrointest. Liver Physiol (2011) 301:G39–G49.

Gooday G.W. Aggressive and defensive roles for chitinases. *EXS* (1999) 87, 157–169.

Gopaul NK, Zacharowski K, Halliwell B, et al. Evaluation of the postprandial effect of a fast-food meal on human plasma F_2-isoprostane and lipid peroxide levels. *Free Radic Biol Med* (2000) 28:806–814.

Guo M. Drosophila as a model to study mitochondrial dysfunction in Parkinson's disease. Cold Spring Hard Perspect. *Med* (2012).

Gutierrez, E., Wiggins, D., Fielding, B., Gould, A.P. Specialized hepatocyte-like cells regulate Drosophila lipid metabolism. *Nature* (2007) 445(7125): 275--280.

Gyde SN, Prior P, Allan RN, *et al.* Colorectal cancer in ulcerative colitis: a cohort study of primary referrals from three centres. *Gut* (1988) 29: 206–17.

Gyde S, Prior P, Dew MJ, Saunders V, Waterhouse JA, Allan RN. Mortality in ulcerative colitis. *Gastroenterology* (1982) 83: 36–43.

Ha E.M., Oh C.T., Bae Y.S., Lee W.J. A direct role for dual oxidase in Drosophila gut immunity. *Science* (2005) 310, 847–850.

Ha, E. M., Lee, K. A., Seo, Y. Y., Kim, S. H., Lim, J. H., Oh, B. H., et al. Coordination of multiple dual oxidase-regulatory pathways in responses to commensal and infectious microbes in drosophila gut. *Nat. Immunol* (2009b) 10, 949–957.

Halliwell B, Zhao K, Whiteman ML. The gastrointestinal tract: a major site of antioxidant action. *Free Radic Res* (2000) 33:819–830.

Hansen J, Gulati A, Sartor RB. The role of mucosal immunity and host genetics in defining intestinal commensal bacteria. *Curr Opin Gastroenterol* (2010) 26(6):564–571.

Hegedus Z, Zakrzewska, A, Agoston VC et al. Deep sequencing of the zebrafish transcriptome response to mycobacterium infection. *Molecular Immunology* (2009) 46 (15): 2918-30.

Helfand S.L., Rogina B. Genetics of aging in the fruit fly, Drosophila melanogaster. *Annu. Rev. Genet* (2003) 37, 329–348.

Hellström PM, Grybäck P, Jacobsson H. The physiology of gastric emptying. Best Pract Res *Clin Anaesthesiol* (2006) 20:397-407.

Hergarden, A.C., Tayler, T.D., Anderson, D.J. Allatostatin-A neurons inhibit feeding behavior in adult *Drosophila*. *Proc. Natl. Acad. Sci* (2012) 109(10): 3967--3972.

Hergovich A., Stegert M.R., Schmitz D., Hemmings B.A. NDR kinases regulate essential cell processes from yeast to humans. *Nat. Rev. Mol. Cell Biol* (2006) 7, 253–264.

Herranz, H., Hong, X., Pérez, L., Ferreira, A., Olivieri, D., Cohen, S.M., Milán, M. The miRNA machinery targets Mei-P26 and regulates Myc protein levels in the Drosophila wing. *EMBO J* (2010) 29(10): 1688--1698.

Herranz, R., Larkin, O.J., Dijkstra, C.E., Hill, R.J., Anthony, P., Davey, M.R., Eaves, L., van Loon, J.J., Medina, F.J., Marco, R. Microgravity simulation by diamagnetic levitation: effects of a strong gradient magnetic field on the transcriptional profile of Drosophila melanogaster. *BMC Genomics* (2012) 13(): 52.

Hiramoto K, Li X, Makimoto M. Identification of hydroxy-hydroquinone in coffee as a generator of reactive oxygen species that break DNA single strands. *Mutat Res* (2001) 419:43–51.

Hoffmann AA , R. J. Hallas , J. A. Dean , M. Schiffer. Low Potential for Climatic Stress Adaptation in a Rainforest *Drosophila*Species. *Science* (2003) 301 no. 5629 pp. 100-102 .

Hong D, Khajanchee YS, Pereira N, et al. Manometric abnormalities and gastroesophageal reflux disease in the morbidly obese. *Obes Surg* (2004) 14:744-9.

Huang, J., Wu, S., Barrera, J., Matthews, K., Pan, D. The Hippo signaling pathway coordinately regulates cell proliferation and apoptosis by inactivating Yorkie, the Drosophila Homolog of YAP. *Cell* (2005) 122(3): 421--434.

Hue S, Ahern P, Buonocore S, et al. Interleukin-23 drives innate and T cell-mediated intestinal inflammation. *J Exp Med* (2006) 203:2473–2483.

Hugot JP, Chamaillard M, Zouali H, Lesage S, Cézard JP, Belaiche J, Almer S, Tysk C, O'Morain CA, Gassull M, Binder V, Finkel Y, Cortot A, Modigliani R,Laurent-Puig P, Gower-Rousseau C, Macry J, Colombel JF, Sahbatou M, Thomas G.in Association of NOD2 leucine-rich repeat variants with susceptibility to Crohn's disease.

Nature (2001) 31;411(6837):599-603.

Ian Spreadbury. Comparison with ancestral diets suggests dense acellular carbohydrates promote an inflammatory microbiota, and may be the primary dietary cause of leptin resistance and obesity. Diabetes Metab Syndr Obes (2012) 5: 175–189.

Inoue, Mayuri; Yokoyama, Yusuke; Harada, Mariko; Suzuki, Atsushi; Kawahata, Hodaka; Matsuzaki, Hiroyuki; Iryu, Yasufumi. Trace element variations in fossil corals from Tahiti collected by IODP Expedition 310: Reconstruction of marine environments during the last deglaciation (15 to 9 ka). *Marine Geology* (2010) 271(3-4), 303-306.

Isono K, Nemoto K, Li K, Takada Y, Suzuki R, Katsuki M, Nakagawara A, Koseki H. Overlapping role for homeodomain-interacting protein kinases hipk1 and hipk2 in the mediation of cell growth in response to morphogenetic and genotoxic signals. *Mol Cell Biol* (2006) 26(7): 2758-71.

Jacoline Gerritsen, Hauke Smidt, Ger T. Rijkers, and Willem M. de Vos. Intestinal microbiota in human health and disease: the impact of probiotics. *Genes Nutr* (2011) 6(3): 209–240.

Jaffin BW, Knoepflmacher P, Greenstein R. High prevalence of asymptomatic esophageal motility disorders among morbidly obese patients. *Obes Surg* (1999) 9:390-5.

Jairam Vanamala, Sridhar Radhakrishnan, Elisabeth Eriksson, Venkata Charepalli, Sung Kim3 and Lavanya Reddivari. High-fat diet induced expansion of colon crypt epithelial proliferative zone towards lumen correlates with elevated innate inflammatory markers in the human-relevant porcine model (123.2). *The FASEB Journal* (2014) vol. 28

Jeanne MR, Wegener C and Michael B . The proportion Convertase encoded by *amontillado* (*amon*) is required in *Drosophila* corpora cardiac endocrine cells producing the glucose regulatory hormones AKH. *Plos Genetics* (2010) 6 issue 5 e1000967.

Jensen J, Pedersen EE, Galante P, Hald J, Heller RS, et al. Control of endodermal endocrine development by Hes-1. *Nat. Genet* (2000) 24:36–44.

Jiang H., Patel P.H., Kohlmaier A., Grenley M.O., McEwen D.G., Edgar B.A. Cytokine/Jak/Stat signaling mediates regeneration and homeostasis in the Drosophila midgut. Cell (2009) 137, 1343–1355.

Jiang H., Edgar B.A. EGFR signaling regulates the proliferation of Drosophila adult midgut progenitors. *Development* (2009) 136, 483–493.

K DiBaise MD, Daniel N Frank PhD and Ruchi Mathur MD, FRCPC.Impact of the Gut Microbiota on the Development of Obesity: Current Concepts. John. Am J Gastroenterol Suppl *(2012) 1:22–27.*

Kalidas S, Smith DP. Novel genomic cDNA hybrids produce effective RNA interference in adult Drosophila. *Neuron* (2002) 33:1787-184.

Kanner J, Lapidot T. The stomach as a bioreactor: dietary lipid peroxidation in the gastric fluid and the effects of plant-derived antioxidants. *Free Radic Biol Med* (2001) 31:1388–1395.

Karam SM. Lineage commitment and maturation of epithelial cells in the gut. *Front. Biosci* (1999) 4:D286–98.

Karantanos T, Markoutsaki T, Gazouli M, Anagnou NP, Karamanolis DG. Current insights into the pathophysiology of Irritable Bowel Syndrome. *Gut Pathog* (2010) 2(1):3.

Katz JP, Perreault N, Goldstein BG, Lee CS, Labosky PA, et al. The zinc-finger transcription factor Klf4 is required for terminal differentiation of goblet cells in the colon. *Development* (2002) 129:2619–28

Kedinger M., Simon-Assmann P., Haffen K. Growth and differentiation of intestinal endodermal cells in a coculture system. *Gut* (1987) 28, 237–241.

Kim YH, Choi CY, Lee SJ, Conti MA, Kim Y.Homeodomain-interacting protein kinases, a novel family of co-homeodomain transcription factors. *J Biol Chem* (199) 273(40):25875-9.

Kentaro Inoue Amy J. Baldwin Rebecca L. Shipman Kyoko Matsui Steven M. Theg and Masaru Ohme-Takagi. Complete maturation of the plastid protein translocation channel requires a type I signal peptidase.*JCB* (2005) (171) ; 3: 425-430.

Kiri Louise Tan, Isabella Vlisidou, and Will Wood. Ecdysone Mediates the Development of Immunity in the *Drosophila* Embryo. *Curr Biol* (2014) 24(10): 1145–1152.

Kirsty Brown, Daniella DeCoffe, Erin Molcan, and Deanna L. Gibson. Diet-Induced Dysbiosis of the Intestinal Microbiota and the Effects on Immunity and Disease. *Nutrients* (2012) 4(8): 1095–1119.

Komuro T., Hashimoto Y. Three-dimensional structure of the rat intestinal wall (mucosa and submucosa). Arch. Histol. *Cytol* (1990) 53, 1–21.

Kuraishi, T., Binggeli, O., Opota, O., Buchon, N., Lemaitre, B. Genetic evidence for a protective role of the peritrophic matrix against intestinal bacterial infection in *Drosophila melanogaster. Proc. Natl. Acad. Sci* (2011) 108(38): 15966--15971.

Kvietys P.R., Granger D.N. Physiology and pathophysiology of the colonic circulation. *Clin. Gastroenterol* (1986) 15, 967–983.

Langholz E, Munkholm P, Davidsen M, *et al*. Colorectal cancer risk and mortality in patients with ulcerative colitis. *Gastroenterology* (1992) 103: 1444–51.

Larsson LI, St-Onge L, Hougaard DM, Sosa-Pineda B, Gruss P. Pax 4 and 6 regulate gastrointestinal endocrine cell development. *Mech. Dev* (1998) 79:153–59.

Lemaitre B., Nicolas E., Michaut L., Reichhart J.M., Hoffmann J.A. The dorsoventral regulatory gene cassette spatzle/Toll/cactus controls the potent antifungal response in Drosophila adults. *Cell* (1996) 86, 973–983.

Lemaitre B., Hoffmann J. The host defense of Drosophila melanogaster. *Annu. Rev. Immunol* (2007) 25, 697–743.

Ley RE, Lozupone CA, Hamady M, Knight R, Gordon JI. Worlds within worlds: evolution of the vertebrate gut microbiota. *Nat Rev Microbiol* (2008) 6(10):776–788.

Ligoxygakis P., Bray S.J., Apidianakis Y., Delidakis C. Ectopic expression of individual E (spl) genes has differential effects on different cell fate decisions and underscores the

biphasic requirement for notch activity in wing margin establishment in *Drosophila. Development* (1999) 126, 2205–2214.

Little TJ, Russo A, Meyer JH, et al. Free fatty acids have more potent effects on gastric emptying, gut hormones, and appetite than triacylglycerides. *Gastroenterology* (2007)133:1124-31.

Lin G., Xu N., Xi R. Paracrine Wingless signalling controls self-renewal of Drosophila intestinal stem cells. *Nature* (2008) 455, 1119–1123.

Lin HC, Doty JE, Reedy TJ, Meyer JH. Inhibition of gastric emptying by sodium oleate depends on length of intestine exposed to nutrient. *Am J Physiol Gastrointest Liver Physiol* (1990) 259:G1031–6.

Lissner L, Levitsky DA, Strupp BJ, Kalkwarf HJ, Roe DA. Dietary fat and the regulation of energy intake in human subjects. *Am J Clin Nutr* (1987) 46:886–92.

Li X, Zhang R, Luo D, Park SJ, Wang Q, Kim Y, Min W. Tumor necrosis factor alpha-induced desumoylation and cytoplasmic translocation of homeodomain-interacting protein kinase 1 are critical for apoptosis signal-regulating kinase1-JNK/p38 activation. *J Biol Chem* (2005) 280(15):15061-70.

Long LH, Lan ANB, Hsuan FTY, et al. Generation of hydrogen peroxide by 'antioxidant' beverages and the effect of milk addition: is cocoa the best beverages. *Free Radic Res* (1999) 31:67–71.

Long LH, Halliwell B. Coffee drinking increases levels of urinary hydrogen peroxide detected in healthy human subjects. *Free Radic Res* (2000) 32:463–467.

Longstreth GF, Thompson WG, Chey WD, Houghton LA, Mearin F, Spiller RC. Functional bowel disorders. *Gastroenterology*. (2006) 130(5):1480-91.

Mackie RI, Sghir A, Gaskins HR. Developmental microbial ecology of the neonatal gastrointestinal tract. *Am J Clin Nutr* (1999) 69(5):1035S–1045S.

Macpherson AJ, McCoy KD, Johansen FE, et al. The immune geography of IgA induction and function. *Mucosal Immunol* (2008) 1:11–22.

Manel Bosch, Florenci Serras, Enrique Martín-Blanco, Jaume Baguñà. JNK signaling pathway required for wound healing in regenerating*Drosophila* wing imaginal discs. *Developmental Biology* (2005) 280(1)73–86.

Mariat D, Firmesse O, Levenez F, Guimarães V, Sokol H, Doré J, Corthier G, Furet JP. The *Firmicutes Bacteroidetes* ratio of the human microbiota changes with age. *BMC Microbiol* (2009) 9:123.

Marshman E, Booth C, Potten CS. The intestinal epithelial stem cell. *Bioessays* (2002) 24:91-98.

Mathilde Gendrin, David P. Welchman, Mickael Poidevin, Mireille Hervé, Bruno Lemaitre. Long-Range Activation of Systemic Immunity through Peptidoglycan Diffusion in *Drosophila. Plos Pathogen* (2009) DOI: 10.1371/journal.ppat.1000694.

Ma X., Torbenson M., Hamad A.R., Soloski M.J., Li Z. High-Fat diet modulates non-CD1d-restricted natural killer T cells and regulatory T cells in mouse colon and exacerbates experimental colitis. *Clin. Exp. Immunol* (2008) 151:130–138.

McVay LD, Keilbaugh SA, Wong TM, et al. Absence of bacterially induced RELMβ reducesinjury in the dextran sodium sulfate model of colitis. *J Clin Invest* (2006) 116:2914–2923.

Membrez M, Blancher F, Jaquet M, et al. Gut microbiota modulation with norfloxacin and ampicillin enhances glucose tolerance in mice. *FASEB J* (2008) 22(7):2416–2426.

Micchelli C.A., Perrimon N. Evidence that stem cells reside in the adult Drosophila midgut epithelium. *Nature* (2006) 439, 475–479.

M J Carter, A J Lobo, S P L Travis in 2004. Guidelines for the management of inflammatory bowel disease in adults. *Gut* (2004) 53:v1-v16 doi: 10.1136.

Mueller S, Saunier K, Hanisch C, Norin E, Alm L, Midtvedt T, Cresci A, Silvi S, Orpianesi C, Verdenelli MC, Clavel T, Koebnick C, Zunft HJ, Doré J, Blaut M. Differences in fecal

microbiota in different European study populations in relation to age, gender, and country: a cross-sectional study. *Appl Environ Microbiol* (2006) 72(2):1027–1033.

Musso G, Gambino R, Cassader M. Obesity, diabetes, and gut microbiota: the hygiene hypothesis expanded? *Diabetes Care* (2010) 33(10):2277–2284.

Nässel DR, Winther AM. Drosophila neuropeptides in regulation of physiology and behavior. *Prog Neurobiol.* (2010) 92(1):42-104.

Naya FJ, Huang HP, Qiu Y, Mutoh H, DeMayo FJ, et al. Diabetes, defective pancreatic morphogenesis, and abnormal enteroendocrine differentiation in BETA2/neuroD-deficient mice. *Genes Dev* (1997) 11:2323–34.

Nehme N.T., Liegeois S., Kele B., Giammarinaro P., Pradel E., Hoffmann J.A., Ewbank J.J., Ferrandon D. A model of bacterial intestinal infections in Drosophila melanogaster. *PLoS Pathog* (2007) 3, e173.

Nenci A, Becker C, Wullaert A, et al. Epithelial NEMO links innate immunity to chronic intestinal inflammation. *Nature* (2007) 446:557–561.

Nateri A.S., Spencer-Dene B., Behrens A. Interaction of phosphorylated c-Jun with TCF4 regulates intestinal cancer development. *Nature* (2005) 437, 281–285.

Ohlstein B., Spradling A. The adult Drosophila posterior midgut is maintained by pluripotent stem cells. *Nature* (2006) 439, 470–474.

Ohlstein B., Spradling A. Multipotent Drosophila intestinal stem cells specify daughter cell fates by differential notch signaling. *Science* (2007) 315, 988–992.

Osterdahl, M et al. Effects of a short-term intervention with a paleolithic diet in healthy volunteers. *Eur J Clin Nutr* (2008) 62(5):682-85.

Pendyala S., Walker J.M., Holt P.R. A high-fat diet is associated with endotoxemia that originates from the gut. *Gastroenterology* (2012) 142:1100–1101.

Pierre Leopold & Norbert Perrimon. Drosophila *and the genetics of the internal milieu. Nature* (2007) 450, 186-188.

Pitsouli C., Apidianakis Y., Perrimon N. Homeostasis in infected epithelia: stem cells take the lead. *Cell Host Microbe* (2009) 6, 301–307.

Poernbacher I, Baumgartner R, Marada SK, Edwards K, Stocker H. *Drosophila* Pez acts in Hippo signaling to restrict intestinal stem cell proliferation. *Curr. Biol* (2012) 22, 389–396.

Poon, P.C., Kuo, T.H., Linford, N.J., Roman, G., Pletcher, S.D. Carbon dioxide sensing modulates lifespan and physiology in Drosophila. *PLoS Biol* (2010) 8(4): e1000356.

Potten CS, Kovacs L, Hamilton E. Continuous labelling studies on mouse skin and intestine. *Cell Tissue Kinet* (1974) 7:271–83.

Powell DW,Mifflin RC,Valentich JD, Crowe SE, Saada JI,West AB. Myofibroblasts. II. Intestinal subepithelial myofibroblasts. *Am. J. Physiol* (1999) 277:C183–20.

Qin J., Li R., Raes J., Arumugam M., Burgdorf K.S., Manichanh C., Nielsen T., Pons N., Levenez F., Yamada T., et al. A human gut microbial gene catalogue established by metagenomic sequencing. *Nature* (2010) 464, 59–65.

Rachael L. Shaw, Alexander Kohlmaier, Cédric Polesello, Cornelia Veelken, Bruce A. Edgar and Nicolas Tapon. The Hippo pathway regulates intestinal stem cell proliferation during Drosophilaadult midgut regeneration. *Development* (2010) 137(24): 4147–4158.

Rajan A, Perrimon N. Drosophila cytokine unpaired 2 regulates physiological homeostasis by remotely controlling insulin secretion. *Cell* (2012) 151(1):123-37.

Rakoff-Nahoum S., Paglino J., Eslami-Varzaneh F., Edberg S., Medzhitov R. Recognition of commensal microflora by toll-like receptors is required for intestinal homeostasis. *Cell* (2004) 118:229–241.

Rakoff-Nahoum S, Medzhitov R. Innate immune recognition of the indigenous microbial flora.*Mucosal Immunol* (2008) 1(Suppl 1):S10–S14.

Razzell W, Evans IR, Martin P and Wood W. Calcium flashes orchestrate the wound inflammatory response through DUOX activation and hydrogen peroxide release. *Curr Biol* (2013) 23(5):424-9.

Rhee S.H., Pothoulakis C., Mayer E.A. Principles and clinical implications of the brain-gut-enteric microbiota axis. *Nat. Rev. Gastroenterol. Hepatol* (2009) 6, 306–314.

Rosetto M., Engstrom Y., Baldari C.T., Telford J.L., Hultmark D. Signals from the IL-1 receptor homolog, Toll, can activate an immune response in a Drosophila hemocyte cell line. Biochem. *Biophys. Res. Commun* (1995) 209, 111–116.

Rubin D.C. Intestinal morphogenesis. Curr. Opin. Gastroenterol (2007) 23, 111–114.

Ryu J.H., Kim S.H., Lee H.Y., Bai J.Y., Nam Y.D., Bae J.W., Lee D.G., Shin S.C., Ha E.M., Lee W.J. Innate immune homeostasis by the homeobox gene caudal and commensal-gut mutualism in *Drosophila*. *Science* (2008) 319, 777–782.

Sajjan, U. S., Yang, J. H., Hershenson, M. B. & LiPuma, J. J. Intracellular trafficking and replication of *Burkholderia cenocepacia* in human cystic fibrosis airway epithelial cells. *Cell Microbiol* (2006) 8, 1456–1466.

Sampson M.N., Gooday G.W. Involvement of chitinases of Bacillus thuringiensis during pathogenesis in insects. *Microbiology* (1998) 144, 2189–2194.

Santiago Vernia, Julie Cavanagh-Kyros, Tamera Barrett, Dae Young Jung, Jason K. Kim and Roger J. Davis. Diet-induced obesity mediated by the JNK/DIO2 signal transduction pathway. *Genes & Dev* (2013) 27:2345-2355.

Satsangi J, M S Silverberg, S Vermeire, and J-F Colombel. He Montreal classification of inflammatory bowel disease: controversies,consensus, and implications. *Gut* (2006) 55(6): 749–753.

Scopelliti, A., Cordero, J.B., Diao, F., Strathdee, K., White, B.H., Sansom, O.J., Vidal, M. Local control of intestinal stem cell homeostasis by enteroendocrine cells in the adult Drosophila midgut. *Curr. Biol* (2014) 24(11): 1199--1211.

Scoville D.H., Sato T., He X.C., Li L. Current view: intestinal stem cells and signaling. *Gastroenterology* (2008) 134, 849–864.

Schirra J, Wank U, Arnold R, et al. Effects of glucagon-like peptide-1(7-36)amide on motility and sensation of the proximal stomach in humans. *Gut* (2002) 50:341-8.

Schneider JM, Brücher BL, Küper M, et al. Multichannel intraluminal impedance measurement of gastroesophageal reflux in patients with different stages of morbid obesity. *Obes Surg* (2009) 19:1522-9.

Schonhoff SE, Giel-Moloney M, Leiter AB. Minireview: development and differentiation of gut endocrine cells. *Endocrinology* (2004)145:2639–44.

Sengupta N., MacDonald T.T. The role of matrix metalloproteinases in stromal/epithelial interactions in the gut. *Physiology* (2007) 22, 401–409.

Shanbhag S., Tripathi S. Epithelial ultrastructure and cellular mechanisms of acid and base transport in the Drosophila midgut. *J. Exp. Biol* (2009) 212, 1731–1744.

Shi Y, Evans JE, Rock KL. Molecular identification of a danger signal that alerts the immune system to dying cells. *Nature* (2003) 425:516–521.

Silverman WK[1], Ortiz CD, Viswesvaran C, Burns BJ, Kolko DJ, Putnam FW, Amaya-Jackson L. Evidence-based psychosocial treatments for children and adolescents exposed to traumatic events. *J Clin Child Adolesc Psychol* (2008) 37(1):156-83.

Simpson SJ, Raubenheimer D. Obesity: the protein leverage hypothesis.*Obes Rev* (2005) 6:133–42.

Sing N, et al. Morphological evolution through integration. A quantitative study of cranial integration in Homo, Pan, Gorilla and Pongo. *J of Human Evolution* (2012) 62 (1). 155-164.

Smythies LE, Sellers M, Clements RH, et al. Human intestinal macrophages display profound inflammatory anergy despite avid phagocytic and bacteriocidal activity. *J Clin Invest* (2005) 115:66–75.

Solinas G, et al. JNK1 in hematopoietically derived cells contributes to diet-induced inflammation and insulin resistance without affecting obesity. *Cell Metab* (2007) 6(5):386–397.

Srigiridhar K, Nair KM. Supplementation with alpha-tocopherol or a combination of alpha-tocopherol and ascorbic acid protects the gastrointestinal tract of iron-deficient rats against iron-induced oxidative damage during iron repletion. *Br J Nutr* (2000) 84:165–173.

Stewart JE, Feinle-Bisset C, Keast RS. Fatty acid detection during food consumption and digestion: Associations with ingestive behavior and obesity. *Prog Lipid Res* (2011) 50:225-33.

Takashi AY. Puckered-GAL4 driving in JNK-Active cells. *Genesis* (2002) 34; 19-22.

Tjonneland A., Overvad K., Bergmann M.M., Nagel G., Linseisen J., Hallmans G., Palmqvist R., Sjodin H., Hagglund G., Berglund G., et al. Linoleic acid, a dietary *n*-6 polyunsaturated fatty acid, and the aetiology of ulcerative colitis: A nested case-control study within a European prospective cohort study. *Gut* (2009) 58:1606–1611.

Toshio Hirano and Masaaki Murakami in The molecular mechanisms of chronic inflammation development. *Front. Immunol* (2012) | doi: 10.3389/fimmu.2012.00323.

Tremblay A, Plourde G, Despres JP, Bouchard C. Impact of dietary fat content and fat oxidation on energy intake in humans. *Am J Clin Nutr* (1989) 49:799–805.

Trinh I, Boulianne GL. Modeling obesity and its associated disorders in Drosophila. *Physiology (Bethesda).* (2013) 28(2):117-24.

Tschöp M, Smiley DL, Heiman ML. Ghrelin induces adiposity in rodents. *Nature* (2000) 407(6806):908-13.

Turner JR. Molecular basis of epithelial barrier regulation: from basic mechanisms to clinical application. *Am J Pathol* (2006) 169:1901–1909.

Uchiyama K., Nakamura M., Odahara S., Koido S., Katahira K., Shiraishi H., Ohkusa T., Fujise K., Tajiri H. *N*-3 polyunsaturated fatty acid diet therapy for patients with inflammatory bowel disease.Inflamm. *Bowel Dis* (2010) 16:1696–1707.

Uhlirova M., Jasper H., Bohmann D. Non-cell-autonomous induction of tissue overgrowth by JNK/Ras cooperation in a Drosophila tumor model. *Proc. Natl. Acad. Sci* (2005) 102, 13123–13128

Vallerie SN, Furuhashi M, Fucho R, Hotamisligil GS. A predominant role for parenchymal c-Jun amino terminal kinase (JNK) in the regulation of systemic insulin sensitivity. *PLoS On* (2008) 3(9):e3151.

Van der Sluis M, De Koning BA, De Bruijn AC, et al. Muc2-deficient mice spontaneously develop colitis, indicating that MUC2 is critical for colonic protection. *Gastroenterology* (2006) 131:117–129.

van Es JH, Jay P, Gregorieff A, van Gijn ME, Jonkheer S, et al. 2005. Wnt signalling induces maturation of Paneth cells in intestinal crypts. *Nat. Cell Biol* (2005) 7:381–86.

Vodovar N., Vinals M., Liehl P., Basset A., Degrouard J., Spellman P., Boccard F., Lemaitre B. Drosophila host defense after oral infection by an entomopathogenic Pseudomonas species. *Proc. Natl. Acad. Sci* (2005) 102, 11414–11419.

Venken KJ, Bellen HJ.Emerging technologies for gene manipulation in Drosophila melnogaster. *Nat Rev Genet* (2005) 6:167-178.

Venken KJ, Bellen HJ. Transgenesis upgrade for Drosophila melanogaster. *Development* (2007) 134: 3571-84.

Wallace D.F., Crawford D.H., Subramaniam V.N. The control of iron homeostasis: Micrornas join the party. *Gastroenterology* (2011) 141:1520–1522. doi: 10.1053/j.gastro.2011.08.018.

Wanders AJ, van den Borne JJ, de Graaf C, et al. Effects of dietary fibre on subjective appetite, energy intake and body weight: a systematic review of randomized controlled trials. *Obes Rev* (2011) 12(9):724–739.

Wang P., Granados R.R. An intestinal mucin is the target substrate for a baculovirus enhancin. *Proc. Natl. Acad. Sci* (1997) 94, 6977–6982.

Weber B, Saurer L, Mueller C. Intestinal macrophages: differentiation and involvement in intestinal immunopathologies. *Semin Immunopathol* (2009) 31:171–184.

Wen L., Ley R.E., Volchkov P.Y., Stranges P.B., Avanesyan L., Stonebraker A.C., Hu C., Wong F.S., Szot G.L., Bluestone J.A., et al. Innate immunity and intestinal microbiota in the development of type 1 diabetes. *Nature* (2008) 455:1109–1113.

Whitworth AJ. Drosophila models of Parkinson's disease. *Adv Genet* (2011) 73:1-50.

Wren AM, Seal LJ, Cohen MA, Bynes AE, Frost GS, Murphey KG, Dhillo WS, Ghatei MA and Bloom SR. Ghrelin enhances appetite and increase food intake in humans. *Journal of clinical Endocrinology and Metabolism* (2001b) 86,5992.

Wren AM, Small CJ, Abbott CR, Dhillo WS, Seal LJ, Cohen MA, Batterham RL, Taheri S, Stanley SA, Ghatei MA and Bloom SR. Ghrelin causes hyperphagia and obesity in rat. *Diabetes* (2001a) 50,2540-2547.

Woods SC, Seeley RJ, Rushing PA, D'Alessio D, Tso P. A controlled high-fat diet induces an obese syndrome in rats. *J Nutr* (2003) 133:1081–7.

Xian kun Zeng, Chhavi Chauhan, and Steven X. Hou. Characterization of Midgut Stem Cell– and Enteroblast-Specific Gal4 Lines in *Drosophila*. *Genesis* (2010) 48(10): 607–611.

Xiao X,Wu ZC, Chou KC. A multi-label classifier for predicting the subcellular localization of gram-negative bacterial proteins with both single and multiple sites. *PLoS One* (2011) 6(6):e20592. doi: 10.1371/journal.pone.0020592.

Young Sik Lee, Kenji Nakahara,John W Pham, Kevin Kim, Zhengying He, Erik J Sontheimer, Richard W Carthew. Distinct Roles for *Drosophila* Dicer-1 and Dicer-2 in the siRNA/miRNA Silencing Pathways. *Cell* (2004) 117(1)69–81.

Zaidman-Remy A., Herve M., Poidevin M., Pili-Floury S., Kim M.S., Blanot D., Oh B.H., Ueda R., Mengin-Lecreulx D., Lemaitre B. The Drosophila amidase PGRP-LB modulates the immune response to bacterial infection. *Immunity* (2006) 24, 463–473.

Zaph C, Troy AE, Taylor BC, et al. Epithelial-cell-intrinsic IKK-β expression regulates intestinal immune homeostasis. *Nature* (2007) 446:552–556.

Zhao K, Whiteman M, Spencer J, et al. DNA damage by nitrite and peroxynitrite: protection by dietary phenols. *Methods Enzymol* (2001)335:296–307.

Zheng Guo, Ian Driver, and Benjamin Ohlstein. Injury-induced BMP signaling negatively regulates Drosophila midgut homeostasis. *Cell Biol* (2013) 201 No. 6 945–961.

Zhengui Xia, Martin Dickens, Joël Raingeaud, Roger J. Davis, Michael E. Greenberg.Opposing Effects of ERK and JNK-p38 MAP Kinases on Apoptosis. *Science* (1995)
270 no. 5240 pp. 1326-1331.

Zhihua Zhang & Chibiao Chen & Jian Sun & Kap Luk Chan. "EM algorithms for Gaussian mixtures with split-and-merge operation." *Pattern Recognition* (2003) 36: 1973–1983.

Zwielehner J, Liszt K, Handschur M, Lassl C, Lapin A, Haslberger AG. Combined PCR-DGGE fingerprinting and quantitative-PCR indicates shifts in fecal population sizes and diversity of *Bacteroides*, bifidobacteria and *Clostridium* cluster IV in institutionalized elderly. *Exp Gerontol* (2009) 44(6–7):440–446.